LUND UNIVERSITY

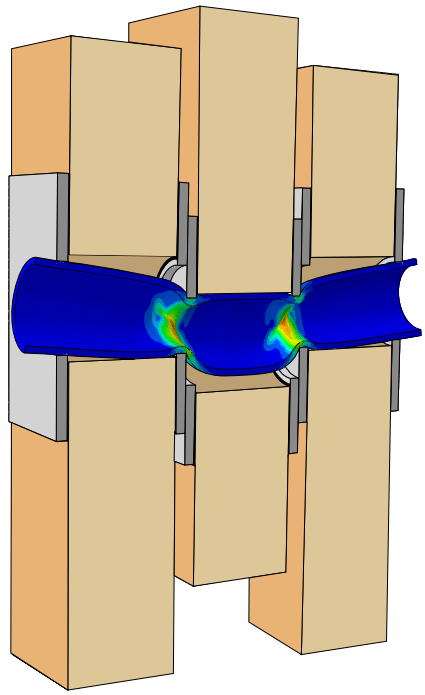

THE SHEAR PLATE DOWEL JOINT

Research on a novel connection for heavy timber structures

GUSTAF LARSSON

Structural Mechanics

Doctoral Thesis

DEPARTMENT OF CONSTRUCTION SCIENCES
DIVISION OF STRUCTURAL MECHANICS

ISRN LUTVDG/TVSM--19/1031--SE (1-145) | ISSN 0281-6679
ISBN 978-91-7895-225-0 (print) | ISBN 978-91-7895-226-7 (pdf)
DOCTORAL THESIS

THE SHEAR PLATE DOWEL JOINT

Research on a novel connection for heavy timber structures

GUSTAF LARSSON

Printed by Media-Tryck LU, Lund, Sweden, August 2019 *(Pl)*.

For information, address:
Division of Structural Mechanics,
Faculty of Engineering LTH, Lund University, Box 118, SE-221 00 Lund, Sweden.
Homepage: www.byggmek.lth.se

Acknowledgements

The work presented in the thesis has been carried out as a joint venture between the divisions of Structural Mechanics and Structural Engineering at the Faculty of Engineering of Lund University. The financial support provided by Formas through grant 2012-879 for the project *Innovative connections for timber construction* and by *Stiftelsen Nils och Dorthi Troëdssons forskningsfond* through grant 893-16 are gratefully acknowledged.

The project started as a joint idea of Professor Per Johan Gustafsson and Professor Roberto Crocetti, two professors who impressed me during my undergraduate studies by their extensive knowledge and enthusiasm. This intriguing combination of subject and expertise made me pursue a PhD in structural mechanics. Many of the ideas central to this work originates from these men and I am very grateful for their inspiring and skilful guidance.

Time passes and main supervisors become co-supervisors and vice versa. I am grateful to Professor Erik Serrano for stepping up as main supervisor, and to Associate Professor Henrik Danielsson for the supervision to the end. I would also like to thank my supervisors Johan Jönsson and Peter Persson for the time shared. It has been a privilege to be able to work with Associate Professor Huifeng Yang at College of Civil Engineering at Nanjing Tech University, and having the external addition to my reference group of Arne Emilsson from Limträteknik AB and Thomas Johansson from Moelven Töreboda AB. An inspiring work climate has been ensured by the staff at Structural Mechanics and Structural Engineering at Lund University.

And finally, to my foremost friend, loving life companion and fiancée Evelina; thank you for being you.

Lund, 15 August 2019

Gustaf Larsson

Abstract

An increased use of wood can reduce the environmental footprint of the building sector. In order to improve the competitiveness of heavy timber structures, the thesis presents a novel type of timber connection with a high degree of prefabrication. The connection includes a resilient bond line, meaning an elastic bond line with low stiffness yet high fracture energy.

It has previously been shown that a large glued joint with a conventional stiff adhesive bond line acting in shear can be made stronger by using a resilient bond line, e.g. by introducing an intermediate rubber foil. The scientific contribution of the thesis starts by comparing such resilient bond lines to conventional non-resilient bond lines. It is shown by numerical analyses that the short-term strength of glued lap joints can be increased by 40–80% by introducing a resilient bond line. Unlike other types of connections, a resilient bond line also enables the possibility to design the stiffness by varying the hardness and thickness of the intermediate bond layer.

The proposed shear plate dowel joint uses a single dowel to transfer load between members. The load transfer from the dowel to the timber element is realised by externally bonded metal plates. The plates are bonded to the element using a resilient bond line, which ensures that the loading is applied to the timber member in uniform shear. Large scale experimental testing has shown an average shear stress over the plate area at failure of 3.1 MPa, while small scale specimens have reached 5.8 MPa. The structural response of the connection for different dowel materials and designs are investigated both numerically and experimentally, and it is shown that increased ductility can be obtained using tubular dowels.

However, the long-term behaviour of the shear plate dowel joint has been found inadequate. A reduction factor k_{mod} of 0.1–0.3 was found for open sheltered climate 50-year period reference, which weakens the benefit of increased load-carrying capacity of the design proposal compared to other contemporary connections. It should be noted that this is an estimate based on 4-month small-scale data extrapolated to 50 years. However, further studies of the duration of load characteristics as well as fire resistance should be conducted prior to structural application.

Populärvetenskaplig sammanfattning

Allt större byggnader uppförs med bärande stomme av trä tack vare teknisk utveckling, modernisering av lagstiftning och inte minst en ökad allmän medvetenhet om hur våra val påverkar miljön. Till skillnad från andra vanligt förekommande byggnadsmaterial som betong och stål är trä ett naturligt material, men det är inte helt utan negativa följder. Trä påverkas negativt av fukt, innehåller kvistar som sänker hållfastheten, blir svagare av belastning över tid och har olika hållfastheter i olika riktningar. Det sistnämnda är praktiskt när man hugger ved, men mer problematiskt när man ska koppla samman olika träelement med hjälp av förband – till exempel sammanfogningen av två plankor med spik. Likt vid vedhuggning kan det kring spikarna uppstå sprickor som kan vara förödande för förbandets styrka. Ett starkt förband måste alltså utnyttja träets goda egenskaper utan att belasta svagheterna.

Träs egenskaper gör det omöjligt att hitta ett förband som passar alla behov, och även om man använder det bäst lämpade förbandet för ändamålet är det likväl ofta konstruktionens svagaste punkt. Detta är ett problem när man nu vill bygga än större träkonstruktioner. Denna avhandling undersöker ett nytt förband vars egenskaper har utretts baserat på moderna funktionskrav.

Grunden i det undersökta förbandet är två stora plattor som limmas på utsidan av träelementet. Limfogen som används är mer eftergivlig än vanliga limfogar, vilket gör att krafter som överförs är jämnt fördelade med följden att hela fogen och därmed förbandet blir starkare. För att sedan föra över krafter från ett element till ett annat används bara *en* kort metallstång (också kallad dymling), vilket gör att montage av förbandet är snabbare jämfört med vanligt förekommande förband.

Forskningen som presenteras i denna avhandling tyder på att det förslagna förbandet är mycket starkt om det belastas under korta tidsperioder, att styvheten enkelt kan anpassas och att förbandet kan utformas så att man i tid hinner upptäcka en eventuell kollaps. Dessvärre är förbandstypen sämre på att ta upp långvariga laster, vilket begränsar användningsområdet. Likt andra förbandstyper har alltså det föreslagna förbandet en del svagheter som bör undersökas vidare innan praktisk tillämpning, men den genomförda forskningen påvisar också nya möjligheter för förband i stora träkonstruktioner.

Contents

Paper D
Analysis of the shear plate dowel joint and parameter studies
Gustaf Larsson, Per Johan Gustafsson, Erik Serrano, Roberto Crocetti
Proceedings of the World conference of timber engineering, 2016.

Paper E
Dowel design of the shear plate dowel joint
Gustaf Larsson, Erik Serrano, Per Johan Gustafsson
Submitted journal paper, 25 June 2019.

Paper F
Duration of load behaviour of the shear plate dowel joint
Gustaf Larsson, Per Johan Gustafsson, Erik Serrano, Roberto Crocetti
Submitted journal paper, 5 March 2019

Part I

Introduction and overview

I
Introduction

While gazing in a large forest, it is easy to be impressed by the sheer size of the trees. The stem is rising high, supporting the branches which in turn support leaves or needles. For millions of years, trees have ever so slowly adapted their characteristics in order to survive in a large variety of habitats.

It is seemingly recent people have begun using timber as an engineered wood product. The once so optimised structure of branches and their efficient joint to the stem is now merely an imperfection in the engineered board as a knot. How to best use timber as a construction material, despite such imperfections, has been studied extensively and will continue to be studied as production methods develop. This work will look at the structural details; namely how timber connections can transfer loads from one timber element to the next in heavy timber structures, while minimizing the effects of these imperfections to ensure efficiency and reliability.

1.1 BACKGROUND

Climate change is a fact, which is putting considerable pressure on the society as a whole to reduce the emission of greenhouse gases. Although the operation stage dominates the life cycle of buildings, the production stage becomes increasingly important in terms of emissions of greenhouse gases [1]. For the construction sector, one possibility is to reduce the use of steel and concrete in favour for timber.

Graded timber of medium strength has indeed higher strength to weight ratio than common

mild steel, but a new set of challenges are introduced. Not only is wood highly anisotropic, i.e. strength and stiffness vary with the orientation of the grain, but wood most often needs to be manufactured into timber in order to be used efficiently. The effects of imperfections, duration of load (DOL), moisture content and understanding in how timber degrades during fire are just some characteristics which differs timber from other building materials.

Timber is used extensively in light framing systems typical for single-family housing, but the increasing interest in large timber structures is made possible by glued laminated timber (GLT) and cross laminated timber (CLT). By aligning and simply gluing the naturally limited cross-sections of timber together, GLT members and CLT panels have significantly increased the load-carrying capacity of timber structures. This enables timber structures to span further and reach higher, and some even propose timber skyscrapers [2]. The work conducted within the thesis is concentrated on such heavy timber structures, leaving light framing systems for others to consider.

Structures are constructed of individual members connected by connections (or joints), and the global behaviour of the entire structure is largely dependent on the characteristics of the connections. New production methods and design approaches are needed in order to make it possible to build timber skyscrapers in the future, including timber connections.

1.2 AIM AND RESEARCH METHODOLOGY

In order to facilitate an increased occurrence and efficiency of heavy timber structures, the general aim of this research project is to

> *Develop a connection design for heavy timber structures suited for industrialized building processes with a high degree of prefabrication.*

This applied science project is well suited for an engineering design process rather than the standard scientific method. Functional requirements are thus identified accordingly and presented in Chapter 2, and these are used to discuss contemporary timber connections. The strengths and weaknesses are emphasized and incorporated into the proposal of a new connection design, here referred to as the shear plate dowel joint (SPDJ). In order to limit the scope of the thesis once the SPDJ design was proposed, the aim was narrowed down to

> *Present computational methods suitable for resilient adhesive bond lines, and evaluate the shear plate dowel joint in terms of functional requirements.*

Although the general aim of the research project includes topics of producibility, the focus in the thesis is put upon achieving an efficient connection design in terms of structural performance. However, some key design aspects of the SPDJ are inherited from a point of view of producibility, although no research effort has been put into these aspects.

In the thesis, a resilient bond line is defined as a bond line with a lower stiffness than conventional adhesive bond lines, yet with a high fracture energy. A resilient bond line can for example be realised by introducing a rubber foil between the adherends, but also by use of an adhesive layer with such properties, see Chapter 4.

Empirical, analytical and numerical modelling are typical types of modelling in timber engineering. Empirical models are based upon observations or experience which is used to formulate a mathematical expression with a predictive power using some chosen input variables. In contrast, analytical formulas are derived to obtain exact solutions and are based upon fundamental theories of physics. Numerical modelling is based upon analytical relations, but typically uses approximate solutions to differential equations to produce results with high accuracy. The finite element (FE) method is the type of numerical modelling exclusively used in the thesis.

Empirical and numerical modelling are in themselves prone to inductive reasoning, which is subject to criticism within philosophy of science. Among the criticisms, and of special concern in engineering, is the problem of formulating generalized conclusions based upon a too small number of observations. By establishing a hypothesis in accordance with hypothetico-deductive reasoning, more general conclusions can be obtained. Although analytical modelling is in general well regarded thanks to the clear physical interpretations, it does not necessarily lend itself better to the favoured hypothetico-deductive reasoning.

In order to obtain a reliable result, the work presented in the thesis includes analytical and numerical modelling, as well as considerable experimental studies.

1.3 ORIGINAL FEATURES AND LIMITATIONS

The original features presented in the thesis comprises:

- Comparison of load-carrying capacity for resilient and non-resilient bond lines, presented in Paper A.
- Experimental comparison of load-carrying capacity for different single dowel connections, presented in Paper B.
- The shear plate dowel joint:
  - Detailed description of the SPDJ, including discussion regarding the functional requirements, is presented in Part I of the thesis.
  - Full scale tests are presented in Paper B.
  - A numerical bond line model is presented in Paper C.
  - Parameter studies regarding e.g. bond line stiffness and shape of the shear plate are investigated in Paper D.
  - The geometry and material of the dowel are analysed in Paper E.

  - Duration of load effects are tested in Paper F.
  - A proposal of a design procedure is presented in Section 5.5.

The presented work has the following general limitations:

- Only static loading is considered.
- The influence of moisture is not considered.
- Conducted experimental work is limited to:
  - The resilient bond line was evaluated using large scale quasi-static tests of double lap joints.
  - The study on single large diameter dowel connections was conducted on large scale quasi-static tests.
  - Dowel design and ductility was evaluated using small scale quasi-static tests in single- and three-member node with the SPDJ.
  - The duration of load study was conducted on small scale SPDJ.
- Numerical work:
  - Wood is modelled as an elastic homogeneous orthotropic material with homogeneous material orientations. If not else specified, a rectilinear model with deterministic timber parameters is used.
  - Glue lines in GLT are not explicitly considered.

1.4 PREVIOUS WORK

Key references to the work conducted within the thesis include analytical as well as experimental work. The novelty of the shear plate dowel joint design lies within the bond line between a steel plate and the exterior of the timber element. To achieve a strong bond over large areas, this bond line has a low shear stiffness yet a high fracture energy. This specific type of adhesive bond line is within the thesis denoted a resilient bond line. The idea was originally presented by Per Johan Gustafsson in 1987 [3], for which the first experimental study was published in 2007 [4].

The SPDJ can be considered a centrically loaded double lap joint, for which the shear stress distribution can be studied analytically using the Volkersen theory presented in 1938 [5]. Originally intended for riveted steel lap joints, it is in the thesis shown that the expression is valid also for the SPDJ using a resilient bond line. However, Volkersen theory is not applicable for common stiff adhesives for which the softening behaviour constitutes a considerable part

of the load-carrying capacity. By use of the equivalent elastic layer approach [3], the softening behaviour can be included in an equivalent linear elastic analysis enabling analytical load capacity predictions using the Volkersen theory.

Key experimental references include the short-term tests on different single dowel designs conducted by Crocetti et al. [6] and Kobel [7]. As one of few found studies on the shear behaviour of timber subjected to long-term loading, the work of Leont'ev from 1961 [8] has been most useful.

A licentiate thesis has preceded this doctoral thesis, using a similar disposition [9]. This doctoral thesis includes all conducted research, including research reported in the licentiate thesis, and thus some context overlaps. In addition to the research included in the licentiate thesis, the thesis contains the additional Papers E and F from which the results are included in the revised Chapter 5 regarding the SPDJ. Remaining chapters of the thesis are also revised and updated as compared to the licentiate thesis.

1.5 OUTLINE

The thesis is divided into three parts, in which Part I presents an introduction to the subject, and puts the conducted research in a wider and more general perspective. A detailed description of a manufacturing method used is found in Part II, which has been used throughout the study. The conducted research is described in detail in Part III, which compiles the research papers.

Part I

Subsequent the introductory chapter you are now reading, the thesis starts by discussing different contemporary timber connections in Chapter 2 by means of functional requirements and possible design improvements. Conducted research is to some extent based upon numerical analysis, thus Chapter 3 attends the methodology used to model timber. Chapter 4 presents the state of the art of resilient bond lines as intended use in civil engineering, including the research conducted in Papers A and C. The shear plate dowel joint is finally presented in Chapter 5, which is the novel connection design of main interest in the thesis. The presentation includes results from Papers B–F, which are discussed in a broader perspective including comparison to existing solutions. Concluding remarks are found in Chapter 6 while a summary of appended papers is found in Chapter 7.

Part II

Part II consist of a single appendix with a detailed description of the manufacturing method of the SPDJ used during the work in the thesis. As discussed in Paper A, the bond between

rubber and timber is highly dependent on this specific methodology and it is hence included.

Part III

Part III of the thesis compiles the appended papers. The papers are not presented in chronological order by publishing date, but rather in a logical order to form a trail of thought similar to the one used in Part I. Paper A studies a special type of adhesive bond line which can be used to increase the load-carrying capacity of adhesive joints. This type of bond line is in Paper B compared to other types of reinforcements of single large diameter dowel connections, which are of interest due to producibility. Combined, Papers A and B motivates the continued work on the shear plate dowel joint by impressing short-term load-carrying capacity. To complement the experimental analyses, an efficient numerical model was developed and published in Paper C. Once an experimental and numerical methodology was established for the shear plate dowel joint, the connection was evaluated in terms of functional requirements as discussed in Section 1.2. Focus was put on the functional requirements regarding structural performance (see Section 2.1), and ductility was investigated in Paper E while duration of load behaviour was studied in Paper F. A more extended summary of the appended papers can be found in Chapter 7.

2
Timber connections

Structures commonly consist of a number of elements assembled by connections. The fundamental purpose of connections is to allow forces from one element to be transferred to the next. This chapter will further specify the functional requirements and highlight the implementation in timber connections. Contemporary connections will then be presented in order to put the thesis into perspective, especially with regards to the slotted-in steel plate connection.

2.1 FUNCTIONAL REQUIREMENTS

It is not far-fetched to consider load-carrying capacity as the primary functional requirement of a connection. However, a strong timber connection can be achieved in numerous ways, and the diverse types of contemporary connections suggest that different functional requirements not only exist, but also vary in importance for different applications. For example, load-carrying capacity and stiffness are usually prioritized in large span structures while appearance and production efficiency can be more important in residential housing and office buildings. Different functional requirements are listed below without any order of importance, based upon a list originally presented by Borg Madsen [10].

Load-carrying capacity

A connection should ideally be able to transmit the internal forces from one structural element to the next, with the same load-carrying capacity and reliability as adopted for the elements

themselves. For many timber connection types used today, this is however not possible. In fact, it is common that the load-carrying capacity of the connection is only 40–60% compared to the capacity of the member [11]. This occurs due to local weakening of the member by cutting or drilling, or due to occurrences of stress concentrations. Stress concentrations in wood are particularly complex to account for since they always have to be put in relation to its corresponding orthotropic material strength, discussed further in Section 3.3. The low tensile strength perpendicular to grain is often the limiting factor in timber connections, which must be considered in the design phase of any strong connection.

For timber, strength should also be discussed in terms of time and climate. Short term strength is typically higher than long term, which is quantified by duration of load (DOL) studies. Strength can also be dependent of the time history of the load which must be considered in design, e.g. for cyclic loading. Strength of timber is typically reduced for increasing moisture content, and the moisture content is in turn related to the relative humidity and temperature of the surrounding air.

Stiffness and deformations

The safety level of structures can often be increased using statically indeterminate systems. The redundancy of such systems enables different load paths in case of member weakening or failure and can thus ensure structural integrity. However, the structural design will become more complicated by introducing several possible load paths, as the load then will be transferred through the structure by the stiffest path possible. The stiffness of such a path depends greatly on the stiffness of the connections, making it an important functional requirement. In order to minimize unwanted deformations in the structure and being able to accurately predict the internal forces of surrounding structural elements, it is important to be able to limit and predict the stiffness and creep behaviour of the connections.

Ductility

Wood is in general a brittle material and can thus fail without the warning sign of excessive deformations. This behaviour is undesirable in structures as loads cannot be redistributed in case of excessive deformations as discussed in the paragraph above, nor does it leave much opportunity for occupants to recognise and avoid danger. A ductile failure allows large deformations prior to system collapse and it is thus a favourable property. Ductility of a timber structure can be achieved by means of other materials and/or a sound structural design, which is of particular importance in seismic regions.

It should also be noted that large deformations also can be obtained without the permanent deformations typically associated with ductility. This can be achieved by use of e.g. rubber-like materials, which is if special interest in the thesis.

Simplicity of design

Simplicity of design relates to the reliability in terms of human error in two aspects. Firstly, it is preferable that the design of a connection is done so that a clear understanding of how forces are transferred in the connection is made possible. Similarly but secondly, the design method of a connection should be straight forward and easy to understand in order to avoid calculation errors.

Producibility

The production of a timber joint includes manufacturing and assembly. A high degree of prefabrication and simple assembly are desirable features, although different connection designs fulfil such requirements to varying degree. Assembly can also be difficult if the connection designs are sensitive to moisture movements and general construction tolerances. Over-sized holes for bolts could simplify the assembly but may significantly decrease the connection stiffness.

Appearance

Wood is often considered an aesthetically pleasant material. To combine aesthetics with functionality is however not an easy task, especially not for connections. An intimate collaboration between the architect, the structural designer and fire protection engineer is thus vital.

Durability

The service life of a connection should not fall short of the service life of the structure which the connection is a part of. Possible degradation due to e.g. corrosion of metallic components and/or moisture of timber members should always be considered. The latter is the more common durability issue, in which detailing is crucial as discussed by e.g. Niklewski [12].

Fire

The fire performance of timber structures has historically limited the use in high-rise buildings. Only in recent years has the improved knowledge of fire design of timber structures combined with technical measures resulted in building code relaxations [13]. However, timber connections still pose a design difficulty in case of fire, mainly due to the typical combination of timber and steel components. Charring will occur on the timber surface, temporarily insulating the material within from degradation while the strength of steel is severely decreased for increasing temperature. A sound connection design should thus have a minimum of exposed steel or enable a simple application of encapsulation.

Costs

As for every project and product, the cost is usually a crucial parameter. About 20–30% of the total cost of a GLT structure is normally spent on the connections [10], a percentage that possibly can be reduced. However, it should be kept in mind that the size of the structural members can be reduced if the load-carrying capacity of the connection matches the capacity of the members, as discussed above. Paradoxically, the total cost of some projects can thus be reduced by increasing the cost of the connection.

Environmental sustainability

Timber engineering has in recent years drawn considerable interest thanks to a growing environmental awareness. Although generally superior to steel or concrete structures in terms of environmental impact, timber engineering can still improve its ecological footprint by e.g. life cycle assessment. Applied to connections, the possibility of reutilization or recycling is beneficial.

2.2 DIFFICULTIES IN TIMBER CONNECTION DESIGN

Although numerous different types of timber connections exist, some general difficulties can be identified in terms of design. At material level, which will be further discussed in Chapter 3, fibre orientation, variability in material properties and brittleness are three characteristics which set the structural behaviour of timber apart from other building materials, e.g. steel.

The material properties of wood vary greatly with orientation of the grain. The most extreme example of this is that the tensile strength of wood perpendicular to grain is only approximately 5% of the parallel to grain tensile strength [14]. This fact is very important to consider in a connection, as fracture perpendicular to grain may occur at low load levels if the design is inadequate. Furthermore, the material properties change not only at different angles to the grain direction, but a great variability is also found for each such material property. In terms of strength, the variability is often considered by differentiating mean strength from characteristic strength, typically being the 5^{th} percentile. These properties also vary with moisture content and duration of load effects, which also must be considered.

The brittleness of timber can be considered a problem at a structural level. For example, in nailed timber connections loaded in tension, Johnsson [15] shows how an increasing number of nails can actually decrease the load-carrying capacity of the joint. This counter-intuitive result is due to the brittle behaviour of wood, as the increased number of nails weakens the timber and may cause block failure, as studied extensively by Jorissen [16]. To fully utilize a nailed connection, each nail must be allowed to yield according to Johansen's yield theory [17].

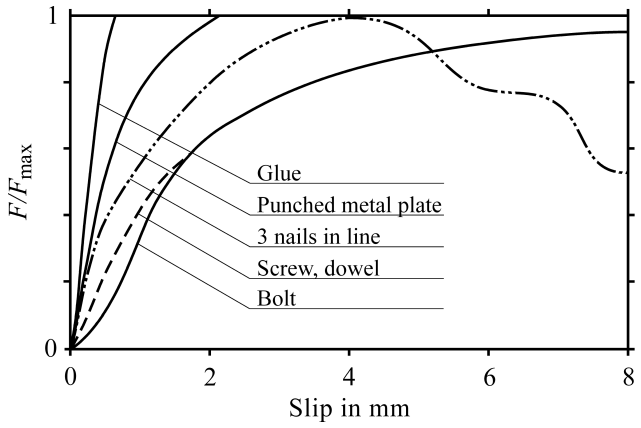

Figure 2.1: Typical normalized load–slip behaviours of different types of fasteners in a single lap joint design. Reproduced from [18].

Of special interest in the thesis is the possibility of assembling different types of fasteners within a single connection, such as a combined glued and bolted connection. The different load–slip behaviour of these fasteners typically limit the level of interaction, as the stiff adhesive typically fails at a deformation which only would allow the bolt to reach a small fraction of its maximum capacity as shown in Figure 2.1 [18]. This problem can be overcome by e.g. careful design of the bond line, which is discussed in Chapter 4.

2.3 CONTEMPORARY CONNECTIONS

In order to propose a novel connection for heavy timber structures, a review of some chosen contemporary connections is presented. The connections represent a range different types of timber connections which can be used in heavy timber structures. The load transfer within the connections is presented along with the prominent features influencing design and performance. The discussion is based upon the functional requirements presented in Section 2.1.

2.3.1 Punched metal plates

Even though typically designed for light structures such as single-family houses, the punched metal plate (PMP), or "truss plate" as it is named in North America, is extensively used throughout the world and thus worth mentioning. As shown in Figure 2.2, the PMP is a combination of nail plates and nails produced by punching edges in galvanized steel plates and bending the formed teeth into position perpendicular to the plate. Due to limitations in the punching process, the steel plate thickness usually does not exceed 2 mm and the PMP is thus bound to be considered a surface connection with a relatively low load-carrying capacity.

Figure 2.2: Punched metal plates, typically used for light timber trusses.

Trusses are formed by pressing the PMP into the wood members using a hydraulic clamp or pushing the whole truss through a large roller press. By such, it is usually not practical to apply PMP on the building site. Common spans for PMP trusses are 9–15 m, but can reach up to 40 m.

The popularity of the PMP is due to the simple manufacturing, ease of use and low production cost. From a design engineer perspective, the connection is however complex. In the European timber design code, Eurocode 5 [19], no less than 11 parameters are needed for full connection characterisation. Poutanen [20] highlighted this complexity in 1989 by comparing seven different design codes, in which an unreasonably large variety of truss sizes was found depending on what type of design code used. More detailed analysis of the PMP is numerically enabled by the use of the Foschi model [21].

The limited teeth length can be considered to cause a surface action of the PMP, which in turn limits the thickness of jointed timber element. Thus it is common that timber trusses using PMP connections are slender. This is not necessarily a problem in residential housing since the truss seldom spans its entire length completely unsupported by interior walls. Many of the design assumptions are also very conservative and as a result, failures are generally rare in the field. However, when using PMP trusses in buildings with clear and long spans, the boundary conditions are not as forgiving. Furthermore, creep deformations significantly higher than the short term elastic deformation have been found [22].

Although popular for shorter spans and smaller dimensions, the size limitations, creep and complex load path makes it unsuitable in heavy timber structures.

2.3.2 Nail plates

The load-carrying capacity of the punched metal plate is limited by the production method, which limits the length and stiffness of the punched-out nails. Naturally, the load-carrying capacity can be increased by using thicker plates and longer nails, but at the cost of production efficiency. These are typically called nailed plate connections, although regional varieties occur.

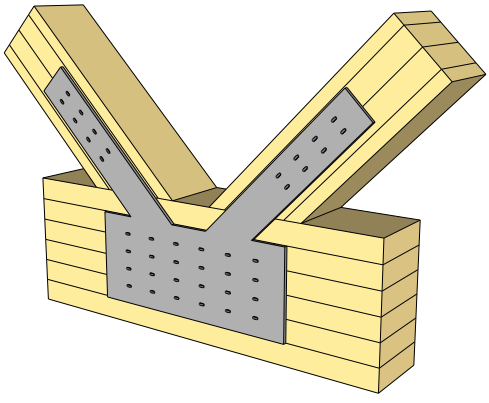

(**a**) Typical truss connection.

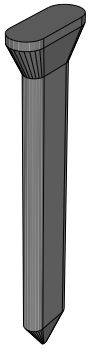

(**b**) The glulam rivet.

Figure 2.3: The glulam rivet is a special type of nail plate designed for heavy timber structures. The design features a rectangular cross-section with rounded corners to maximize bending resistance and minimize grain impact. The tapered head causes hoop tension in the nail plate.

The nail plate design has been further improved by Borg Madsen using Canadian glulam rivets [10]. The system is shown in Figure 2.3 which illustrates two key features which distinguishes it from typical nail plates. The first of the two key features is the shape of the nail cross-section. Instead of round or close to square, the rivets are made rectangular with rounded corners. This allows the rivet to have increased bending stiffness with, if inserted correctly with its longest side parallel to grain, a minimal impact on the wood grain which reduces the risk of premature splitting. As pre-drilling is not required, fibres are left intact and only slightly bend when the rivet is inserted. The second key feature is the tapered head of the rivet, which causes significant hoop tension in the plate as the rivet is driven in, ensuring a tight fit. The result is a strong cantilevering component with a similar effect to cold-riveting, and hence the name. [10]

Among the benefits of nailed plates, and of glulam rivets, is the well-established manufacturing process. By small design alterations from the nail plate, the glulam rivet offers a stronger and stiffer connection more suited for heavy structures. However, the installation of any type of nail plate is labour-intensive if used on heavy timber structures due to the large number of rivets which must be inserted. Even though the large number of nails/rivets may prove useful in earthquake design, it is probably not favourable in environments prone to moisture content variations due to the typical shrinkage and swelling of timber, and the typical subsequent splitting.

2.3.3 Slotted-in steel plates

The large number of nails in nail plate type connections can be reduced by increasing the diameter of the nail, then typically denoted a dowel. Dowel-type connections are common in timber engineering, and an elegant way of using them in heavy timber structures is in combination with one or more slotted-in steel plates as shown in Figure 2.4. The steel plates are used to transfer load between members, while the dowels transfer load between the steel plates and the timber member. The capacity of a single dowel is increased by the number of inserted plates, but limited by brittle failure of the remaining timber.

As the steel is embedded in timber, slotted-in steel plates are not only protected from fire, but also usually considered as aesthetically pleasing. Slotted-in steel plates do not eliminate the risk of brittle failure, but the risk can be reduced by using small diameter dowels as well as using adequate plate spacing and end distances.

The dimensions and number of steel plates and dowels are increased for higher load-carrying capacities. Thinner slotted-in plates can be pierced by self-perforating dowels which reduces the number of operations needed for installation. This method is also very efficient to obtain joints with high stiffness as the slip is minimized. However, thicker steel plates or larger dowel diameters requires pre-drilling, which must be done with a high degree of precision in order to enable assembly at the building site while limiting the connection slip. Although less fasteners than in nail plate type connections are used, the number of dowels can still be significant and require considerable assembly times. Additionally, the cuts made to insert the steel plates weaken the timber members.

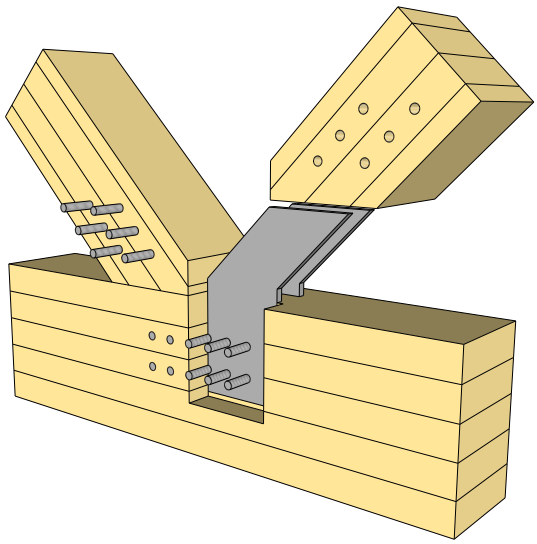

Figure 2.4: Slotted-in steel plates used in a truss node.

2.3.4 Expanded tube fasteners

Expanded tube fasteners are considerably less common than slotted-in steel plates, but the design can be considered more innovative. The design shown in Figure 2.5 was proposed by Leijten [23] in an effort to improve stiffness and ductility of timber connections.

The most prominent feature of the design is the expanded tube. After being inserted in the timber elements similar to a dowel-type connection with some clearance, the tube is expanded radially using a hydraulic jack to ensure a close to perfect fit. The fit reduces the initial slip to a minimum, which also improves the load-carrying capacity of the expanded tube in moment resisting connections. The material used in the tubes are galvanized gas pipes of low grade, which causes a ductile failure response of the connection.

The tube expansion causes tensile stresses perpendicular to grain in the timber elements, which requires reinforcement in order to prevent splitting. Thus, the second prominent feature of this connection is the use of densified veneer wood, which is a special type of plywood material with increased strength (further presented in Paper E). It can be seen in Figure 2.5 as darker layers, which are bonded to the timber element using conventional structural adhesives.

The minimal slip combined with ductile failure and possibility of moment resistant connections make this design appealing. However, considerable amount of the production is needed to be carried out at the production site for heavy timber structures. Furthermore, larger and stiffer tubes are needed for heavier loads, which requires heavier hydraulic jacks that are not suited to be hand-held. Although very strong, densified veneer wood is more expensive than steel.

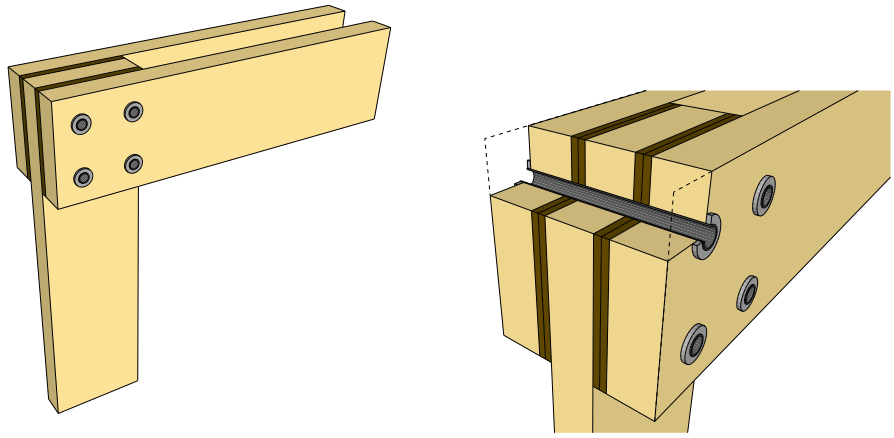

(a) Moment stiff portal corner joint.

(b) A cut through an expended tube fastener after assembly. The tube expansion ensures a close to perfect fit.

Figure 2.5: Expanded tube fastener as proposed by Leijten [23].

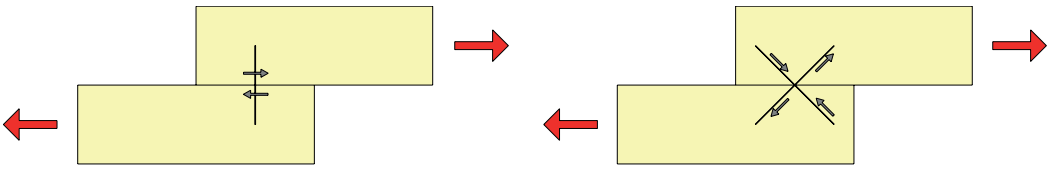

Figure 2.6: Schematic comparison between traditional and inclined screws in lap joints.

2.3.5 Screws and rods

Screws are used extensively in timber engineering and in construction in general. Traditionally, fasteners are placed perpendicular to the connection of two adjacent members and will typically carry load in shear. However, screws typically have a considerable withdrawal capacity if inserted at an angle to the grain, as shown in Figure 2.6, making such arrangement often preferable. By inclining the screws typically 45°, it is possible to minimize shear action in favour for axial action thus increasing the load-carrying capacity and the stiffness of the connection. Tests indicate that by inclining the screws, the load-carrying capacity can be increased by more than 50% while the slip modulus increases by a factor of up to 12 compared to traditional screws [24]. To enable easy on-site assembly, inclined screws can be used in combination with tenon joints.

The inclined screws can be driven on-site by simple means. Furthermore, the very limited aesthetic impact of the joint is also a positive feature of the design. However, the load-carrying capacity is in general smaller than in e.g. connections made of slotted-in steel plates and dowels, making the inclined screws less suitable for heavy structures. Nevertheless, the load-carrying capacity and stiffness can be increased using threaded bars in combination with adhesive, resulting in so-called bonded-in rods [25]. Such a system can typically be used as a connection or as a reinforcement in a similar manner as screws [26]. An advantage for bonded-in rods over screws is the increased load-carrying capacity when inserted parallel to grain.

2.3.6 Wood adhesive joints

Adhesives are an important part of modern timber engineering, which typically requires larger cross-sections than a single timber plank can procure. These larger cross-sections of timber can be obtained by joining planks in lengthwise direction using adhesives, and stacking the planks to create glued laminated timber (GLT). Furthermore, massive timber panels can be produced by gluing planks in a crosswise manner to form cross-laminated timber (CLT), a product that has become increasingly popular in recent years. In the manufacturing of both products, an arbitrary length of each timber plank is made possible by finger joints, which is also an adhesive joint. However, this compilation of timber connections regards the connection *between* different timber members, where adhesives are considerably less common.

The use of timber in structural systems is sometimes questioned due to the large variation

in the mechanical properties of timber, further discussed in Chapter 3. Similar arguments are often also put forward for structural adhesive joints; they possess a number of favourable characteristics, but they are difficult to inspect and their reliability is often doubted. This is probably the main reason for the scarce usage of such type of joint. To utilize the favourable characteristics, adhesive joints must be recognized by skilled design and craftsmanship in a controlled environment.

One of the favourable characteristics of adhesive joints is the load-carrying capacity, for which a comparison is shown in Figure 2.7. Four different types of double lap joints are presented, all with a design load of approximately 150 kN but obtained at different lap lengths based upon empirical design rules. The comparison is presented in [27], but the adhesive lap joint is here added with an average shear stress at failure of 1.8 MPa, according to Eurocode 5 and well below recorded values in Paper A. Similar comparison was also conducted by Adams and Wake in [28]. The adhesive joint is the smallest and thus most material efficient. In addition to high load-carrying capacity, Adams and Wake also argue that adhesive joints have better durability than corresponding mechanical fasteners since the adhesive used is fully resistant to weathering, compared to steel which will rust if not protected.

There are however disadvantages using adhesive connections. The adhesive bond requires a controlled environment during gluing and curing, which is difficult to obtain on-site. Curing pressure and a curing time is needed at a specific temperature and relative humidity range to obtain the desired results. It is furthermore difficult to inspect an adhesive joint since it would then be necessary to dismantle the entire connection. The effects of some of these disadvantages can be minimized using a resilient bond line as presented in Chapter 4.

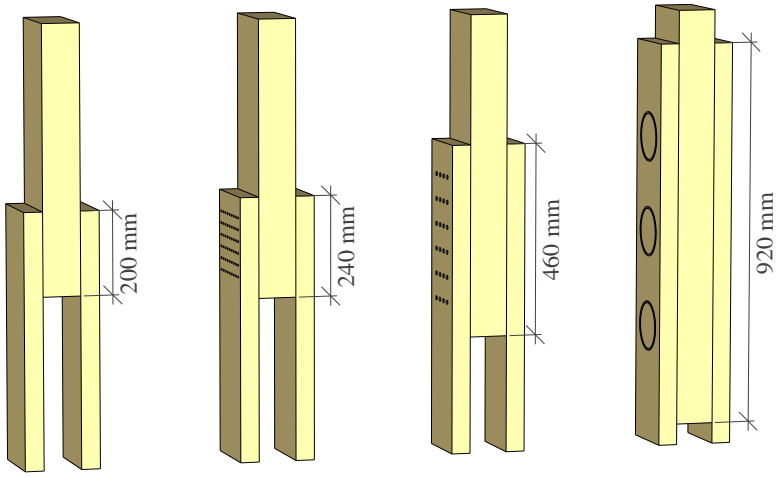

Figure 2.7: Four different double lap joints with similar tensile load capacity using (from left): PUR adhesive; 2×6×9 nails of 5 mm diameter; 4×6 screws of 10 mm diameter; and 2×3 split rings with 120 mm in diameter. The illustration is drawn to scale and based upon [27].

2.4 POSSIBLE DESIGN IMPROVEMENTS

A reasonable design basis for any type of connector is to match the member characteristics as close as possible. For example, material efficiency of the structure is reduced if the connection requires an increase in member dimensions, and the connection is not designed properly against fire if it loses load-carrying capacity prior to the members. This type of thinking limits the level of optimisation of some functional requirements, while others can be improved endlessly such as production cost. A third category of functional requirements will always be subjected to subjective assessment, which of course is a typically difficult basis for optimisation.

The orthotropic nature of wood in combination with complex structures requires a surprisingly large number of different types of connections for different situations. The aim of the thesis regards connections in heavy timber structures with a high degree of prefabrication, a distinction which enables a ranking among the functional requirements and limits the number of possible design solutions.

One of the most typical connection types used for heavy timber structures today is slotted-in steel plates. The design suggested in the thesis should thus exceed the performance of slotted-in steel plates in one or more aspects, of which cost is the one indirectly highlighted in the project aim (c.f. Section 1.2). Some possible improvements as compared to slotted-in steel plates can be identified as:

- Higher load-carrying capacity at long term loads, limited by ductile failure.
- A designable stiffness with high prediction accuracy.
- Lower the production cost by minimizing material usage and production time (especially on-site).
- A connection design suitable for tension and bending action.

3
Wood mechanics

Evolution has spent millions of years devising an arrangement which allow trees to reach as much sunlight as possible. The area of active photosynthesis is maximized by growing tall and branching out. However, this also increases the wind loading which requires each branch to carefully be jointed to the stem by knots. This is typically achieved by locally varying the fibre orientation of the wood, which acts as a local reinforcement.

In order to use the material wood in buildings, it is typically engineered into timber. In timber, the varying fibre orientation from the knots are now, in fact, a defect. This distinction between wood and timber is important, as "timber is as different from wood as concrete is different from cement", as nicely put by Borg Madsen [29].

In this chapter, the modelling choices from wood to timber will be discussed along with material properties of spruce, the most commonly used wood species in northern Europe for structural applications. The structure of wood is only discussed briefly, but further reading can be found in e.g. Bodig and Jayne [30] and Dinwoodie [31]. The mechanics presented in this chapter is implemented in numerical finite element (FE) analysis, which is used throughout the thesis.

3.1 THE DIFFERENT SCALE LEVELS OF TIMBER

Wood is an organic composite built up mainly of cellulose, hemicellulose and lignin which together forms fibres which mostly are aligned close to parallel to the stem. The characteristic annual growth rings are formed depending on what time of year the cells are grown; the lighter

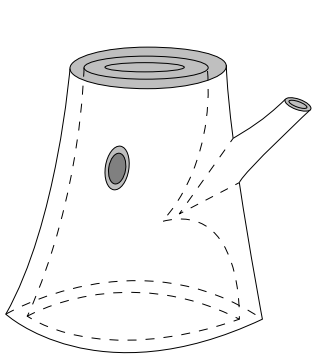

(a) Tree stem with natural growth characteristics.

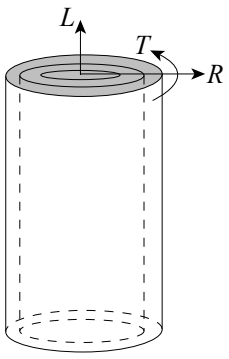

(b) Cylindrical tree stem model with principal directions.

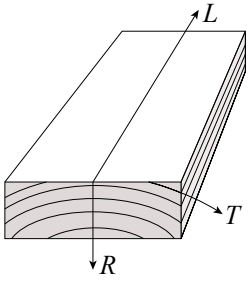

(c) Timber with a cylindrical coordinate system

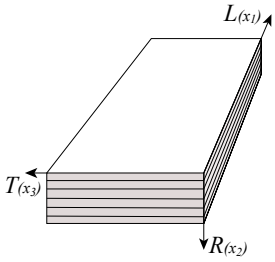

(d) A rectilinear orthotropic model of timber.

Figure 3.1: The reduction of a tree stem to a timber plank model. Based upon [30].

but thicker rings of earlywood and the darker and stronger rings of latewood. As the round stem is of limited use in timber construction, the trees are commonly sawn into timber.

Depending on the type of problem investigated, timber needs to be considered at different scale levels. Cellulose, hemicellulose and lignin are considered the ultrastructural level whereas fibres are represented at the microstructural level. Clear wood is normally regarded as the macroscopic level [32], which is characterised by a distinction between the three orthogonal directions in relation to the growth rings and fibre direction: longitudinal (L), radial (R) and tangential (T), see Figure 3.1. A clear wood specimen has parallel fibre direction and does not contain defects such as knots.

How these defects are considered differs for different engineering problems. Commonly used, also in the thesis, is that they are treated implicitly in the material properties rather on the geometry itself. Not only is it common to ignore geometrical defects as shown in Figure 3.1 (b), but for some problems the effects of the growth ring curvature are also negligible, and a rectilinear material model can be used (d). This assumption typically introduces larger errors for cuts taken near the pith than for cuts taken in the periphery, while the error is minimized if the cut is kept small in relation to the distance from the pith.

Compared to other building materials such as steel or reinforced concrete, wood shows a higher degree of variation in terms of properties. Not only is it orthotropic, but also hygroscopic with properties varying with moisture content and thus affected by air humidity. Timber is produced from a very large variety of logs cut from different trees grown in varying conditions. Additionally, the properties also vary within a single tree from the pith and outwards, but also from lower parts of the tree to the higher. While steel and concrete are manufactured according to well-established procedures with low variability, timber is a natural product which must be graded. It is evident that every single sawn timber element for structural use should be individually tested and sorted, which is done using non-destructive evaluation and statistical relationships. The variability of timber properties is the cost of wood being a natural material, which must be considered using sound engineering judgement.

3.2 WOOD ELASTICITY

A convenient way to represent wood at the macroscopic level as a 3D continuum, is to use Hooke's generalized law as given in Equation 3.1 using Voigt matrix form. The constitutive law assumes small strains and has been adapted to the principal directions of wood, namely the longitudinal, radial and tangential directions referring to the annual growth rings, see Figure 3.1. Robert Hooke stated the law in 1660 as *ut tensio, sic vis* – "As the extension, so the force" [33] which relates material stresses σ to the elastic strains ε according to Equation 3.1.

$$\boldsymbol{\varepsilon} = \mathbf{C}\boldsymbol{\sigma} \tag{3.1}$$

where

$$\boldsymbol{\varepsilon} = \begin{bmatrix} \varepsilon_{LL} & \varepsilon_{RR} & \varepsilon_{TT} & \gamma_{LR} & \gamma_{LT} & \gamma_{RT} \end{bmatrix}^T \tag{3.2}$$

$$\boldsymbol{\sigma} = \begin{bmatrix} \sigma_{LL} & \sigma_{RR} & \sigma_{TT} & \tau_{LR} & \tau_{LT} & \tau_{RT} \end{bmatrix}^T \tag{3.3}$$

The symmetric elastic flexibility tensor $\mathbf{C}$ in Equation 3.4 is valid for orthotropic materials and organizes the moduli of elasticity E_i and shear G_{ij} along with Poisson's ratio ν_{ij}, where i, j are the principal directions L, R, T [30]. It should be noted that wood is assumed an orthotropic material, for which the principal directions can be defined by the stem (as in Figure 3.1) or by the local fibre orientation which typically circles around the stem.

$$\mathbf{C} = \begin{bmatrix} \frac{1}{E_L} & -\frac{\nu_{LR}}{E_R} & -\frac{\nu_{TL}}{E_T} & 0 & 0 & 0 \\ & \frac{1}{E_R} & -\frac{\nu_{TR}}{E_T} & 0 & 0 & 0 \\ & & \frac{1}{E_T} & 0 & 0 & 0 \\ & & & \frac{1}{G_{LR}} & 0 & 0 \\ & \textit{sym.} & & & \frac{1}{G_{LT}} & 0 \\ & & & & & \frac{1}{G_{RT}} \end{bmatrix} \tag{3.4}$$

Table 3.1: Elastic parameters for softwood from literature. Stiffness [MPa], density [kg/m^3] and Poisson's ratio at room temperature and a moisture content of 12%.

Species/Class	ref	E_L	E_R	E_T	G_{LR}	G_{LT}	G_{RT}	ρ
Norway spruce	[14]	9 040	790	340	640	580	30	400
Timber, C24	[35]	11 000	370	370	690	690		420
GLT, GL24h	[36]	11 500	300	300	650	650	65	420
Timber, C30	[35]	12 000	400	400	750	750		460
GLT, GL30h	[36]	13 600	300	300	650	650	65	480
		ν_{LR}	ν_{RL}	ν_{LT}	ν_{TL}	ν_{RT}	ν_{TR}	
Norway spruce	[14]	0.50	0.11	0.66	0.06	0.84	0.34	

The elastic parameters found in Equation 3.4 are material dependent and determined by tests. Comprehensive compilations for various wood species can be found in e.g. [31] and [34]. Dahl [14] presents in a recent study a comprehensive test program in order to identify the properties of Norway Spruce (*Picea Abies*), a species commonly used as timber in Sweden. His findings are presented in Table 3.1 along with mean stiffness values of some strength classes of timber as defined in EN 338:2016 [35] and GLT in EN 14080:2013 [36]. It can be seen that the European standards do not distinguish radial from tangential direction, thus taking one further step of simplifying the structure of wood to only parallel and perpendicular to grain, i.e. transverse isotropy. Neither Poisson's ratio is considered of interest in the standards. Dahl argues that some of the discrepancies between his results and the standard possibly is due to the fact that the material sample was partly ungraded, but the differences between clear wood and structural timber also affect the results.

Considering the height of a tree and wind action upon it, it is reasonable to expect a high stiffness parallel to grain. The elastic property which stands out is the very low rolling shear stiffness G_{RT}. This difference in stiffness causes some interesting phenomena, e.g. how a uniform load causes a considerable non-uniform stress distribution within the cross-section as seen in Figure 3.2 [37, 38]. The practical influence of the low rolling shear stiffness has previously been limited, but it does to a large extent affect the behaviour of the increasingly popular CLT panels subjected to varying bending as well as the connection design studied the thesis.

The linear elastic parameters presented above are valid only up to the limit of proportionality after which non-linear behaviour is typically found prior to failure as shown in Figure 3.3. However, the non-linearities of wood are often of limited influence in timber engineering, and thus often disregarded. Elasto-plastic material models can be suitable in compression parallel and perpendicular to grain, but the mechanisms are profoundly different from those in metal where elasto-plastic models are commonly used.

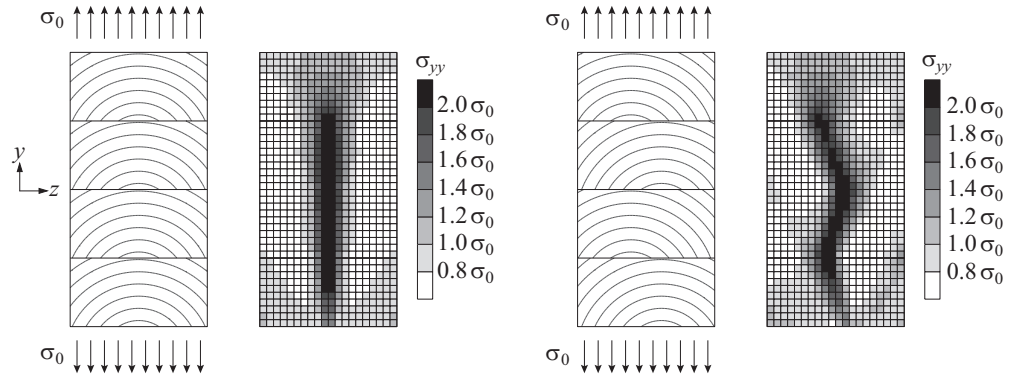

Figure 3.2: Although subjected to uniformly applied load σ_0, a GLT cross-section will experience a non-uniform stress distribution σ_{yy} due to different stiffnesses in different material directions. From Danielsson [39].

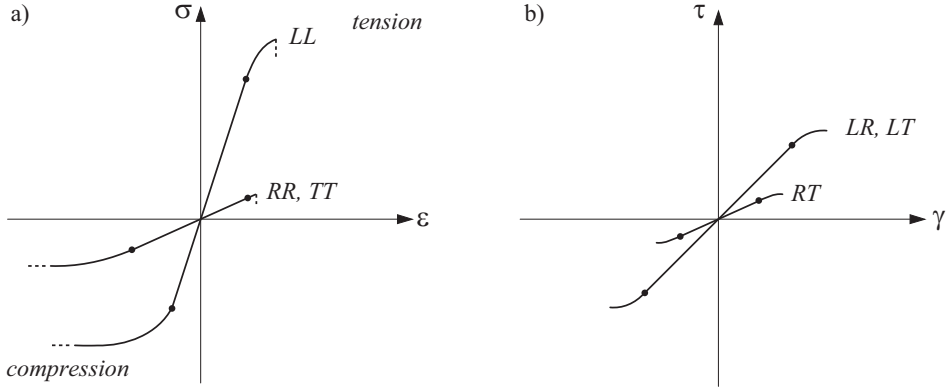

Figure 3.3: Schematic illustration of wood subjected to normal (a) and shear (b) action. The limits of proportionality are shown by dots. From Danielsson [39].

3.3 WOOD FAILURE

Like all structural materials, wood will eventually fail if subjected to increasing load. Similarly to the elastic properties, also the strength properties of wood are of orthotropic nature. However, distinction must now also be made between compressive and tensile action. As seen in Figure 3.3, failure typically occurs close to the limit of proportionality making wood a brittle material, in which excessive deformations seldom are experienced prior to failure. For timber, strength properties are typically expressed in terms of stress at failure, and determined by uniaxial tests. To evaluate combined stress states, different failure criteria can be used in order to evaluate the load-carrying capacity. Focus will here be put on stress-based failure criteria and fracture mechanics.

Table 3.2: Wood and timber strength properties [MPa] for spruce.

Species/Class	ref	f_{Lt}	f_{Lc}	f_{Rt}	f_{Rc}	f_{Tt}	f_{Tc}	f_{LR}	f_{LT}	f_{RT}
Norway spruce	[14]	63	29	4.9	3.6	2.8	3.8	6.1	4.4	1.6
Spruce	[41]	75	50	4.9	7.0			8.6		
Timber, C24	[35]	14.5	21	0.4	2.5	0.4	2.5	4.0	4.0	
GLT, GL24h	[36]	19.2	24	0.5	2.5	0.5	2.5	3.5	3.5	1.2
Timber, C30	[35]	19	24	0.4	2.7	0.4	2.7	4.0	4.0	
GLT, GL30h	[36]	24	30	0.5	2.5	0.5	2.5	3.5	3.5	1.2

3.3.1 Strength properties

Handbooks and standards in timber engineering commonly refer strength values as the lower 5^{th} percentile of the distribution of graded structural timber. For engineering purposes, such strength values are evaluated on test specimens large enough to include defects in order to represent actual structural elements. The resulting strengths should therefore be considered defined on element level rather than at a single material point level [40].

Tests of clear wood specimens are however also conducted. Comprehensive experimental studies have been conducted on clear wood by e.g. Dahl [14] and Eberhardsteiner [41], whose results are compiled in Table 3.2 along with the properties of structural timber and GLT according to EN 338:2016 [35] and EN 14080:2013 [36]. The strengths f_{ij} are defined in the principal directions $i = L, R, T$ in compression and tension $j = c, t$. Shear strengths are direction independent and all strengths are defined positive.

Among the parameters influencing the strength of wood, size effects can be somewhat counter-intuitive as larger specimens fail at lower average stress levels than smaller specimens [42]. It can however be explained using Weibull weakest link theory [43] due to the presence of defects, as the probability of a large weakness occurring in the most loaded section is higher for a large specimen than for a small. The theory assumes that the weaknesses are of random size and position within the element, and that the material is brittle [44]. These effects are typically included in building codes specifying timber characteristics, such as Eurocode [35, 36]. These effects are to a large extent however avoided in the small clear wood specimens, such as tested by Dahl [14] (see Table 3.2).

3.3.2 Failure criteria

In practical timber engineering, the performance of a component is commonly assessed by a linear elastic stress analysis with a stress-based failure criterion. It is a convenient approach which enables assessment of the strength also by analytical hand calculations. However, the method is typically used on a single point assuming that no stress redistribution occurs. Al-

though wood is brittle, the single point evaluation can result in too conservative predictions of load-carrying capacity if large stress gradients occur within the member. Predictions can be improved using several different techniques, such as using a non-linear material model, stress averaging over a certain area or analysing crack propagation.

Regardless of what method used, the combined state of stress must be evaluated by a failure criterion in each material point in order to asses a reasonable failure. Failure criteria typically look different for different materials, and three commonly used for timber are the maximum stress criterion, the Norris criteria [45] and the Tsai-Wu criterion [46].

Maximum stress criterion

The maximum stress criterion is a common and simple failure criterion used for both uni-axial and multiaxial stress states. The criterion assumes that a material can withstand each stress component in the LRT-system independent of the other stress components, i.e. does not consider stress interaction. As a single stress component reaches its strength, failure occurs according to Equation 3.5 as given for 3D analysis.

$$\max\left\{\frac{|\sigma_{LL}|}{f_{Li}}, \frac{|\sigma_{RR}|}{f_{Ri}}, \frac{|\sigma_{TT}|}{f_{Ti}}, \frac{|\tau_{LR}|}{f_{LR}}, \frac{|\tau_{LT}|}{f_{LT}}, \frac{|\tau_{RT}|}{f_{RT}}\right\} = 1 \tag{3.5}$$

The strengths with respect to normal stresses may have different values regarding compression or tension ($i = c, t$). If a material point experiences significant stresses in several directions, the maximum stress criterion is seldom an accurate description of material failure, and typically not conservative.

Norris criteria

Stress interaction can be achieved by means of the Norris criteria [45]. Instead of looking at a single stress ratio individually, a sum of several is used as shown in Equation 3.6 for the 3D case.

$$\max\left\{\begin{array}{l}\left(\frac{\sigma_{LL}}{f_{Li}}\right)^2 + \left(\frac{\sigma_{RR}}{f_{Ri}}\right)^2 + \left(\frac{\tau_{LR}}{f_{LR}}\right)^2 - \frac{\sigma_{LL}}{f_{Li}}\frac{\sigma_{RR}}{f_{Ri}} \\ \left(\frac{\sigma_{LL}}{f_{Li}}\right)^2 + \left(\frac{\sigma_{TT}}{f_{Ti}}\right)^2 + \left(\frac{\tau_{LT}}{f_{LT}}\right)^2 - \frac{\sigma_{LL}}{f_{Li}}\frac{\sigma_{TT}}{f_{Ti}} \\ \left(\frac{\sigma_{RR}}{f_{Ri}}\right)^2 + \left(\frac{\sigma_{TT}}{f_{Ti}}\right)^2 + \left(\frac{\tau_{RT}}{f_{RT}}\right)^2 - \frac{\sigma_{RR}}{f_{Ri}}\frac{\sigma_{TT}}{f_{Ti}}\end{array}\right\} = 1 \tag{3.6}$$

The Norris criteria are commonly used for timber. However, as tensile and compressive strengths differ, the criteria must be applied in a piece-wise manner. Each of the equations represents a closed surface in the respective stress space.

Tsai-Wu criterion

The stress interaction of the Norris criteria is often considered sufficient, but the piece-wise application of the criteria is sometimes undesirable. The Tsai-Wu criterion [46] uses matrix notation to form a more efficient failure criterion according to Equation 3.7, which also allows for different tensile and compressive strengths.

$$\bar{\boldsymbol{\sigma}}^T \bar{\mathbf{q}} + \bar{\boldsymbol{\sigma}}^T \bar{\mathbf{P}} \bar{\boldsymbol{\sigma}} = 1 \tag{3.7}$$

where $\bar{\boldsymbol{\sigma}}^T$ is defined in Equation 3.3. The stress interaction is obtained using the Tsai-Wu matrices $\bar{\mathbf{q}}$ and $\bar{\mathbf{P}}$ given by [14]

$$\bar{\mathbf{q}} = \begin{bmatrix} F_{LL} \\ F_{RR} \\ F_{TT} \\ 0 \\ 0 \\ 0 \end{bmatrix} \quad \text{and} \quad \bar{\mathbf{P}} = \begin{bmatrix} F_{LLLL} & F_{LLRR} & F_{LLTT} & 0 & 0 & 0 \\ & F_{RRRR} & F_{RRTT} & 0 & 0 & 0 \\ & & F_{TTTT} & 0 & 0 & 0 \\ & & & F_{LRLR} & 0 & 0 \\ & \textit{sym.} & & & F_{LTLT} & 0 \\ & & & & & F_{RTRT} \end{bmatrix} \tag{3.8}$$

Uniaxial tensile and compression strengths along with shear strengths are used to define the parameters F_{ii}, F_{iiii} and F_{ijij} according to

$$\begin{aligned} F_{ii} &= 1/f_{it} - 1/f_{ic} && i = L, R, T \\ F_{iiii} &= 1/\left(f_{it} f_{ic}\right) && i = L, R, T \\ F_{ijij} &= 1/f_{ij}^2 && i, j = L, R, T \, (i \neq j) \end{aligned} \tag{3.9}$$

The remaining strength interaction coefficients F_{iijj} must be determined by uniaxial off-axis or biaxial tests. The coefficients must satisfy Equation 3.10 in order to produce a closed and convex failure surface. The inequality is for example satisfied for $F_{iijj} = 0$ as F_{iiii} and F_{jjjj} are defined positive, which is a simplification often used. A special case in timber engineering is how the shear strength increases if simultaneously subjected to compression, which can be achieved by considering F_{iijj} [47].

$$F_{iiii} F_{jjjj} - F_{iijj}^2 \geq 0 \qquad i, j \quad = L, R, T \, (i \neq j) \tag{3.10}$$

The Tsai-Wu criterion presents an effective method to evaluate the combined state of stress in an orthotropic material. However, the main difficulty is to determine the strength interaction coefficients [48].

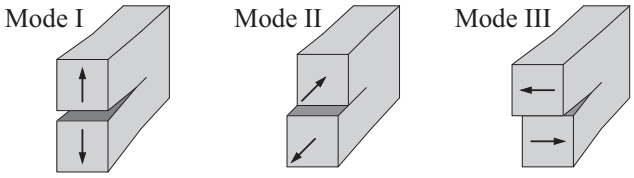

Figure 3.4: The three fundamental modes of fracture deformation. From Danielsson [39].

3.3.3 Fracture mechanics

A stress-based failure criterion is a powerful tool to evaluate the load-carrying capacity of structures. However, the typical use of such failure criteria does not consider cracks, which are very common in timber failures. For many timber engineering applications, the crack propagation is of little concern for the typical load-carrying capacity analysis. However, it will be shown that for the type of connection investigated in the thesis, the fracture properties are of great interest.

Fracture mechanics is the branch of solid mechanics which studies structural failure due to separation of material, i.e. the formation and propagation of cracks. The microscopic mechanisms which govern the separation and predictions from a macroscopic point of view are both topics of interest in order to predict the load-carrying capacity of structural members. [49]

There are only three basic modes of relative displacement in the vicinity of a crack, which are illustrated in Figure 3.4: the opening mode I, the in-plane shear mode II, and the out-of-plane mode III. It is in practical applications common that load causes a mixed mode displacement for which fracture occurs in mixed mode. The combination of mode I and II is most common, which is also the case for the problems studied in the thesis.

The orthotropic nature of wood complicates the discussion of crack orientations, as six possible orientations of plane cracks are made possible as shown in Figure 3.5. The nomenclature is such that the first index indicates the direction normal to the crack plane, while the second indicates the straightforward direction of the crack length extension. Combined with the three fracture modes in Figure 3.4, this will sum up to 18 different basic fracture situations. In general, wood will typically show a different resistance to each such basic fracture situation [50]. For example, the high tensile strength in the longitudinal direction will result in high resistance to mode I crack growth for LR and LT orientations.

Fracture resistance can be defined by material stiffness and the fracture energy G_f. G_f is defined as the energy required to bring a unit area of the material from unloaded state to complete fracture. In case of pure shear, the mathematical definition is found in Equation 3.11.

$$G_f = \int_0^\infty \tau \ \mathrm{d}\delta \tag{3.11}$$

where δ is the crack opening deformation. It should be noted that the fracture energy G_f in

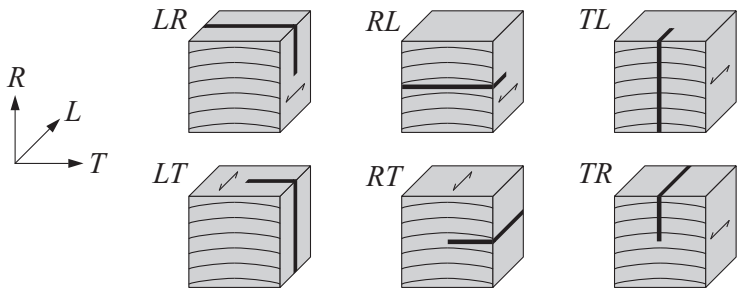

Figure 3.5: Crack plane orientation relative to the LRT directions. From Danielsson [39].

general differs from the critical energy release rate G_c. While G_f refers to a single material point during fracture, G_c represents the energy dissipated at the distinct tip of a progressing sharp crack. However, in the case of a material with a small fracture process region in relation to other dimensions, G_f and G_c are the same.

Various test setups can be used to determine the fracture energy of wood, also dependent on what crack mode is of interest. Commonly used for mode I is the single edge notched beam design (SENB), whereas small-scale notched specimen can be used for both mode I and II. A compilation of results found in literature is shown in Table 3.3 for spruce and pine. The fracture surface orientation is in the table given by the direction of the surface normal. The material directions for mode II test results are oriented so that the crack planes were exposed to longitudinal shear, i.e. τ_{RL} for crack plane orientation R and τ_{TL} for crack plane orientation T. Of special interest in the thesis is mode II in tangential direction for Norway spruce as it is the dominating orientation in GLT lap joints.

Table 3.3: Fracture properties for spruce and pine found in literature. Density ρ in kg/m³, moisture content u in percent, fracture energy G_f in J/m² and material strength f in MPa.

Mode I				Orientation R		Orientation T	
Species	ref.	ρ	u	$G_{f,RR}$	f_{Rt}	$G_{f,TT}$	f_{Tt}
Scots pine	[51]	450	8	450	5.3	550	4.1
Scots pine	[51]	470	10	445	5.0	500	4.2
Scots pine	[51]	470	13	535	4.5	460	4.0
Scots pine	[51]	460	26	515	4.1		
Norway spruce	[52]	463	13			298	3.3
Mode II				Orientation R		Orientation T	
Species	ref.	ρ	u	$G_{f,RL}$	f_{LR}	$G_{f,TL}$	f_{LT}
Scots pine	[51]	460	13	815	11		
Norway spruce	[52]	463	13			965	8.4
Norway spruce	[53]		14			1240	9.8

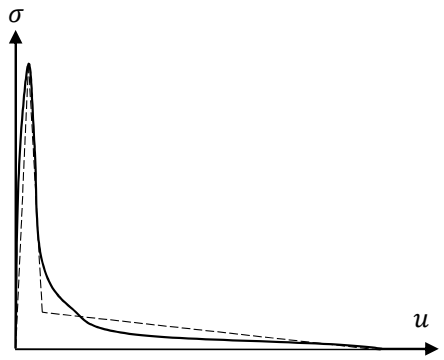

Figure 3.6: A schematic σ–u curve of wood in tension perpendicular to grain with a typical bilinear approximation. The curve is obtained by a displacement-controlled tensile test.

Traditional fracture mechanics considers the effect of pre-existing cracks, often under the assumption that cracks of limited size are always present in materials due to e.g. manufacturing methods or material behaviour. Intense research in the traditional linear elastic fracture mechanics (LEFM) was conducted during mid-20th century due to its application on vehicles, ships and aircraft.

Later developments in the field distinguish from LEFM by the possibility to regard material non-linearity outside the crack tip, the limited stress capacity and/or the non-linear stress-deformation performance of the material at the crack tip. This can be achieved using various approaches, of which a more direct one is done by characterisation of fracture properties of the material by a stress-deformation relation which includes material softening, here denoted a σ–u curve.

The σ–ε curve shows the properties of the material outside the fracture region while the σ–u curve shows the properties within. As crack opening does yield deformations without arising stresses, relevant measures must include certain material length, e.g. a finite thickness. By including such model in a finite element analysis, it is possible to calculate how the fracture process region initiates and propagates as the external action is increased. A schematic σ–u curve of wood is shown in Figure 3.6, plotted alongside a typical bilinear approximation.

It is shown in Chapter 4 how this type of non-linear fracture mechanics (NLFM) analysis is vital for an accurate determination of timber lap joints using conventional adhesives.

3.4 NUMERICAL ANALYSIS

The work presented in the thesis is to a large extent based upon numerical analysis by means of the FE method. The mechanics of wood presented in this chapter is incorporated in the

analysis procedure using the general-purpose FE software Abaqus [54].

The method of implementation varies slightly between the different aspects of this work, and details are presented in the appended papers. The timber has typically been modelled as a rectilinear linear elastic material with a deterministic stress-based failure criterion, but also stochastic analyses have been conducted. The detailed implementation of the failure criteria varies, but a great effort has been put into experimental verification which will be evident in the following Chapters 4 and 5.

4
The resilient bond line

The scientific contribution of the thesis is presented in the following two chapters, starting here by research conducted on a type of adhesive bond line with low shear stiffness yet high fracture energy, within the thesis denoted a resilient bond line. The resilient bond line is compared to conventional non-resilient bond lines in a lap joint configuration shown in Figure 4.1. The chapter is based upon Papers A and C, combining experimental and numerical work.

4.1 BACKGROUND

While studying the Volkersen theory [5] regarding the shear stress distribution of lap joints, Gustafsson [3] found that the fracture energy rather than shear strength in terms of maximum stress is decisive for the load carrying capacity. He also found that a relevant measure of the fracture energy of the bond line is found by including the elastic part of the stress vs. deformation response. A schematic response curve is shown in Figure 3.6, which also is valid for shear stresses associated with lap joints.

As common adhesives are very stiff, elastic part of the stress–deformation response is usually of very limited size. However, the elastic part can be made considerably larger using a bond line with low shear stiffness, which would then increase the load carrying capacity of lap joints. Such a bond line, with low shear stiffness yet high fracture energy, is in the thesis denoted a resilient bond line. To lower the stiffness of the bond line, a rubber layer can be introduced as schematically shown in Figure 4.1, or by introducing an adhesive of low stiffness.

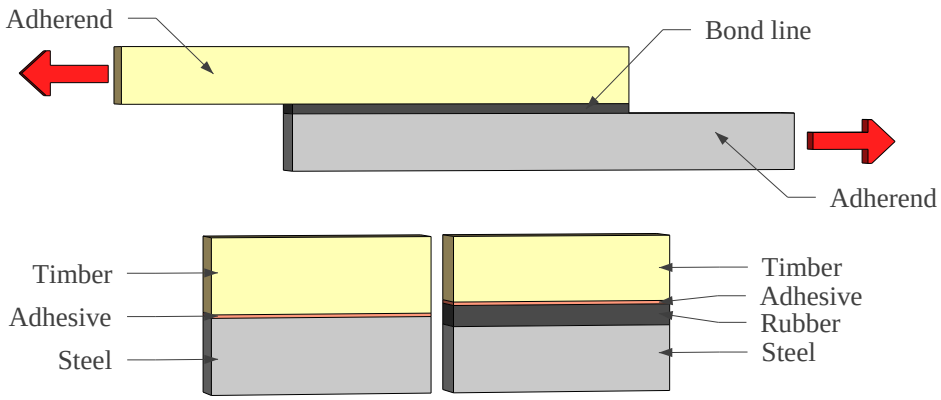

Figure 4.1: The nomenclature of a single lap joint and the schematics of non-resilient bond line using a conventional stiff adhesive (left) and resilient bond line using a material of low shear stiffness yet high fracture energy, here by introducing a rubber layer (right).

The effect of a resilient bond line can also be discussed in terms of shear stress distribution over the lap length. Common adhesives typically have a high stiffness which do not allow the axial strains of the adherends to act independently. This causes shear stress concentrations at the ends of the joint as shown in blue in Figure 4.2. The material strength is reached at a low external load, and fracture is thus initiated prematurely. By having a low stiffness, the resilient bond line enables different axial strains of the adherends, resulting in a close to uniform shear stress distribution over the joint area. Figure 4.2 is based upon numerical results at maximum load carrying capacity, where softening is considered for the non-resilient bond line. As the area under the respective curves represent the total applied load, it is clear that the resilient bond line has a much higher load carrying capacity. The shear stress distribution of the resilient bond line can also be determined, with good agreement, using the Volkersen theory [5] shown as Equation 4.1.

$$\tau_3(x) = C_1 \cosh(\omega x) + C_2 \sinh(\omega x) \tag{4.1}$$

The constants C_1 and C_2 depend on boundary conditions. For the studied compression-compression case, the constants can be determined according to Equation 4.2 [55]. The shear stress distribution of the bond line (index 3) is thus governed by the properties of the two adherends (indices 1 and 2) and the bond line properties: cross-sectional area A, longitudinal stiffness E, bond line length L, width b_3, thickness t_3 and shear stiffness G_3.

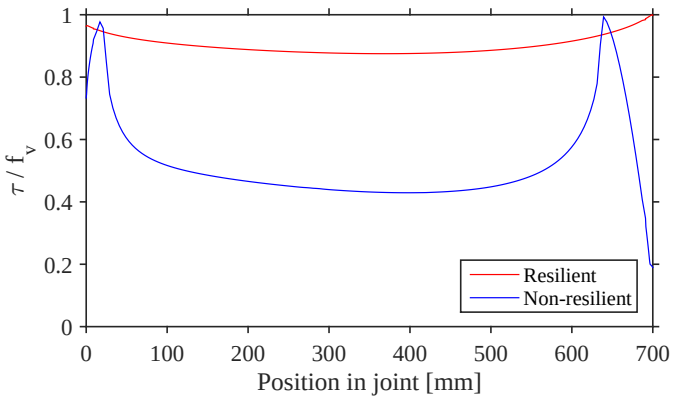

Figure 4.2: A comparison of the shear stress distribution in a common non-resilient bond line and in a resilient bond line at failure by numerical analysis. Bilinear softening is used in the FE model. Geometry and loading are shown in Figure 4.4, using a lap length of 700 mm.

$$C_1 = \frac{PG_3}{t_3\omega}\left(\frac{1}{E_1A_1\tanh(\omega L)} + \frac{1}{E_2A_2\sinh(\omega L)}\right)$$
$$C_2 = \frac{PG_3}{t_3\omega}\left(\frac{-1}{E_1A_1}\right) \tag{4.2}$$

$$\omega L = L\sqrt{\frac{G_3b_3(1+\alpha)}{t_3E_1A_1}} \qquad \alpha = \frac{E_1A_1}{E_2A_2} < 1.0 \tag{4.3}$$

Studies of resilient bond lines are found in several publications [4,56,57], typically using a 1 mm thick rubber foil to promote the low shear stiffness needed. The stiffness of a lap joint with resilient bond line is similar to a conventional nailed joint, although the resilient bond line shows an elastic behaviour up to large loads unlike the plastic behaviour of nailed joints due to yielding. In the comprehensive test series conducted by Gustafsson [4] it is shown, among other things, that the resilient bond line can be used to create interaction between dowel-type fasteners and adhesive, since the two components have similar shear stiffnesses.

4.2 NUMERICAL MODELLING OF BOND LINES

Numerical studies have been used in order to investigate the differences in terms of load capacity and stiffness between resilient and non-resilient bond lines, such as presented in Figure 4.2. Due to the different characteristics of the bond line, two different numerical models have been used.

4.2.1 Non-resilient bond lines

Conventional bond lines used in timber engineering are made using stiff structural adhesives. The high stiffness causes stress concentrations where fracture is initiated, and the importance of the material softening behaviour for the total load carrying capacity has been shown in several studies [58, 59] and Paper C. NLFM is thus needed, and a bilinear softening behaviour is typically used in the thesis as presented in Section 3.3.3, in combination with a linear elastic material response of the adherends for which a stress based failure criterion is to be fulfilled. A continuum-based modelling of the adhesive layer can be obtained using cohesive elements in which the adhesive has a finite thickness.

4.2.2 The resilient bond line

The resilient bond line, as defined in the thesis, is made of elastomeric materials, typically rubber. The main specific property of those materials is the ability to sustain large straining without permanent deformation [60]. From a modelling point of view, rubber is a hyperelastic material characterised by low and non-linear elastic stiffness and a high Poisson's ratio, see Figure 4.3.

In order to model rubber numerically, hyperelastic models are typically based upon the assumption of isotropic behaviour throughout deformation history and thus being able to de-

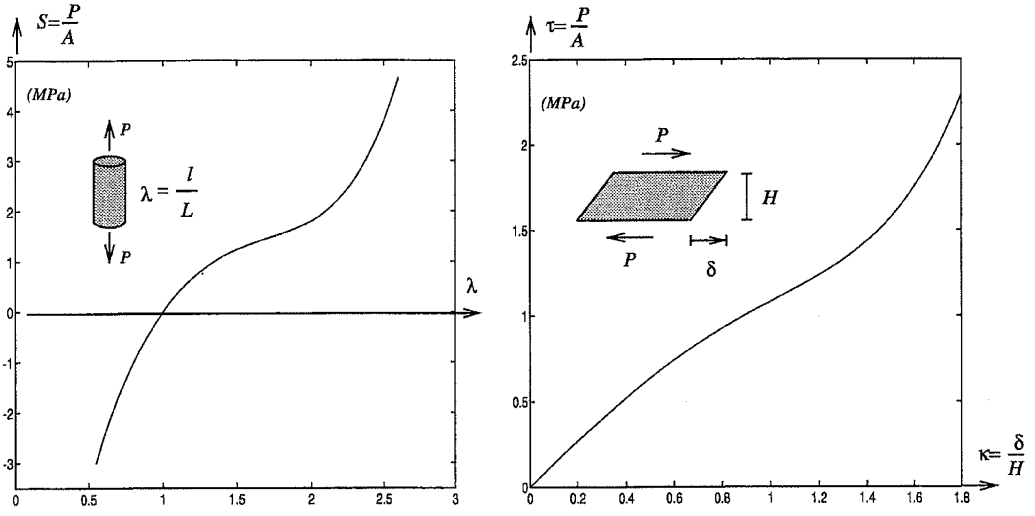

Figure 4.3: Typical non-linear elastic behaviour of rubber subjected to normal stresses (left) and in shear stresses (right). l is the deformed length while L is the undeformed, together defining the stretch λ. From Austrell [60].

scribe the material model in terms of strain energy potentials [54]. Typical forms of strain energy potentials used for rubber are the polynomial Yeoh and neo-Hookean forms, for which the specific coefficients for a resilient bond line is presented in Paper E and by Danielsson and Björnsson [61]. Non-linear geometry and special finite elements must be used in order to obtain reasonable numerical results. More comprehensive reading on the mechanical properties of rubber can be found in e.g. [62].

As seen in Figure 4.3, rubber can be modelled as linear elastic in shear with reasonable accuracy. This is often desirable in order to minimize the computational cost of an analysis. Paper C shows that this is indeed possible for the shear plate dowel joint with reasonable accuracy, if special consideration is made to the high normal stiffness shown by rubber in plane strain conditions. The simulation procedure presented in Paper C is used in Paper A.

4.3 COMPARATIVE STUDY OF DOUBLE LAP JOINTS

The study of double lap joints, published in Paper A, was intended as an experimental verification of the close to uniform shear stress distribution shown by analytical and numerical calculations, especially for long lap joints. A test series with dominant shear action was conducted in order to investigate the increase in load-carrying capacity made possible by the uniform stress distribution. The geometry of the double lap joint is presented in Figure 4.4, where a constant cross-section where used for the various overlap lengths. The lap width was 225 mm, while the width of the GLT elements were 230 mm and 280 mm for the outer and centre members respectively. Three different lap lengths of 200, 400 and 700 mm were used in a comparative study between resilient and non-resilient bond lines. Independent numerical and analytical analyses were conducted using material properties found in literature, with total load carrying capacity and stiffness as the main characteristics investigated.

A comparison in terms of a numerical study of the shear stress distribution at failure of the two bond line types is shown in Figure 4.2. The shear stress distribution is also shown in Figure 4.5, where non-resilient bond line (b) has been loaded until failure at 720 kN assuming a shear strength of 4.4 MPa. The propagating crack tip is visible as a stress concentration which has propagated from the top and downwards. The same load is applied to the resilient specimen (a) for which a more uniform stress distribution is found, with lower maximum stresses as a result.

The load-carrying capacity of the lap joints were evaluated for increasing lap length by means of the analytical Volkersen theory, numerical FE simulations and full scale tests as presented in Figure 4.6. The Volkersen theory [5, 55] considers a linear elastic shear action without bending of the adherends. The effect of the linear material model, which does not include material softening, is visible in Figure 4.6 as the large difference in predicted load carrying capacity of the non-resilient bond line between the analytical Volkersen prediction and the numerical results. Although dramatically improved accuracy for the resilient bond line, the limitation of no bending is shown to affect the prediction of shorter lap joints.

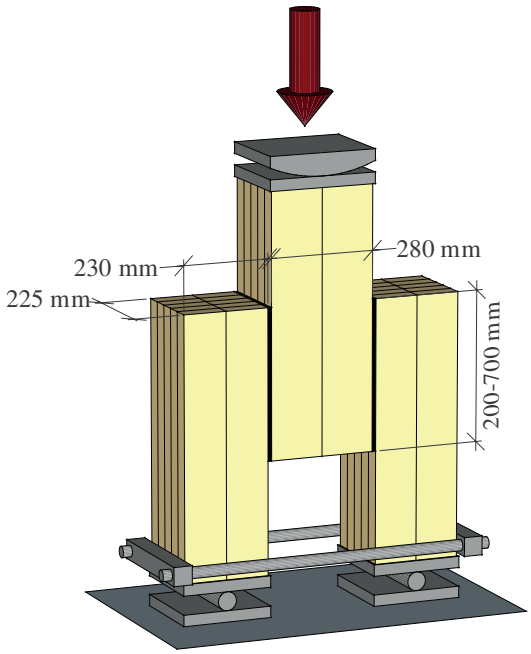

Figure 4.4: Double lap joint design used in the experimentally and numerically comparative study between resilient and non-resilient bond lines.

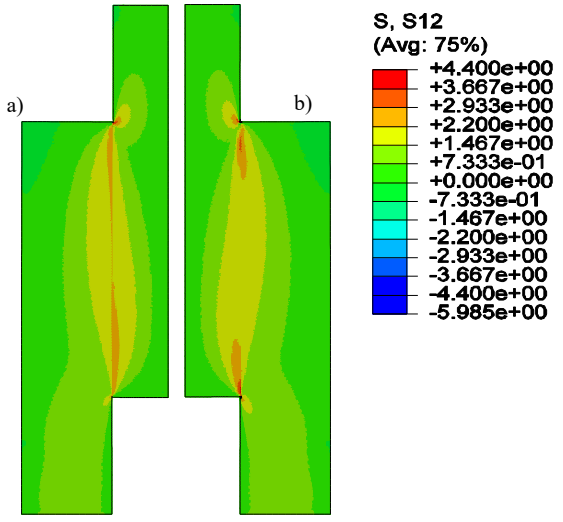

Figure 4.5: A comparison between the resilient (a) and non-resilient bond line (b) in terms of shear stress distribution in a 700 mm lap length. The non-resilient bond line is loaded to failure at 720 kN and corresponding load is applied to the non-resilient specimen.

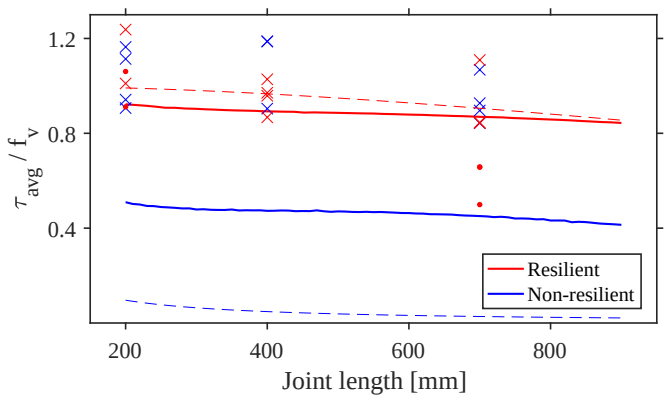

Figure 4.6: Numerical results (lines) of experimental setup compared to experimental data (markers). Wood failure close to the bond line is marked with × while dots mark premature adhesion failures. The solid lines are numerical FE results while the dashed lines are analytical results according to Volkersen theory, using shear strength $f_v = 4.4$ MPa.

A reasonable resemblance between the numerical, analytical and experimental results are found for the resilient bond line. Although considering the softening behaviour with material data presented in literature, little resemblance is found between the numerical model of the non-resilient bond line and the test results. The experimental study indicates similar load carrying capacities for resilient and non-resilient bond lines, which is not in agreement with numerical findings nor previously presented results [4] and Paper B. It is reasonable to assume that several influencing factors have led to the increase in load-carrying capacity, among which the influence of boundary conditions is deemed most influential. Other factors comprise a possible underestimation of the fracture energy, influence of the softening behaviour and size effects. This is further discussed in Paper A.

4.4 DISCUSSION

In terms of structural performance, load-carrying capacity and stiffness are of high interest. Load-carrying capacity is the fundamental property of a connection as to be able to withstand the forces occurring in a structure. However, the forces occurring are typically dependent on the stiffness of the connections, as the load is transferred by the stiffest load path possible. Thus, in order to have control over the actual load path, the stiffness of the connections must be known. An even greater degree of control can be obtained if the stiffness of the connections can be designed. The results indicate that a resilient bond line can increase the load-carrying capacity of long lap joints in comparison to non-resilient bond lines, and allowing the joint stiffness to be designed to specifications.

Table 4.1: Results of bond lines presented in Paper A. Mean load-carrying capacity [kN], mean average shear stress at failure [MPa] and mean stiffness [kN/mm] of 700 mm double lap joints of the four resilient bond lines and a reference of a conventional stiff adhesive (PUR). t is the bond line thickness [mm].

Type	t	Load capacity	Stress	Stiffness
SBR/NR	3.5	1290[1,2]	4.1	190
CR	0.5	360[3]	1.2	720
IT	2.0	760[3]	2.4	270
CO	1.5	730[3]	2.3	260
PUR	-	1290[2]	4.1	5470

1) Premature failure specimens excluded.

2) Failure in wood close to bond line.

3) Bond line failure in the adhesive/wood interface.

A great variability in rubber properties can be obtained using different fillers during the production, and also several different types of rubbers are produced. In terms of properties relevant for structural applications, the different products vary in e.g. durability, creep, usable temperature ranges, strength and stiffness. Not only can the elastic properties of the material be varied using fillers, but the thickness of the rubber included in the bond line can be chosen in a lap joint design. This combination enables a vast range of possible effective stiffnesses, which can enable interaction in terms of load-carrying capacity between a resilient bond line and e.g. dowel-type connections.

Tests of four types of resilient bond lines are presented in Paper A and the results are summarized in Table 4.1. Two rubbers were tested: A mixture of natural rubber (NR), styrene-butadiene rubber (SBR) and chloroprene rubber (CR). In addition, two elastomeric adhesives were also tested: SikaTack Move IT (IT) and Collano RESA HLP-H (CO). Although CR was found unsuitable for the application due to low load-carrying capacity, the thinner bond line used increases the connection stiffness as shown in Figure 4.7. The tested resilient bond lines are plotted in colour, where the great variability in stiffness can be seen. Slip curves of different types of connectors will typically never be identical, but an interaction in terms of load-carrying capacity can theoretically be obtained if the different types are active in the same slip region.

Paper A also discusses the importance of the correct rubber treatment needed to adhere rubber to wood using conventional adhesives, which includes submerging the rubber in concentrated sulfuric acid. The study shows an increase in terms of load-carrying capacity of the rubber-adhesive interface by 60 times when comparing no treatment to the one used. In terms of load carrying capacity of a joint, correct rubber treatment is thus vital for the structural integrity. This sensitivity is a clear potential drawback of the technique, but can possibly be eliminated by developing a standardized treatment procedure with simple inspection techniques as partly

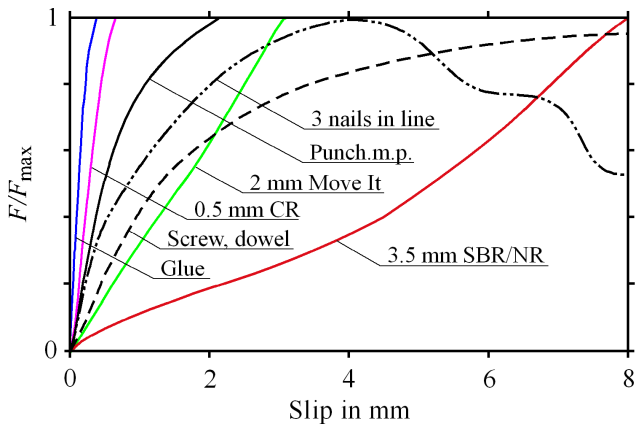

Figure 4.7: Slip comparison between common connectors and the resilient bond line.

suggested in Paper A. The production method used during the experimental work presented in the thesis is specified in Appendix A. The use of concentrated sulfuric acid over diluted is of special importance if the rubber is vulcanized to steel, as the high concentration will actually prevent steel corrosion [63].

Resilient bond lines can typically be used whenever a conventional non-resilient bond line can be used. However, a higher production cost and lower stiffness is not suitable for all applications. Continuous bond lines in structural elements such as GLT and CLT are best made by a non-resilient bond line for common uses. The resilient bond line is typically advantageous in applications when large forces are to be transferred in relatively small areas, such as in connections. The bond line can also be used to increase deformation capacity in elements when resistance to dynamic loads and/or impact loads is needed.

The double lap joint is not common in modern timber engineering. It can be used to splice timber elements lengthwise, but GLT can today be produced in large lengths thus minimizing material use and improving design aspects, although length is typically limited by transportation possibilities and production facilities. However, the key concept of this study is not the double lap joint itself, but rather the resilient bond line which is further used in the shear plate dowel joint presented in Chapter 5.

5 The shear plate dowel joint

The aim of this project is to develop a novel connection for heavy timber structures suitable for a high degree of prefabrication. In Section 2.4, the slotted-in steel plate connection was identified as a contemporary timber connection often used in modern heavy structures. However, this type of connection necessitates a large number of high precision dowels which in turn requires extensive production time. When designing a new heavy timber connection, it is not far-fetched trying to reduce the number of fasteners to a minimum. The challenges of reducing the number of dowels to a single one are discussed in this chapter, after which the shear plate dowel joint is presented and evaluated in terms of functional requirements.

5.1 REINFORCEMENT OF A SINGLE DOWEL

In order to reduce the number of fasteners, one must consider the brittle nature of wood which often limits the load-carrying capacity of the connection due to premature splitting. Typically found in building codes today are minimum distances from dowels to member edges and between different dowels [19]. These distances are used to reduce the risk of premature splitting in the connection, which typically occurs due to the wedge action at the contact area between the dowel and timber, causing tensile stresses perpendicular to grain. It is not uncommon that these geometrical restrictions are the parameters that govern the cross-sectional dimension of the timber members. This subsequently reduces the utilization factor of the member in span and thus causes excessive material use.

One of these geometrical restrictions is the dowel to member end distance which should ex-

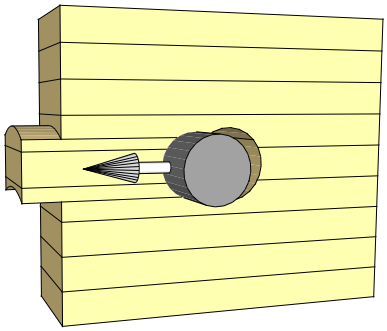

Figure 5.1: Typical plug shear failure when using a large diameter dowel without reinforcement.

ceed $7d$ according to Eurocode, were d is the dowel diameter. This recommendation is given in order to avoid splitting, and based upon the earliest documented experiments on timber bolted connections [64]. A considerable amount of research effort has since been put into this behaviour, with noticeable contributions by Johansen and Jorissen [16,17], typically on smaller dowels.

Compared to the large number of dowels needed in slotted-in steel plate connections, a highly efficient on-site production would be obtained if a single dowel could be used. However, the considerably larger dowel required in a single fastener design is instead prone to plug shear failure as shown in Figure 5.1. With a single large diameter dowel as the only fastener in the connection, the $7d$ end distance would result in bulky and unpractical nodes. Several studies have aimed at minimizing the required distance between mechanical fasteners and member end by e.g. self-tapping screws [65] and fibre textiles [66, 67], but also for a single large diameter dowel using different types of reinforcements [68].

Assuming that the production efficiency of a single dowel joint design is worth investigating as a competitor to slotted-in steel plates, several different reinforcement designs are possible in order to avoid the brittle shear plug failure. Some small-scale experimental tests were conducted by Crocetti et al. [6], which led to two individual full-scale test series conducted by Kobel [7] and Yang et al. The latter study was conducted at College of Civil Engineering at Nanjing Tech University, China, and is included as Paper B in the thesis. The two full-scale test series were conducted in a manner in which direct comparison is made possible. Some of the tested joints from this combined effort are illustrated in Figure 5.2, where it should be noted that all specimens have the same dimensions of GLT and dowel, but different reinforcement techniques.

The results are compiled in Table 5.1 using a GLT cross-section of 405×140 mm^2 and a dowel diameter of 90 mm. The dowel was located at an end distance of $3.5d$, which is half of the recommended distance according to Eurocode 5 [19]. The reference case without any reinforcement is found having an average load-carrying capacity of approximately 130 kN, at which point a shear plug failure occurred. An increased load-carrying capacity was found using all

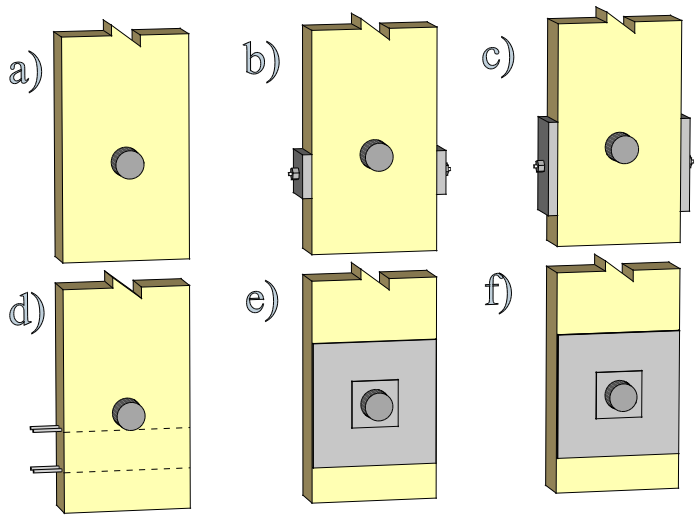

Figure 5.2: Different reinforcement techniques tested for single large dowel joints in Paper B and [7], using a GLT cross-section of 405×140 mm² and a dowel diameter of 90 mm. a) Non-reinforced reference, b) single rod, c) prestressed rod, d) 4 screws, e) glued steel plate and f) glued steel plate using a resilient bond line.

reinforcement techniques, but often with questionable results in comparison to production time and competing heavy timber connections. While the steel plate joint with a conventional stiff adhesive bond line showed a premature failure at 220 kN in the steel-adhesive interface, the steel plate with a resilient bond line outperformed all other reinforcement types by a vast margin at an average load-carrying capacity of 990 kN. The failure load indicates an average shear stress at failure of 3.3 MPa for the plate with dimensions 400×400 mm², considering the oversized timber hole of 102 mm in diameter.

Table 5.1: Average experimental load-carrying capacity and stiffness of the single dowel designs shown in Figure 5.2.

Specimen	Capacity [kN]	Stiffness [kN/mm]
a) No reinforcement[1]	134	308
b) Rod	195	-
c) Rod, prestressed	298	-
d) Screws[1]	237	336
e) Glued steel plate joint[2]	220	-
f) SPDJ 400×400–90	990	484

1) From [7]

2) Premature failure in steel-adhesive interface

The experimental results provided enough confidence of the glued steel plate with a resilient bond line to continue the investigation. The name that was assigned to this particular type of solution is the shear plate dowel joint.

5.2 THE SHEAR PLATE DOWEL JOINT DESIGN

The SPDJ consists of only four components: the timber element, the steel plate, the dowel and the bond line. The joint is shown in an exploded view in Figure 5.3, where the bond line is divided into an adhesive layer and a rubber foil. Although simple in terms of components, there are some key design aspects in order to optimize the performance.

The dowel must be strong enough to enable forces to be transferred from one element to another. Furthermore, it must be placed in such way that direct contact between the dowel and timber element is prevented, in order to reduce the risk of shear plug failure. This is achieved by using a larger hole in the timber than in the steel shear plate and thus all load applied to the connection is transferred to the timber element in shear over the plate area, rather than by contact between the dowel and the timber.

The shear plates are bonded to the timber element using a resilient bond line. The testing of lap joints presented in Paper A suggested that a resilient bond line using rubber sheeting was strongest. The rubber can be vulcanized directly onto the steel plate with sufficient strength. The steel plate with rubber is then bonded to the timber element using a conventional stiff adhesive, by strictly following the procedure found in Appendix A. The introduction of the

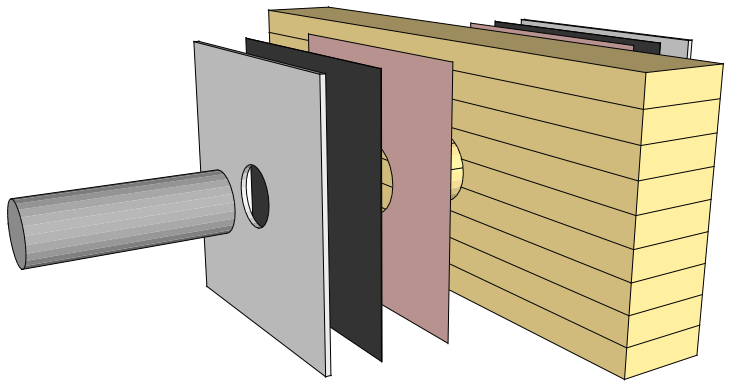

Figure 5.3: Exploded view of the SPDJ. From left: A single steel dowel; steel plate with hole size matching the dowel; rubber foil vulcanized to the steel plate; structural adhesive and then the GLT member with oversized hole to ensure no direct contact between dowel and timber.

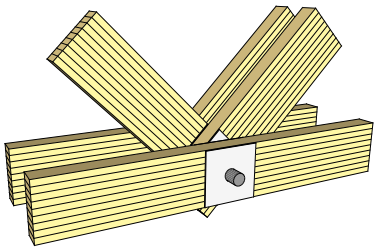

(a) Stacking truss node.

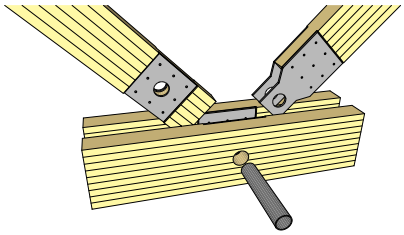

(b) Reduced truss node, see Section 5.3.5.

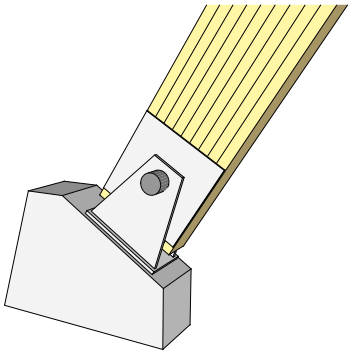

(c) Arch springing.

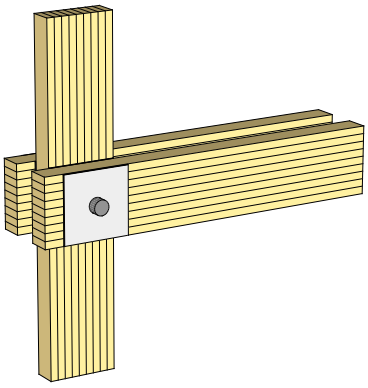

(d) Beam-column connection.

Figure 5.4: Possible uses of the shear plate dowel joint.

rubber not only enables a stronger connection, but also enables the possibility of designing the connection stiffness by choosing a rubber foil with adequate thickness and/or shear stiffness.

This combination of external plate and a single dowel is the basis for the shear plate dowel joint. In order to specify the geometry in text, the nomenclature 400×400–90 is introduced, denoting a shear plate size of 400×400 mm² with a 90 mm dowel. Four possible uses of the SPDJ are presented in Figure 5.4.

Typically, new design concepts introduce uncertainties and possible weaknesses. Therefore, a great effort has been put in this investigation to identify and analyse possible risks related to the design of the SPDJ, which is presented next. A summary in terms of the functional requirements is presented in Section 5.4.

5.3 INVESTIGATED DESIGN ASPECTS

The design of the shear plate dowel joint introduces new possibilities as well as difficulties. In this section, design aspects included in the conducted research are discussed in relation to the global behaviour of the connection.

5.3.1 Stresses over the bond line

It is shown in Chapter 4 how the resilient bond line enables a close to uniform shear stress distribution over long lap joints. However, the SPDJ is not a conventional lap joint between timber and steel elements due to the hole and interaction with the dowel. Furthermore, the limited size of the steel plates does not necessarily make it possible to neglect bending due to eccentricity.

The eccentricity in question is the distance between the steel plate on which the load is applied to the member, and the line of action within the timber member. The eccentricity causes bending of the plate, and of special concern is peel stresses which occur close to the plate perimeter. However, more prominent peel stresses are caused by the interaction between the dowel and the plate.

Typical distributions of shear and normal stresses perpendicular to the bond line within the SPDJ are shown in Figure 5.5. Shear stresses are shown in (a) where some stress concentration occur where the load is applied. Normal stresses are shown in (b), where peel stresses are shown in red. Fortunately, the location of the maximum peel stress do not coincide with the location of the maximum shear stress, which is the dominant stress component.

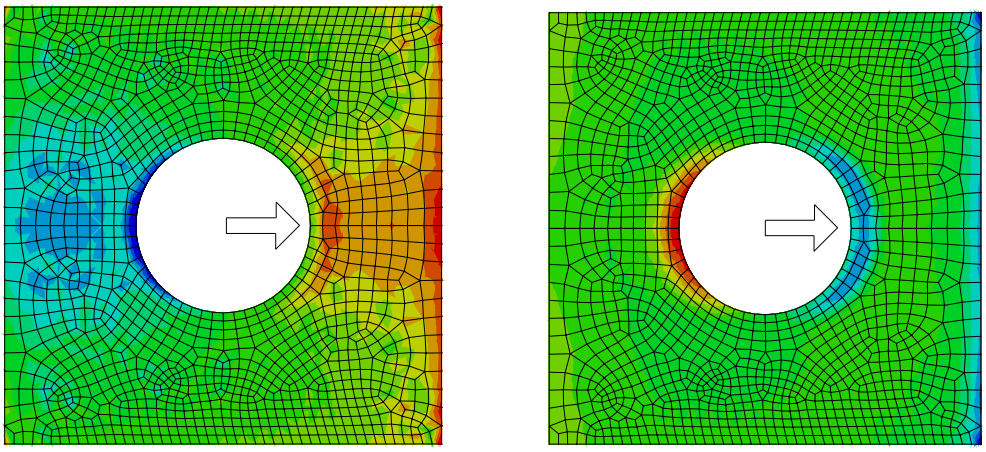

(a) Shear stress distribution. Colour limits are 3.5 MPa (blue) and 6.5 MPa (red). Green represents a stress of 5 MPa.

(b) Distribution of normal stresses perpendicular to grain. Colour limits are –6 MPa (blue) and 6 MPa (red, peel stress). Green represents zero stress.

Figure 5.5: Typical distribution of dominant stresses of the SPDJ bond line, shown here is a SPDJ 200×200–70. The load is applied in rightward direction, and stresses are shown at ultimate load as predicted by Weibull theory to 360 kN. Further reading in Paper E.

5.3.2 Stiffness of the bond line

Slip and large deformations in connections are typically undesired in structures. By using adhesives, the initial slip is reduced to a minimum. However, introducing a low stiffness material in the load path, such as rubber, does increase the deformations of the connection. The shear stiffness of the rubber layer and its thickness are of vital importance in determining the global stiffness of the connection. It has been shown that the SPDJ connection can in fact be designed stiffer than a common dowel or nailed joint [4].

In order to quantify the connection stiffness, a parameter study was conducted in Paper D. The resilient bond line in the SPDJ consists of a rubber layer with governing shear loads. In such a case, the stiffness of the bond line is dependent of the stiffness and thickness of the bond line material. The force–displacement curve has a fairly linear behaviour for rubber loaded in shear, and it typically varies in the range of 0.35–2.75 MPa (35–80° Shore A) [69]. In addition to this relatively wide range, the thickness can be chosen typically from 0.5–30 mm. By combining these two variables, the stiffness of the SPDJ can actually be designed to meet specific requirements, a possibility that is rather uncommon in other connection types. The basic concept is explained and to some extent studied in Section 4.4 and Paper A. The stiffness of the joint can be designed varying the rubber hardness and thickness with only a small influence on the load-carrying capacity. Decreasing bond line stiffness leads to a small increase of the load-carrying capacity of the connection, c.f. Paper D.

A rubber sheeting of stiffness 1.1–1.2 MPa (60–61° Shore A) and thickness of 1.0–1.1 mm has been used for the experimental studies of the SPDJ in the thesis, which results in a stiffness comparable to dowel joints used in timber structures today.

5.3.3 The shape of the shear plate

As discussed in Chapter 4, the key aspect of the resilient bond line is that a close to uniform shear stress distribution can be obtained over the bonded area. A perfectly uniform stress distribution would render the possibility to adopt an arbitrary plate shape without affecting the load-carrying capacity. However, this is not the case as a perfectly uniform shear stress distribution is not obtained, but also since the interaction of peel stresses must be considered (see Section 5.3.1). It is thus of interest to investigate the shape of the steel plate reinforcement.

Shear stress distribution over the bonded area can be theoretically determined using the Volkersen theory, as discussed in Section 4.1 and Paper C. Although a fairly uniform shear stress distribution is found for resilient bond lines, slightly higher shear stresses occur at the plate edges in the direction of the load. On the contrary, the theory predicts that the load-carrying capacity of a lap joint is directly proportional to the width of the bond line. It is thus favourable to choose a wide plate, possibly close to the width of the timber element.

The stress concentrations around the hole can be minimized by reducing the bonded area in the vicinity of the hole in direction of the load as shown in Figure 5.6. The results found in

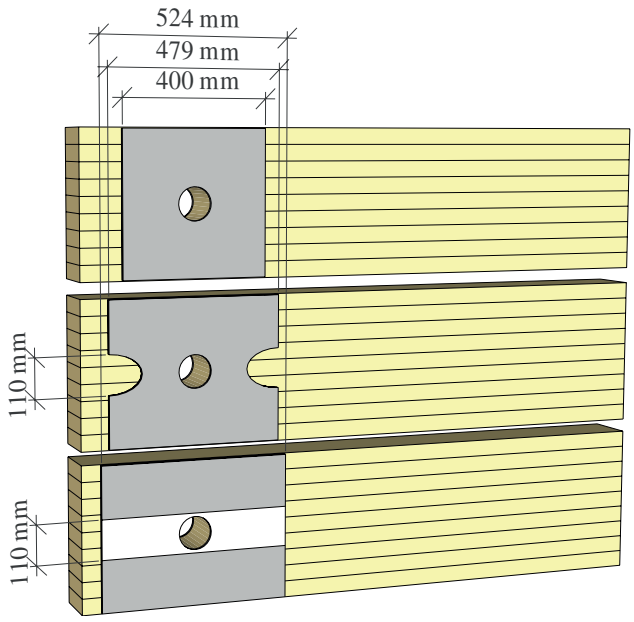

Figure 5.6: Alternative plate designs to the SPDJ studied in Paper D: The original square design (top), elliptical cut-outs (middle) and the strip design (bottom). All designs have the same bond area.

Paper D suggest an increase in load-carrying capacity for a given bonded area for the design alternatives (b) and (c). However, the increased efficiency is not deemed high enough to justify the increased production time and material usage, and the standard rectangular (here square) shape remains.

The thickness of the plate is limited by bearing strength and local instability around the dowel hole, discussed in Section 5.3.5. Local thickening of the plate around the hole can be used to optimize material usage.

5.3.4 Load angle

It is possible to use the SPDJ for several different applications, but characteristics such as material strength will vary depending on the direction of the applied load compared to the fibre direction. If not else specified, all presented tests and analyses in the thesis have been done for loading parallel to grain. However, loading perpendicular to grain will occur in e.g. a beam-column connection such as shown in Figure 5.4d. This loading mode was included in Paper F, where the load-carrying capacity of small scale SPDJ was experimentally investigated on specimens such as those illustrated in Figure 5.7.

The experimentally determined short-term nominal shear stress at failure is presented in Figure 5.8 and compared with the shear strengths presented in Table 3.2. It can be seen Figure 5.8

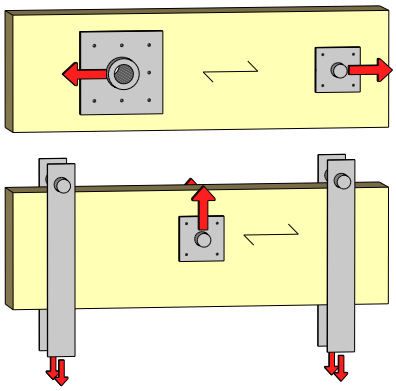

Figure 5.7: Test specimens of small scale SPDJ 65×65–20 loaded parallel and perpendicular to grain, top and bottom illustration respectively.

that loading the SPDJ parallel to grain is on average close to twice as strong as when loaded perpendicular to grain. It is also noticeable that the average strength of the SPDJ is considerably higher than the clear wood specimens used as reference [14], despite the occurrence also of peel stresses in the bond line and a possible size effect [70].

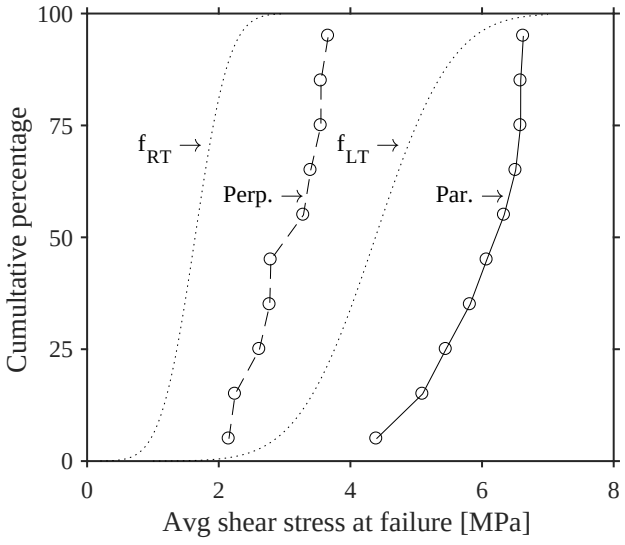

Figure 5.8: Cumulative distribution function of short-term strength of small scale SPDJ loaded both parallel (solid line) and perpendicular to grain (dashed line). Dotted lines represent shear strength in RT and LT directions respectively, according to Table 3.2 [14].

5.3.5 Ductility and dowel design

One of the major benefits of the SPDJ is the limited number of components, which also limit the number of possible failure modes to the following:

- Dowel shear and/or bending failure
- Plate bearing failure
- Bond line shear failure, including
  - Brittle wood failure close to bond line
  - Adhesive failure in wood-rubber inter-layer
  - Rubber failure
  - Vulcanization failure
- Timber element tensile failure

Using the manufacturing method proposed in Appendix A, the typical failure mode observed during the experimental work is wood failure close to the bond line. However, such a brittle failure is undesirable for timber connections as discussed in Section 2.1. The brittle behaviour can be avoided by redirecting the failure from wood to a ductile material such as steel, i.e. the plate and dowel in the SPDJ. By such, ductility can either be achieved in the steel plate by allowing plastic bearing deformations within the limits of the over-sized timber hole. This possibility was studied by Lefèvre [71], who found only a limited amount of ductility possible, which it was difficult to practically design for. A second possibility of achieving a ductile behaviour is by means of dowel deformations as studied in Paper E, for which some results are included here.

The ductility of the SPDJ can dramatically be increased if the dowel is designed with a hollow cross-section, i.e. a tube. The dimensions of the tube should then be chosen so that a ductile pipe-crushing failure mode occurs prior to the brittle bond line timber failure. This will increase the global connection ductility at the expense of total load-carrying capacity, and be made possible by the ductility of steel. This has been tested experimentally and numerically for single- and three-member nodes as shown in Figure 5.9. The difference in test configurations is the possible bending of the dowel in the three-member node.

The ductile response of the three-member node is illustrated on the thesis cover. In order to obtain a ductile failure while minimizing the loss in total load-carrying capacity, it was found that the diameter of the dowel should be 30–40% of the plate side length while the ratio between inner and outer diameter of 0.85–0.90. Paper E also experimentally investigates the possibility of using other dowel and plate materials, yet steel plate and dowel remain the most viable commercial alternative.

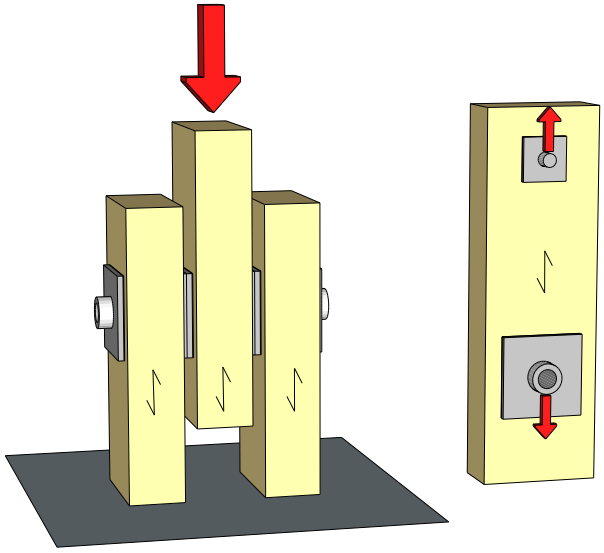

Figure 5.9: Experimental test setup to study the global response for different dowels. A three-member node to the left and a single-member node to the right. Please compare to the with Figure 5.4.

During the study presented in Paper E, it was found that the outermost steel plate of the outer members in the three-node configuration was poorly utilized in terms of carrying load due to dowel deformations. This has been considered in the so-called reduced truss node shown in Figure 5.4b, which omits these outermost plates which forces the dowel to transfer load by dominating shear. This dowel shear action is also made possible by the alternative design of a diagonal, which uses extruded plates to minimize the GLT element stacking in width direction. The design of the dowel is thus simplified by not using the outermost shear plates but using extruded plates of one diagonal GLT element. The strength of the connection can be increased by using the screws applied for curing pressure during production. By recessing the plates in the timber elements, a smooth outer surface can be obtained which can increase aesthetics and simplify external fire cladding.

5.3.6 Duration of load effects

Buildings are generally designed for a life span of 50–100 years [72]. Although on occasion argued too short, it is still a considerable time during which the load-carrying structure must uphold its characteristics as discussed in Section 2.1. In terms of the SPDJ, of special concern is the rubber material used in the resilient bond line in terms of strength and stiffness. The strength of rubber is known to decrease when subjected to long term loading [60], but also prone to creep considerably more than wood [61]. Also of concern is the duration of load effects of timber in shear, a property still not well documented at the time of writing the thesis. In order to investigate the duration of load (DOL) effects on the SPDJ, an experimental study was

conducted which is presented in detail in Paper F. A constant load methodology was adopted in open sheltered conditions, during which deformations and time to failure were recorded. Small scale SPDJ specimens were loaded both parallel and perpendicular to grain, see Figure 5.7.

The duration of load behaviour of timber subjected to bending is well documented, with a typical reduction factor of 0.5 adopted in building codes for permanent load in open sheltered conditions [19]. Significantly larger reduction factors were found during the study of the SPDJ, suggesting reduction factors of 0.1 and 0.3 for specimens loaded parallel and perpendicular to grain, respectively. This is to be considered a relatively rough estimate based on a 50-year extrapolation of 3-month data. However, it must be concluded that the proposed SPDJ is not efficient in terms of long duration loads in outdoor sheltered conditions without possible improvements (e.g. screws), and that further studies are needed in order to verify the use in other climate classes.

5.4 ASSESSMENT OF THE FUNCTIONAL REQUIREMENTS

This section discusses the shear plate dowel joint in terms of the ten functional requirements presented in Section 2.1. The discussion is based upon available research results presented within the thesis whenever applicable, and sound engineering judgement when no data exist. A summary is found in Table 5.2.

It is evident from Papers B and E that the SPDJ has a high load-carrying capacity in terms of short-term loading. The resilient bond line enables the possibility to increase the load-carrying capacity of the connection by simply increasing the shear plate area in order to match design loads. However, the duration of load tests presented in Paper F indicate a rapid strength degradation over time in open sheltered conditions. The design is thus expected to be useful for short duration loads such as impact loads, wind gusts or some types of dynamic loading.

Stiffness is a key point of interest within the thesis, as being one of the two fundamental requirements of the resilient bond line, in addition to high fracture energy. The preferred method of achieving a resilient bond line is by means of an intermediate rubber layer. Rubber is manufactured with a high accuracy of the shear stiffness [69], which together with various thicknesses of the layer offer the rather uncommon possibility to *design* the elastic response of the connection with high predictability.

Papers B and F present the ultimate load-carrying capacity of the SPDJ design limited by brittle wood shear failure close to the bond line. Paper E investigates the possibility of achieving a ductile failure behaviour by adopting a steel dowel with a hollow cross-section. The study verifies the concept and presents suitable geometries for the dowel, and the results are included in Section 5.3.5 and 5.5.

The SPDJ is a simple design concept with a clear load path. Papers A and C also indicate the applicability of the Volkersen theory to the resilient bond line, making it possible to determine the timber failure load using a single analytical expression with reasonable agreement. The

joint is also expected to be efficient to produce as the steel plates can be mounted onto the GLT member at the production facility, leaving only alignment and mounting of the single dowel on-site. A weakness during manufacturing is the treatment sensitivity discussed in Paper A, and the practicality of the acid rinse. A detailed description of the production method used can be found in Appendix A.

Appearance is subjective, but modern architecture seems more willingly to include an exposed load-carrying structure of timber than of concrete or steel. Nevertheless, the truss node in Figure 5.4a has the potential weakness of having to stack the members in the out-of-plane direction, creating wide nodes in comparison to e.g. slotted-in steel plates. The stacking of member can be minimized using a design alteration illustrated in Figure 5.4b. Also, the steel components of the SPDJ can be replaced by other materials as discussed in Paper E.

Of the resilient bond lines tested in Paper A, an SBR rubber foil was found most reliable in terms of adhesion properties and short-term strength. The idea of subjecting rubber to high permanent loads are often met with healthy scepticism regarding durability. However, the DOL-study published in Paper F highlights the fact that timber subjected to shear loading over time is in itself also very limiting. The study indicates that shear strength is decreasing more rapidly with loading over time than commonly used relations of bending strength over time, such as the Madison curve [73] or by Pearson [74]. As such, it was found that the DOL behaviour of the connection in open sheltered conditions is limited, and thus the connection in current configuration should not be used for high permanent loads.

Study of the fire behaviour of the SPDJ was *not* within the scope of this research. However, it is plausible that the current design configuration must be covered entirely by insulating materials to ensure safety according to modern fire standards. Concerns have arisen regarding the

Table 5.2: Summarized characteristics of the SPDJ based upon the functional requirements; weak performance (–), satisfactory performance (∼) and good performance (+). Characteristics of the three last functional requirements are *not* supported by scientific data presented in the thesis, but based upon sound engineering judgment of available data.

Load-carrying capacity	∼
Stiffness and deformations	+
Ductility	+
Simplicity of design	+
Producibility	∼
Appearance	∼
Durability	–
Fire	–
Costs	∼
Sustainability	∼

decreased yielding point of steel at elevated temperatures, melting of rubber and the influence of charring on the superficial shear strength. The proposed reduced truss node illustrated in Figure 5.4b is possibly more effective than a stacking truss node in terms of fire performance.

The production cost of the joint is not known at this point. In comparison to slotted-in steel plates, the SPDJ is expected to be more labour intense off-site while less on-site, a combination often claimed being cost effective. Approximately the same amount of material is needed for both types of connections, but the easy dismantling of the SPDJ suggests that it can be reused. However, recycling might be cumbersome due to the bonding of different materials.

5.5 PROPOSAL OF DESIGN GUIDELINES

The research conducted on the shear plate dowel joint is within this section summarized to a set of design guidelines. The guidelines are aimed at the timber engineer and regards the use of the shear plate dowel joint in single- and three-member nodes, see Figure 5.9. Please note that the presented guidelines only reflect conducted research, and some key aspects highlighted in Section 5.4 are not considered, e.g. fire resistance. A verification of the proposed guidelines is presented in Section 5.5.3, but is only made to the limited amount of test configurations presented within the thesis. For these tests, the adhesive and rubber strengths exceed the shear strength of the timber members.

5.5.1 Load-carrying capacity

The load-carrying capacity of the shear plate dowel joint is verified by considering the locally reduced timber cross-section, the size of the shear plate and the geometry of the dowel. The necessary considerations are presented below.

Timber element

The timber element should be designed according to current building codes. A conservative approach should be used by assuming that the entire normal force of the timber element is transferred through the reduced cross-sectional area around the centrically placed single large diameter hole. The end distance consistently used within the thesis is $3.5d$, where d denotes the outer diameter of the dowel. The proportionality to the dowel diameter is based on Eurocode 5 specifications for dowel connections [19], but reduced by half in comparison to Eurocode recommendations. However, as the typical timber failure mode is different from that found in conventional dowel connections, it might prove more relevant to keep the end distance proportional to a side length of the plate.

The hole in the timber should be made larger than the diameter of the dowel to allow for the shear displacement of the plate. The tensile elongation at break of typically used rubbers

seldom exceed 600% [69], and shear deformation at failure is typically significantly lower. It is thus reasonable to design for a 6 mm clearance if a rubber thickness of 1 mm is used, which is preferred.

Shear plate

The shear plate is recommended to have a square shape with a centrically placed hole with a diameter suitable to fit the dowel. Equation 5.1 is proposed to determine the design load capacity of a single timber element, F_{Rd}. The equation is based on the effective shear area A_{eff}, the design shear strength of the timber f_{vd} and a coefficient to consider phenomena regarding the specific connection design k_{SPDJ}.

$$F_{Rd} = f_{vd} A_{eff} k_{SPDJ} \tag{5.1}$$

The design shear strength of the timber f_{vd} is determined according to current building codes for shear parallel to grain or shear perpendicular to grain (rolling shear) in connections, depending on the direction of loading. The effective shear area A_{eff} is the total for the member, i.e. for two plates and accounting for the size of the larger hole made in the timber element. The effective shear area is thus found as $A_{eff} = 2\left(L^2 - \pi d_w^2/4\right)$ were L is the square plate side length and d_w is the diameter of the hole in the timber element.

The SPDJ coefficient k_{SPDJ} is defined in Equation 5.2. The three parameters k_i refer to additional duration of load considerations, interaction between shear and peel stresses in the bond line and dowel bending, respectively.

$$k_{SPDJ} = k_1\, k_2\, k_3 \tag{5.2}$$

The duration of load behaviour of the SPDJ was investigated in Paper F. The study indicates an increased degradation of load-carrying capacity over time while subjected to permanent load in comparison to timber in bending, which the reduction factor k_{mod} of Eurocode 5 is based on. The additional reduction is considered by the coefficient k_1, which is presented in Table 5.3.

Peel stresses are developed within the bond line due to the eccentric position of the external plates and local interaction with the dowel, see further in Section 5.3.1. The interaction between shear and peel stresses must be considered, which is made possible by the reduction coefficient k_2.

The peel stress reduction coefficient k_2 is determined from results presented in Paper E. The ratio between the numerically predicted capacity of the connection and the analytical shear capacity of the bonded area was determined, assuming perfect plasticity while regarding size effects according to Weibull [43]. Using the geometrical guidelines for the connection suggested in this Section 5.5, $k_2 = 0.8$.

Table 5.3: Reduction factor k_{mod} from Eurocode 5 (GLT, service class 1-2) and Paper F, which the additional reduction factor k_1 for the SPDJ is based on.

	Load-duration class	EC5	SPDJ par	SPDJ perp
k_{mod}	Short term	0.90	0.9	0.9
	Permanent	0.60	0.1	0.3
k_1	Short term		1.0	1.0
	Permanent		0.15	0.5

The single dowel will be exposed to pronounced bending if the SPDJ is used in e.g. a beam-column connection as seen in Figure 5.4d (in contrast to e.g. an arch springing in Figure 5.4c). If three timber elements are connected, the outermost plates of the outer members will not be efficiently used due to dowel bending. This is regarded in design by the factor k_3, which reduces the load-carrying capacity of the outer members of a 3-member node. For a single-member configuration, $k_3 = 1$, while for three-member nodes $k_3 = 0.75$ for outer members (outermost plates are typically carrying 50% of the loading of the inner plates). This factor is only valid for the suggested geometries of the inner plates and the dowel geometries suggested in the following section.

The thickness of the plate is determined by the bearing strength according to current building codes. Material efficiency can be increased by local thickening around the hole, but it should be ensured that the bond area remains flat. It should also be noted that the two plates must be aligned in order to ensure the intended load-carrying capacity.

The resilient bond line

The proposed connection (and thus Equation 5.1) utilizes a resilient bond line achieved by conventional stiff adhesive and a thin rubber layer. It is essential that the materials used, as well as bond strengths, exceed the shear strength of timber.

It is recommended to use a rubber thickness of 1 mm with a stiffness of approximately 60° Shore A (shear modulus of 1.2 MPa). The stiffness of the connection is then comparable to dowel-type connections. A suitable rubber type is either a styrene-butadiene rubber (SBR) or a mix of SBR and natural rubber (SBR/NR). The rubber should be vulcanized to the steel plate, and then be treated with concentrated sulphuric acid prior to bonding to timber, see Appendix for details. If the rubber is properly prepared, several types of adhesives are feasible although a 2-component polyurethane reactive adhesive (2C PUR) has been used throughout the thesis.

Dowel

The dowel is the single element transferring loads from one member to the next. Maximum load-carrying capacity is reached for solid dowels, where the capacity is limited by brittle failure of the timber closest to the bond line. A ductile behaviour can be achieved by redirecting failure from timber to steel by designing the dowels as tubes, which is typically preferred and studied in Paper E.

The diameter of the steel dowel should be in the range of 30–40% of the plate side length. Closer to 30% is suitable for single-member configurations (see Figure 5.4c), where the tube is primarily loaded in shear. Closer to 40% is suitable for three-member configuration (see Figure 5.4d), where the dowel is also subjected to bending. To achieve some ductility in the connection, a ratio between inner and outer diameter of the steel tube of 0.85–0.90 is suitable regardless of configuration type. It should be noted that it is difficult to ensure a ductile failure throughout the service life of the connection as the ductility is dependent on the ratio of load-carrying capacity between the timber and dowel. Although the structural behaviour of the steel dowel is comparably stable over time, the behaviour of timber has a high variability, are prone to size effects and changes over time if subjected to load.

In addition to these geometrical recommendations, the shear capacity of the dowel should be checked according to applicable codes.

5.5.2 Stiffness

The service life stiffness of the shear plate dowel joint is dominated by the stiffness of the rubber layer. While non-linear in tension, rubber can be approximated by linear elasticity in shear with reasonable accuracy. This lends itself well for simple predictions of the global connection stiffness by means of Equation 5.3.

$$K_{ser} = \frac{G}{t} A_{eff} \tag{5.3}$$

where K_{ser} is the connection stiffness, G is the shear modulus of the rubber expressed in stress/strain, t the rubber layer thickness and A_{eff} the effective bond area (same as in Equation 5.1). It should be noted that dowel bending is neglected, which can occur in e.g. three-member nodes (see Figure 5.9). Furthermore, the stiffness of the timber is not considered although experimental data suggests a lower stiffness for loading perpendicular to grain. A comparison between experimental data and predictions is found in Table 5.4.

In structural engineering applications, material stiffnesses are conveniently expressed in terms of stress/strain. However, the stiffness of rubbers (and other polymers and elastomers) are often expressed in terms of the Shore scale. The scale is based upon resistance to indentation,

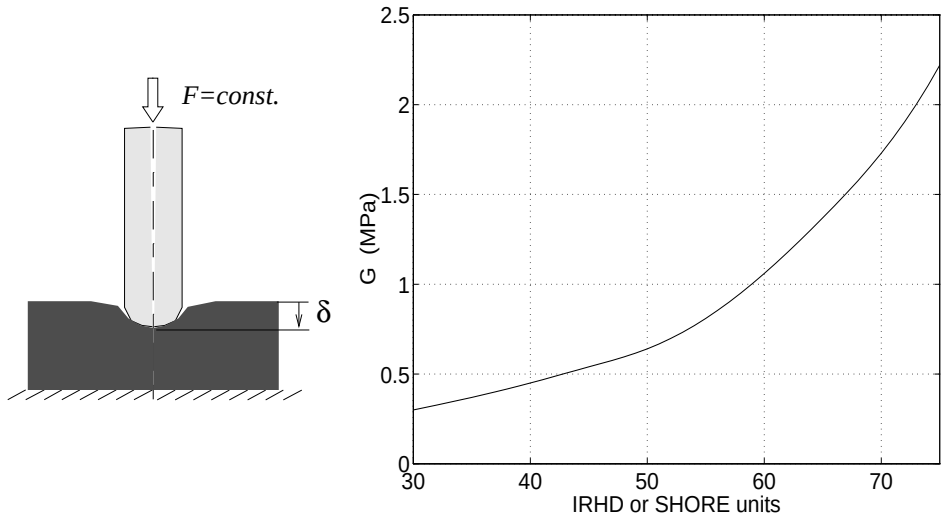

Figure 5.10: Illustration of the measurement of stiffness unit Shore alongside the relation between the shear modulus G and the rubber hardness in Shore units. Illustration from [60].

for which a high number indicates a higher resistance. The principle of the measurement is illustrated in Figure 5.10, alongside a conversion plot between shear stiffness and Shore units.

5.5.3 Verification

Experimental test results are compiled alongside predictions based upon Equations 5.1 and 5.3 in Table 5.4. The presented experimental data is the average of n identical tests using solid or close to solid dowels, with the coefficient of variation within parenthesis. The dominant failure mode for solid dowels is shallow timber shear failure, as is expressed by Equation 5.1. Although the recommended dowel geometries promote ductile failure by pipe crushing prior to brittle timber failure, the recommendations are made to minimize the loss of load-carrying capacity and a comparison is thus considered possible.

The predicted design capacities of the connections are consistently lower than the average capacities obtained in the tests. While conservative, it can be argued that the safety margin is too large for smaller specimens. The main contribution to this large difference is the shear strength, suggested by Eurocode to $f_{vd} = 2.4$ MPa (GLT in service class 1–2, $\gamma_M = 1.3$) for short duration loads parallel to grain in comparison to the presented test results which indicates an average shear stress at failure of $3 - 6.5$ MPa. The higher average stress at failure is found for smaller connections, which indicates a size effect suggesting that the excessive safety margin is necessarily not excessive for the larger shear plate dowel joints needed in heavy timber buildings. A higher average shear stress at failure than suggested by Eurocode is also found for loading perpendicular to grain, where $f_{vd} = 0.9$ MPa (GLT in service class 1–2, $\gamma_M = 1.3$)

Table 5.4: Verification of presented design equations on conducted tests. All test data average values from solid dowels, with the coefficient of variation in parenthesis.

Specimen[1]	Type[2,3]	n[4]	Capacity [kN]		Stiffness [kN/mm]	
			Test	Eqn 5.1	Test	Eqn 5.3
400×400–90	Single, ∥	3	990 (11%)	585	450 (3%)	346
120×120–45	3-node, ∥	3	130 (5%)	35	23 (7%)	28
65×65–20	Single, ∥	10	40 (12%)	12	13 (13%)	8
65×65–20	Single, ⊥	10	20 (18%)	4	7 (22%)	8

1) Geometry specified by plate dimensions and dowel diameter.

2) Single- or three-member configuration, see Figure 5.9.

3) Loaded parallel (∥) or perpendicular (⊥) to grain.

4) Number of specimens tested.

compared to 3.0 MPa found experimentally.

A reasonable accuracy of the stiffness was found. It should be noted that Equation 5.3 tends to underestimate the stiffness of single-member configurations while overestimating the stiffness of three-member configurations. This can possibly be explained by the limitations of the equation, but is considered within engineering accuracy.

6
Concluding remarks

The aim of the research presented in the thesis is to evaluate the shear plate dowel joint in terms of functional requirements. The thesis work has been focused on the mechanical behaviour of the connection, although some design features are related to production efficiency. The mechanical behaviour has been evaluated by experimental as well as numerical studies, for which specific methods for the resilient bond line have been presented. The main contributions of the conducted research can be concluded to the following two statements:

- A bond line with low stiffness yet high fracture energy can increase the load-carrying capacity of large lap joints. Such properties can be obtained by using an intermediate layer of thin rubber.
- The shear plate dowel joint is a timber connection suitable for large short-term loads.

More detailed conclusions and proposals for further research is presented in this chapter.

6.1 CONCLUSIONS

Resilient bond lines

The general conclusion of the study in Paper A is that a bond line with low stiffness yet high fracture energy can increase the load-carrying capacity of lap joints by reducing stress concentrations, despite to some degree conflicting experimental results. The technique is typically

applicable whenever a conventional adhesive bond line is applicable, and introduces the possibility of designing the shear stiffness by means of stiffness and thickness of the intermediate layer, typically rubber. A high sensitivity to the manufacturing method of the bond between rubber and wood has been found, for which detailed instructions are found in Appendix A.

The low stiffness of the resilient bond line is also preferred over conventional stiff adhesives in terms of computational effort. The load-carrying capacity of conventional bond lines are highly dependent on fracture softening, which requires non-linear numerical analysis. This is not the case for resilient bond lines, for which good predictions of the load-carrying capacity can be obtained analytically and by hand calculations using the Volkersen theory for lap joints. If a non-prismatic geometry of the lap joint is used, as is the case for the SPDJ, numerical analysis is preferred. An efficient linear bond line model for such cases is presented in Paper C, which also enables predictions of load-carrying capacity by means of single point stress evaluation in a combined stress state.

The shear plate dowel joint

The overall aim of the research project was to develop a good connection design for heavy timber structures. After the full-scale tests published in Paper B, it became evident that the shear plate dowel joint was a design concept worth further investigation.

The design combines the strengths of the resilient bond line with the simplicity of a single dowel as the only load transferring element, suggesting a fast installation and a high degree of possible prefabrication. The possibility of designing the stiffness of the connection is numerically verified in Paper E, where it was also concluded that the externally bonded steel plate preferably is square-shaped. Ductility can be introduced by using a tubular dowel as suggested in Paper E, where suitable geometrical relationships between the dowel and the steel plate was established.

The duration of load behaviour of small scale SPDJ loaded parallel and perpendicular to grain was investigated in open sheltered conditions and published in Paper F. It was expected that the intermediate rubber layer would limit the long-term strength, but it was found that timber in shear was also limiting the total load-carrying capacity over time. The investigation concludes that the SPDJ, in current design and materials, is not suitable for long-term loads in varying moisture conditions.

The combined research effort of the shear plate dowel joint design is included in the proposed design guidelines presented in Section 5.5, including DOL reduction factors and suitable geometries.

6.2 FURTHER RESEARCH

An assessment of the shear plate dowel joint in terms of the functional requirements is presented in Section 5.4, where some areas not yet studied are specified in Table 5.2. Of key importance prior to structural application is the behaviour of the connection when subjected to fire, something which has not yet been studied. However, it can be argued that the duration of load results presented in Paper F are of such limiting character that further studies of the connection design is of little practical interest. Before such dismissal is made, the procedure of the DOL study should be thoroughly reviewed in order to verify that the results are independent of the specific parameters used.

It should be noted that the resilient bond line possibly can be used wherever a conventional stiff bond line is used. Unpublished data suggests that simple lap joints are less affected by the duration of load than found for the SPDJ, see further in Paper F. The resilient bond line can be used to increase the load-carrying capacity or lower the stiffness. Further research is however needed to develop a production methodology with minimal variance in the achieved bond strength. It would also be interesting to further study the unexpected good performance of non-resilient bond lines in Paper A in order to determine causality. In terms of technical applications, it would be interesting to study vibration reduction effects by use of resilient bond lines.

The reasons of the poor duration of load performance of the connection is of more general use in timber engineering. During the course of the study, the limited amount of literature on duration of load behaviour of timber subjected to shear became evident. In addition, the very few results found in literature were contradictory in terms of relation to the generally used Madison curve [73]. Constant loading was applied to shear blocks in indoor climate by Leont'ev, finding the Madison curve for bending being *non-conservative* [8]. The opposite conclusion was found by Spencer [**?**], finding the Madison curve conservative by studying tube torsion in a controlled environment. A different duration of load behaviour should be expected for timber subjected to shear compared to bending, but there is an apparent lack of data to suggest a relation.

7 Summary of appended papers

Six papers are appended to the thesis, to which summaries are presented below. The summaries differs from the respective abstracts in order to also present a line of argument. The contribution of the author of the thesis is indicated for each paper. Some results and conclusions drawn in the appended papers are included in Part I of the thesis.

Paper A

Use of a resilient bond line to increase strength of long adhesive lap joints
G. Larsson, P.J. Gustafsson, R. Crocetti
European Journal of Wood and Wood Products, 76:401–411, 2018.

Conventional non-resilient bond lines are compared to resilient bond lines in terms of load carrying capacity and stiffness of long lap joints. A comprehensive comparative study is conducted numerically, analytically and experimentally, for which different results were obtained for the three methods used. The numerical and analytical results indicate an increase in load-carrying capacity by use of a resilient bond line, while the experimental results do not indicate a significant difference. Difficulties in achieving a strong bond between the adhesive and the rubber are discussed, but also the influence of softening behaviour and boundary conditions. Despite the experimental results, the authors conclude that resilient bond lines can increase the load-carrying capacity of long lap joints.

The thesis author performed the research tasks including the experimental and numerical work, and writing the article. The co-authors contributed during the planning of the experimental work, and reviewed the manuscript.

Paper B

Experimental study on innovative connections for large span timber truss structures
H. Yang, R. Crocetti, G. Larsson, P.J. Gustafsson
Proceedings of IASS W.G. 12 + 18, 2015.

On-site assemblage can be made more efficient by the use of a single large dowel compared to typical contemporary multi-dowel connections. Reinforcements are however needed in order to prevent premature splitting failure, and several different reinforcing techniques are compared experimentally in this article. 15 full scale quasi-static tensile tests of 5 different designs were conducted on glulam members with identical connections at each end of each specimen. An increase in load-carrying capacity was found for all reinforcement techniques, but the shear plate dowel joint outperformed the others by use of a resilient bond line.

The study was planned and conducted by assistant professor Huifeng Yang of the College of Civil Engineering, Nanjing Tech University, China. The thesis author contributed to the experimental work conducted in China and to the writing of the paper.

Paper C

Bond line models of glued wood-to-steel plate joints
G. Larsson, P.J. Gustafsson, E. Serrano, R. Crocetti
Engineering Structures, 121: 160–169, 2016.

As the experimental results of the shear plate dowel joint were promising, development of a representative and efficient numerical bond line model was of interest. Such model is presented in Paper C with good agreement with the experimental results of the resilient bond line tested in Paper B.

The numerical analysis also provided means to evaluate the potential of the premature failure of the non-resilient specimens presented in the Paper B. The importance of fracture softening on the load-carrying capacity is highlighted, yet the resilient bond line was still considerably stronger. Comparison is also made to the analytical Volkersen theory describing the shear stress distribution of lap joints.

The analytical and numerical work was conducted by the thesis author, and writing the majority of the paper. Co-authors assisted in planning of the study, writing shorter sections of the paper and reviewing. This is the first journal paper published by the author.

Paper D

Analysis of the shear plate dowel joint and parameter studies
G. Larsson, P.J. Gustafsson, E. Serrano, R. Crocetti
Proceedings of the World conference on timber engineering, 2016.

This conference paper is a direct follow-up of Paper C, in which the previously presented bond line model is used to conduct parameter studies of the shear plate dowel joint. The study is primarily focused on the shape of the bonded shear plate and the thickness of the bond line. Issues relating to applicability and practical implications of the alternative designs are investigated and discussed, for which it is concluded that the original square design is preferred, although not being the strongest.

The thesis author carried out all simulations and wrote the paper while the co-authors assisted in reviewing.

Paper E

Dowel design of the shear plate dowel joint
G. Larsson, E. Serrano, P.J. Gustafsson, H. Danielsson
Journal paper submitted 25 June, 2019.

Until this point, the shear plate dowel joint failed in a brittle manner by using a solid dowel with a diameter of approximately 30% of member height. This journal paper shows, both experimentally and numerically, that a ductile failure can be made possible by instead using tubular dowels. Based on numerical parameter studies of the dowel geometry, guidelines are presented in order to obtain a ductile failure at a reasonable load level.

The thesis author carried out the planning and execution of this study, and writing the paper. Co-authors assisted in general supervision and reviewing.

Paper F

Duration of load behaviour of the shear plate dowel joint
G. Larsson, P.J. Gustafsson, E. Serrano, R. Crocetti
Journal paper submitted 5 March, 2019.

The duration of load behaviour of the shear plate dowel joint was studied in open sheltered conditions. It was found that the load-carrying capacity of the connection was significantly reduced over time. For the design configuration used in the tests, high permanent loading is not advised. The duration of load performance of the connection is limited by the duration of load performance of timber subjected to shear loading; a topic not well documented in literature. Very few studies have been conducted, in which conflicting results are presented.

The thesis author conducted the experimental study and wrote the paper. The co-authors were involved in the planning, and assisted in the reviewing-process.

References

[1] Dodoo, A., Gustavsson, L., Sathre, R. (2016), *Climate impacts of wood vs. non-wood buildings*, Tech. rep., The Swedish Association of Local Authorities and Regions.

[2] Green, M.C., Karsh, J.E. (2012), *Tall Wood*, Canadian Wood Council.

[3] Gustafsson, P. (1987), *Analysis of generalized Volkersen-joints in terms of non-linear fracture mechanics*, Mechanical Behaviour of Adhesive Joints 139–150.

[4] Gustafsson, P. (2007), *Tests of full size rubber foil adhesive joints*, Tech. Rep. TVSM-7149, Division of structural mechanics, Lund University.

[5] Volkersen, O. (1938), *Die Nietkraftverteilung in zugbeanspruchten Nietverbindungen mit konstanten Laschenquerschnitten*, Luftfahrtforschung **15**(1/2), 41–47.

[6] Crocetti, R., Axelson, M., Sartori, T. (2010), *Strengthening of large diameter single dowel joints*, Tech. Rep. 2010:14, SP Technical Research Institute of Sweden.

[7] Kobel, P. (2011), *Modelling of strengthened connections for large span truss structures*, Master's thesis, Division of structural engineering, Lund University.

[8] Leont'ev, N. (1961), *Long term resistance of spruce wood to shear along the grain*, Russian. Lesn. Z. Archangel'sk **4**(4), 122–124.

[9] Larsson, G. (2017), *High capacity timber joints - Proposal of the Shear plate dowel joint*, Licentiate thesis, Division of structural mechanics, Lund University.

[10] Madsen, B. (2000), *Behaviour of timber connections*, Timber Engineering Ltd.

[11] Jensen, J.L. (1994), *Dowel-type fastener connections in timber structures subjected to short-term loading*, Ph.D. thesis, Statens byggeforskningsinstitut – Aalborg University.

[12] Niklewski, J. (2018), *Durability of timber members: Moisture conditions and service life assessment of bridge detailing*, Ph.D. thesis, Division of structural engineering, Lund University.

[13] Östman, B., Brandon, D., Frantzich, H. (2017), *Fire safety engineering in timber buildings*, Fire Safety Journal **91**, 11–20.

[14] Dahl, K.B. (2009), *Mechanical properties of clear wood from Norway spruce*, Ph.D. thesis, NTNU Trondheim.

[15] Johnsson, H. (2004), *Plug shear failure in nailed timber connections. Avoiding brittle and promoting ductile failures*, Ph.D. thesis, Luleå University of Technology.

[16] Jorissen, A.J.M. (1998), *Double shear timber connections with dowel type fasteners*, Heron **44**(3), 163–186.

[17] Johansen, K. (1949), *Theory of timber connections*, in: *International Association of Bridge and Structural Engineering*, vol. 9, 249–262.

[18] Larsen, H.J. (2003), *Introduction: Fasteners, Joints and Composite Structures*, in: S. Thelandersson, H. Larsen (eds.), *Timber Engineering*, chap. 16, 303–314, Chichester West Sussex.

[19] EN 1995-1-1:2004, *Eurocode 5: Design of timber structures – Part 1-1: General – Common rules and rules for buildings*.

[20] Poutanen, T.T. (1989), *Analysis of trusses with connector plate joints*, in: *Proceedings of the Second Pacific Timber Engineering Conference, University of Auckland, New Zealand, 28-31 August 1989 Volume 1*, 155–159.

[21] Foschi, R.O. (1977), *Analysis of wood diaphragms and trusses. Part II: Truss-plate connections*, Canadian Journal of Civil Engineering **4**(3), 353–362.

[22] Feldborg, T., Johansen, M. (1981), *Wood trussed rafter design: Strength and stiffness tests on joints. Long-term deflection of W-trussed rafters*, Statens Byggeforskningsinstitut, SBI.

[23] Leijten, A. (1998), *Densified veneer wood reinforced timber joints with expanded tube fasteners*, Ph.D. thesis, TU Delft.

[24] Blass, H.J. (2003), *Joints with Dowel-type Fasteners*, in: S. Thelandersson, H. Larsen (eds.), *Timber Engineering*, chap. 17, 315–332, Chichester West Sussex.

[25] Bengtsson, C., Johansson, C.J. (2002), *GIROD – Glued-in rods for timber structures*, Tech. Rep. 2002:26, SP Technical Research Institute of Sweden.

[26] Tlustochowicz, G., Serrano, E., Steiger, R. (2010), *State-of-the-art review on timber connections with glued-in steel rods*, Materials and Structures **44**(5), 997–1020.

[27] Natterer, J., Sandoz, J.L., Rey, M. (2004), *Construction en bois: matériau, technologie et dimensionnement*, Traité de génie civil de l'Ecole polytechnique fédérale de Lausanne, Presses Polytechniques et Universitaires Romandes.

[28] Adams, R.D., Wake, W.C. (1984), *Structural adhesive joints in engineering*, Elsevier Applied Science Publishers Ltd.

[29] Madsen, B. (1992), *Structural behaviour of timber*, Timber Engineering Ltd.

[30] Bodig, J., Jayne, B.A. (1982), *Mechanics of wood and wood composites*, Van Nostrand Reinholt Publishing.

[31] Dinwoodie, J. (2000), *Timber – Its nature and behaviour*, E&FN Spon, 2 edn.

[32] Persson, K. (2000), *Micromechanical modelling of wood and fibre properties*, Ph.D. thesis, Division of structural mechanics, Lund University.

[33] Petroski, H. (1996), *Invention by Design: How Engineers Get from Thought to Thing*, Harvard University Press.

[34] Hearmon, R.F.S. (1948), *The elasticity of wood and plywood*, HM Stationery Office London.

[35] EN 338:2016, *Structural timber - Strength classes*.

[36] EN 14080:2013, *Timber structures - Glued laminated timber and glued solid timber - Requirements*.

[37] Astrup, T., Clorius, C.O., Damkilde, L., Hoffmeyer, P. (2007), *Size effect of glulam beams in tension perpendicular to grain*, Wood Science and Technology **41**(4), 361–372.

[38] Aicher, S., Dill-Langer, G. (2005), *Effect of lamination anisotropy and lay-up in glued-laminated timbers*, Journal of structural engineering **131**(7), 1095–1103.

[39] Danielsson, H. (2013), *Perpendicular to grain fracture analysis of wooden structural elements-Models and applications*, Ph.D. thesis, Division of structural mechanics, Lund University.

[40] Thelandersson, S. (2003), *Introduction: Wood as a construction material*, in: S. Thelandersson, H. Larsen (eds.), *Timber Engineering*, chap. 2, 15–22, Chichester West Sussex.

[41] Eberhardsteiner, J. (2013), *Mechanisches Verhalten von Fichtenholz: Experimentelle Bestimmung der biaxialen Festigkeitseigenschaften*, Springer-Verlag.

[42] Aicher, S., Dill-Langer, G., W, K. (2002), *Evaluation of different size effect models for tension perpendicular to grain*, in: *CIB-W18 Timber Structures, meeting 35*, 35-6-1.

[43] Weibull, W. (1939), *A statistical theory of the strength of materials*, 151, Generalstabens litografiska anstalts förlag.

[44] Johansson, M. (2015), *Structural properties of sawn timber and engineered wood products*, in: E. Borgström (ed.), *Design of timber structures*, vol. 1, chap. 2, 26–67, Swedish Forest Industries Federation, 2 edn.

[45] Norris, C.B. (1962), *Strength of orthotropic materials subjected to combined stresses*, FPL-1816. Madison, Wis. : U.S. Dept. of Agriculture, Forest Service, Forest Products Laboratory .

[46] Tsai, S.W., Wu, E.M. (1971), *A general theory of strength for anisotropic materials*, Journal of composite materials **5**(1), 58–80.

[47] Swiss Society of Engineers and Architects (2012), *Timber beams notched at the support*, SIA 265.

[48] Mascia, N.T., Nicolas, E.A., Todeschini, R. (2011), *Comparison between Tsai-Wu failure criterion and Hankinson's formula for tension in wood*, Wood Research **56**(4), 499–510.

[49] Hellan, K. (1985), *Introduction to fracture mechanics*, McGraw-Hill.

[50] Haller, P., Gustafsson, P.J. (2002), *An overview of fracture mechanics concepts*, Rep. No. RILEM TC **133**.

[51] Boström, L. (1994), *The stress-displacement relation of wood perpendicular to the grain*, Wood science and technology **28**(4), 309–317.

[52] Riberholt, H., Enquist, B., Gustafsson, P., Jensen, R. (1992), *Timber beams notched at the support*, Tech. Rep. TVSM-7071, Division of structural mechanics, Lund University.

[53] Stefansson, F. (2001), *Fracture analysis of orthotropic beams - Linear elastic and non-linear methods*, Licentiate thesis, Division of structural mechanics, Lund University.

[54] Dassault Systèmes (2017), *Abaqus Analysis User's manual*.

[55] Gustafsson, P. (2008), *Tests of Wooden Cleats Oriented Along Fibre*, Tech. Rep. TVSM-7155, Division of structural mechanics, Lund University.

[56] Gustafsson, P. (2008), *Stress equations for 2D lap joints with a flexible bond layer*, Tech. Rep. TVSM-7148, Division of structural mechanics, Lund University.

[57] Gustafsson, P. (2006), *A structural joint and support finite element*, Tech. Rep. TVSM-7143, Division of structural mechanics, Lund University.

[58] Serrano, E. (2000), *Adhesive joints in timber engineering. Modelling and testing of fracture properties*, Ph.D. thesis, Division of structural mechanics, Lund University.

[59] Wernersson, H. (1994), *Fracture characterization of wood adhesive joints*, Ph.D. thesis, Division of structural mechanics, Lund University.

[60] Austrell, P.E. (1997), *Modeling of elasticity and damping for filled elastomers*, Ph.D. thesis, Division of structural mechanics, Lund University.

[61] Björnsson, P., Danielsson, H. (2005), *Strength and creep analysis of glued rubber foil timber joints*, Master's thesis, Division of structural mechanics, Lund University.

[62] Freakley, P., Payne, A. (1978), *Theory and Practice of Engineering with Rubber*, Applied Science Publishers.

[63] Ellison, B., Schmeal, W. (1978), *Corrosion of steel in concentrated sulfuric acid*, Journal of the Electrochemical Society **125**(4), 524–531.

[64] Trayer, G.W. (1932), *The bearing strength of wood under bolts*, US Department of Agriculture, Forest Service, Forest Products Laboratory.

[65] He, M.j., Liu, H.f. (2015), *Comparison of glulam post-to-beam connections reinforced by two different dowel-type fasteners*, Construction and Building Materials **99**, 99–108.

[66] Windorski, D.F., Soltis, L.A., Ross, R.J. (1997), *Feasibility of fiberglass-reinforced bolted wood connections*, US Department of Agriculture, Forest Service, Forest Products Laboratory.

[67] Haller, P., Birk, T., Offermann, P., Cebulla, H. (2006), *Fully fashioned biaxial weft knitted and stitch bonded textile reinforcements for wood connections*, Composites Part B: Engineering **37**(4), 278–285.

[68] Pavković, K., Rajčić, V., Haiman, M. (2014), *Large diameter fastener in locally reinforced and non-reinforced timber loaded perpendicular to grain*, Engineering structures **74**, 256–265.

[69] Trelleborg (2015), *Sheeting & Matting - Industrial & Wear resistant*.

[70] Colling, F. (1986), *Influence of volume and stress distribution on the shear strength and tensile strength perpendicular to grain*, in: *CIB-W18 Timber Structures, meeting 19*, 19-12-3.

[71] Lefèvre, C. (2015), *Reinforcement of a large diameter single dowel joint*, Master's thesis, University of Mons.

[72] EN 1990, *Eurocode 1: Basis of structural design*.

[73] Wood, L. (1951), *Relation of Strength of Wood to Duration of Load*, Tech. Rep. 1916, US Department of Agriculture, Forest Service, Forest Products Laboratory.

[74] Pearson, R. (1972), *The effect of duration of load on the bending strength of wood*, Holzforschung-International Journal of the Biology, Chemistry, Physics and Technology of Wood **26**(4), 153–158.

Part II

Appendix

Manufacturing of the SPDJ

The shear plate dowel joint relies on a strong bond between rubber and timber. As shown in Paper A, a surface treatment of the rubber is crucial as initial testing indicates that the load-carrying capacity is increased by up to 60 (!) times between treated and untreated samples. This increase shows the significance of having a detailed manufacturing procedure to ensure the proper strength and strength variability of the bond line. This appendix summarizes the author's experiences over the years of this study but should not be considered a final manufacturing procedure. As such, the instructions are often complemented with comments. The treatment of rubber is based upon a work of Magnus Wikström, as presented by Per Johan Gustafsson [4].

A.1 GENERAL PROCEDURE

The general procedure of the production of the shear plate dowel joint is presented below, for which the treatment of rubber is further specified in Section A.2. Proposed design guidelines of the connection can be found in Section 5.5.

1. Create steel plates of the appropriate size. Create appropriate holes for the single dowel as well as the screws used to apply curing pressure.
2. A standard vulcanization procedure is used to bond the rubber to the steel plate. Note that only the hole for the large single dowel should be made. The curing screws easily penetrates the rubber, which makes the adhesive application less untidy.
3. Prepare the rubber surface for bonding to wood (see details in Section A.2 below).
4. Create GLT elements of proper size. Drill the over-sized holes for the dowels with a diameter dependent on dowel diameter and the thickness of the rubber layer. Drill from both sides to prevent splintering.
5. Clean the rubber surface of the steel and rubber plate using water and ethanol.
6. Plane the GLT surface to obtain a fresh timber surface in accordance with EN 14080 [36].

7. Apply the adhesive onto the GLT element according to manufacturer's specifications and mount the plate.
8. Apply curing pressure using appropriate screws.
9. Remove all excessive adhesive around the plate and inside the dowel hole.

Step 1–4 can be done prior to bonding (at least up to 3 months) while the bonding steps 5–9 must be carried out within 24 hours. The adhesive used throughout this work is the 2-component polyurethane SikaForce 7710 with hardener 7020. However, initial testing suggests that the bond between the treated rubber surface and timber surface is insensitive to the specific adhesive used. The rubber used is either pure SBR (styrene-butadiene-rubber) or a mix of SBR and natural rubber.

A.2 TREATMENT OF RUBBER

The difficulty of achieving a strong bond between the rubber and adhesive is due to the low surface energy of many types of rubbers, including SBR and natural rubber [4]. In order to achieve a strong bond, the adhesive used must have an even lower surface energy. This is rarely the case, and poor or no adhesion follows. Instead of creating a new type of adhesive, it is more convenient to increase the surface energy of the rubber by sanding and etching in concentrated sulphuric acid. The presented method shows how the surface energy of the rubber can be increased, which is valid regardless if the rubber is vulcanized to a steel plate or not.

Procedure

1. Scrub the rubber surface under running water.
2. Sand the rubber surface with 100-grit paper, preferably using a random-orbit sander. The sanding is rather aggressive and is completed when the shiny surface has turned entirely matt.
3. Again scrub the rubber surface under running water.
4. Wash the rubber surface with ethanol.
5. Etch the rubber by submerging the specimen (with the vulcanized steel plate) in concentrated sulphuric acid for *30 seconds* (not more, not less).
6. Rinse the specimens in water for 15–30 minutes.
7. Wipe with a clean cloth and leave to dry in air.

Comments on the procedure

The acid etching is conducted by submerging the rubber in concentrated sulphuric acid (>95%, room temperature). The high concentration is used both in order to obtain the right etching, but also to *reduce* the corrosion rate of the steel plate compared to lower concentrations of the same acid [63]. This counter-intuitive behaviour of steel in *concentrated* sulphuric acid is due to the interaction of sulphate. The acid is preferably poured into a resistant container which is large enough for one specimen (e.g. polypropylene plastic).

Subsequent the acid etching, the specimens should be rinsed in water for 15–30 minutes. This is preferably made by using a large container of water for which the water is continuously changed.

Etching of the rubber can be made in advance to bonding the plates to the GLT members. Successful bonding has been made in laboratory conditions up to three months after etching, but no detailed study of the durability of the etching procedure has been conducted in the presented work.

Part III

Appended publications

Paper A

European Journal of Wood and Wood Products (2018) 76:401–411
https://doi.org/10.1007/s00107-017-1264-x

ORIGINAL

Use of a resilient bond line to increase strength of long adhesive lap joints

Gustaf Larsson[1] · Per Johan Gustafsson[1] · Roberto Crocetti[2]

Received: 2 January 2017 / Published online: 16 November 2017

Abstract
The load capacity of long adhesive lap joints is often governed by stress concentrations at the lap ends. This paper investigates a method to minimize these stress concentrations by using a bond line with low shear stiffness and sufficient strength, here denoted as a resilient bond line. The resilient bond line is intended to increase the load carrying capacity of long lap joints by achieving a more uniform shear stress distribution while maintaining an elastic joint behaviour without damage or plastic deformation. The study comprises analytical, numerical and full-sized experimental work on double lap joints with lengths 200–700 mm comparing conventional stiff bond lines to resilient bond lines. Different resilient bonds lines were obtained by using rubber-like adhesives and by having a rubber mat within the bond line. An analytical definition of a 'long' lap joint is suggested and a study of adhesive-rubber bonding is also presented. The numerical analysis clearly indicates that an increase in load carrying capacity is made possible using resilient bond lines. A good agreement is also found between the numerical results and the analytical Volkersen theory, indicating that reasonable strength predictions can be obtained by hand calculations if the joint is designed in order to minimize the influence of peel stress. The experimental results of the resilient bond line verify the numerical findings, although production difficulties decrease the statistical significance of the result. On the contrary, the experimental results of the conventional bond lines significantly exceeded the numerical predictions, showing similar load carrying capacities to the resilient bond line. This is probably due to the specific boundary conditions used in the test setup. Despite some contradictory experimental results, the conclusion of this study is that the efficiency of long lap joints can be increased by the use of a bond line with low shear stiffness and sufficient strength.

1 Introduction

Lap joints have historically been used in engineering as a simple means of assembling structural members. Lap joints are today still used on a variety of materials, but the early examples are mainly for wood. Standing for well over a millennium, high-rise Japanese pagodas as well as the slightly younger Nordic stave churches are good examples of how timber can be assembled for durability, in which some joints are based upon a lap joint design (Sumiyoshi and Matsui 1991; Zwerger 2000). Today's efficient production and optimized material usage often rule out the old production methods and lap joints are hence rarely seen in modern timber structures. However, the resilient adhesive lap joints studied herein might prove to again increase the competitiveness of lap joints in heavy timber structures.

The use of long adhesive lap joints with conventional stiff bond lines is limited in terms of load carrying capacity. The utilization rate of the bond line is kept low due to high stress concentrations at lap ends. With the aim of increasing the load carrying capacity, it was realized that the stress concentrations in lap joints can be minimized if an elastic bond line with low shear stiffness and high strength is used. This combination of a bond line with low stiffness and high strength is henceforth denoted as a resilient bond line, which also relates to the elastic response to high strains common for the elastomers used. A test series based upon the idea of using an intermediate rubber foil was conducted without any comparisons to conventional stiff bond lines (Gustafsson 2007). As damage typically occurs at low load levels for this type of adhesives, the behaviour is typically non-resilient. Further work has since been conducted on resilient bond lines using different types of rubbers (Danielsson and

✉ Gustaf Larsson
gustaf.larsson@construction.lth.se

[1] Division of Structural Mechanics, Lund University, P.O. Box 118, 221 00 Lund, Sweden

[2] Division of Structural Engineering, Lund University, P.O. Box 118, 221 00 Lund, Sweden

Björnsson 2005), other full scale tests of innovative timber joints using the technique (Yang et al. 2015) and a numerical bond line model has been presented (Larsson et al. 2016).

Previous studies indicate that the length of the adhesive lap joint is a key factor in the comparison between conventional bond lines and bond lines with lower shear stiffness, in which the latter is more effective for longer joints. An analytical approach is here proposed in order to define an upper length limit for the lap joint length after which a resilient bond line is favourable. One type of resilient bond lines studied herein is achieved by using an intermediate rubber layer between the timber adherends. However, previous studies indicate difficulties in achieving a strong bond between the adhesive and rubber. Thus, parameter study regarding the rubber treatment is also added to this study.

The present paper aims to determine the possible effect of using a resilient bond line in full scale wooden lap joints by a comparative study. The study comprises:

- An analytical definition of a 'long' lap joint.
- Experimental study of rubber-adhesive bonds for different rubber treatments.
- A full scale experimental test series of double lap joints with lap lengths from 200 to 700 mm. Conventional stiff bond lines are compared to low stiffness resilient bond lines, but also different techniques to achieve a resilient bond line are tested.
- Numerical and analytical analyses of an ideal lap joint comparing geometrically similar resilient and non-resilient bond lines. Sensitivity analysis according to the method of factorial design is also conducted.

2 Methods

Double adhesive lap joints were tested experimentally in full scale quasi-static shear tests, accompanied by numerical analyses. Rational design equations can possibly be derived from analytical expressions based upon Volkersen theory (Volkersen 1938). The study aims at investigating possible benefits of using a resilient bond line for large lap joints, in which a conventional stiff adhesive bond line is used as reference.

2.1 Tests

2.1.1 Test series

Double adhesive lap joints with increasing lap lengths according to Fig. 1 were used in the test series, in which the bond line material varied according to Table 1. The height of the test specimens was 225 mm, and the width was

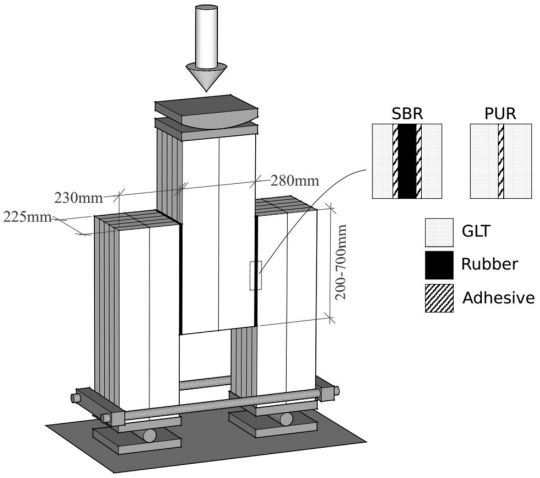

Fig. 1 Double lap joint test setup

230 and 280 mm for the side members and centre member respectively.

To achieve a resilient bond line, a sheeting made from a mix of natural rubber (NR) and styrene-butadiene rubber (SBR) was primarily used, denoted as the SBR specimens in Table 1. The conventional stiff bond line was the PUR-series which consisted of a 2-component polyurethane (PUR), the same as used for the rubber specimens, see Fig. 1. These two types of specimens were used for the lap length investigation ranging from 200 to 700 mm. One additional specimen of each type with 700 mm lap length was included to investigate the effects of boundary conditions, denoted SBR/PUR-700 s and further discussed in Sect. 2.1.4.

In order to possibly simplify the manufacturing process of resilient bond lines, three additional types were added to the test series. The use of chloroprene rubber sheeting (CR) was intended to possibly decrease preparation work while rubber can be replaced entirely by using resilient adhesives such as SikaTack Move IT (IT) and Collano RESA HLP-H (CO).

The SBR/NR used was 3.5 mm thick with a hardness of 60 shore A (1.2 MPa), tensile strength $f_t \geqslant 17.5$ MPa and an elongation at failure of 400%. The CR was 0.5 mm thick with a density of 1.30 g/cm^3, tensile strength $f_t \geqslant 13$ MPa and an elongation at failure of $\geqslant 250\%$ according to ISO standards. The hardness was the same as for the SBR/NR.

The resilient adhesive SikaTack Move IT is a 1C PUR with a shear modulus of 65 shore A (1.4 MPa), a shear strength of 5 MPa and an elongation at failure of 300%. Collano RESA HLP-H is a 2C PUR casting resin with granular additive, being the softest and weakest material tested with a shear modulus of 30 shore A (0.4 MPa), a tensile strength of 0.8 MPa and an elongation at failure of approximately 260%.

Table 1 Specimen and bond line specifications

Specimen	Joint length (mm)	Rubber	Adhesive	No. tests
SBR-200	200	SBR/NR, 3.5 mm	SikaForce 7710 + hardener 7020	4
SBR-400	400	SBR/NR, 3.5 mm	SikaForce 7710 + hardener 7020	4
SBR-700	700	SBR/NR, 3.5 mm	SikaForce 7710 + hardener 7020	6
PUR-200	200	–	SikaForce 7710 + hardener 7020	4
PUR-400	400	–	SikaForce 7710 + hardener 7020	4
PUR-700	700	–	SikaForce 7710 + hardener 7020	4
CR-700	700	CR, 0.5 mm	SikaForce 7710 + hardener 7020	2
IT-700	700	–	SikaTack Move IT, 2 mm + Sika Primer-3 N	2
CO-700	700	–	Collano RESA HLP-H, 1.5 mm	2
SBR-700 s	700	SBR/NR, 3.5 mm	SikaForce 7710 + hardener 7020	1
PUR-700 s	700	–	SikaForce 7710 + hardener 7020	1

In comparison, the shear stiffness of conventional bond line is approximately 1000 MPa (Wernersson 1990).

2.1.2 Rubber-adhesive bonding

The generally low surface energy of rubber is problematic in terms of adhesion as the adhesive used must have an even lower surface energy in order to achieve a strong bond (Dillard and Pocius 2002). However, this is seldom the case and poor adhesion, or no adhesion at all, follows.

It is a relative difference in surface energy that has to be obtained, which can be done by modifying either the rubber or the adhesive. In this study, the surface energy of the rubber was increased by sanding and etching in concentrated sulphuric acid. Clean surfaces were obtained by rinsing the specimens in water and ethanol. To obtain the best possible results of the test series, additional tests were conducted to investigate the influence of the rubber treatment. Simple rubber-adhesive-rubber peel tests were conducted according to Fig. 2 using 3.5 mm SBR/NR rubber and 2C PUR adhesive with a thickness less than 0.5 mm. Using two nominally equal test specimens, the effect of each process step was investigated: water rinsing, ethanol rinsing, sanding and acid etching. Two different time durations of sanding and etching were tested. The acid etching was conducted with 97% sulphuric acid at room temperature.

2.1.3 Manufacturing

Glued laminated timber (GLT) of strength class GL30c (Norway spruce) with a cross-sectional depth of 225 mm was paired using SikaBond 545 to obtain the required dimensions shown in Fig. 1. The thickness of the laminations was 45 mm. The test setup introduces eccentricity which gives rise to perpendicular to grain tensile stress within the centre member with possible premature splitting. To avoid possible splitting and to minimize possible secondary effects on the bond line the largest specimens were reinforced by means of 2–3 6.5 × 220 mm screws inserted perpendicular to grain at the low end. The density of the tested GLT was 440–460 kg/m^3 at an average moisture content of 8.7% during testing.

Fig. 2 Rubber-adhesive adhesion tensile test. Bonded area was 50 × 50 mm^2

The manufacturing method used for the bond line was dependent on the bond line material, and all methods were verified by tests. The method used for the SBR/NR is presented in detail in Gustafsson (2007), which involves sulphuric acid treatment of the rubber prior to application of the adhesive according to the results of the rubber-adhesive bonding tests. The same gluing technique was used for the SBR/NR specimens as for the PUR specimens. The GLT was planed within 2 h prior to bond line gluing. All adhesive was applied to the GLT surfaces, one-sided for each bond, and cured at room temperature with manually applied curing pressure using 4–6 sash clamps. Dependent on the adhesive used, the pressure was typically applied for 24 h and the specimens stored for a minimum of one week prior to testing.

The manufacturer of the CR recommended the use of CR-based contact adhesive for application, but pre-testing indicated low strength. To obtain the best result, the CR was also treated with sulphuric acid according to Gustafsson (2007) and 2-component PUR adhesive was used.

The resilient adhesive in the IT specimens was applied using a motorized mobile caulking gun after application of the primer. A maze of adhesive strings was applied to the wood surface, which were flattened out by applying compression between the two adherends. The thickness of the bond line was ensured by 2.0 mm rubber distances. Due to the manual string-wise application, the bond line was not entirely continuous making the nominal bond line area smaller than intended with typically 90–95% coverage. The low viscosity of Collano RESA HLP-H enabled pouring of the adhesive on to the substrate, ensuring 100% coverage if the 1.5 mm rubber distances are disregarded. The CO specimens were stored for one month prior to testing to ensure proper hardening.

2.1.4 Setup and loading procedure

The experimental test setup is shown in Fig. 1. The test is designed to primarily fail in shear, in which the horizontal shackle at the base of the specimen reduces the effect of leg splitting during the displacement controlled quasi-static loading. The shackle was made of up to UPE 80 beams and 8.8 M16 rods. Steel plates were used in order to uniformly distribute the bearing stress between the points of load application and the end grain.

The loading procedure was conducted according to the European Standard EN 26891 for timber structures. The load is applied up to 40% of the estimated failure load F_{est}, then reduced to 0.1 F_{est} before loaded to failure at an actuator speed of 1.1 and 1.5 mm/min for non-resilient and resilient bond lines, respectively. The relative shear displacement over the bond line was measured centrically on both sides using four LVDTs with 140 mm length of stroke. The measurement points were located 25 mm from the bond line on either side. The load was measured internally in the hydraulic press, which was calibrated up to 500 kN with a maximum error less than approximately 2%.

Possible failure modes include bond line failure in the wood/adhesive interface, rubber/adhesive interface, rubber failure, wood failure close to bond line by shear/peel stress interaction and wood tensile crack perpendicular to grain along the centreline of the specimen due to leg splitting. Except rubber failure, all these failure modes were visible in the experimental study. However, only wood failure close to bond line by shear/peel stress interaction is studied in the numerical analyses as further discussed in the following section.

In addition to the test setup shown in Fig. 1, the influence of support conditions was experimentally investigated. The main part of the study was conducted using steel plates covering the entire end-grain area of the specimens where the forces were applied. The steel plates to some extent prevent failure due to block shear. The test specimens SBR-700s and PUR-700s were made to experimentally evaluate this restriction by reducing the end grain area covered by the steel plate. The steel plate covering the end grain of the top member was reduced in width, allowing 40 mm free end grain on each side.

2.2 Numerical strength analysis

Numerical analyses with linear and non-linear fracture modelling were performed to determine a general length to load bearing capacity behaviour for resilient and non-resilient bond lines, respectively. The simulations were performed in plane stress 2D by means of finite element modelling using the commercial general-purpose FE software Abaqus. The model consists of wood and a bond line, which is represented by a cohesive layer with a single element in the thickness direction. The bond line thus represents either (1) the adhesive or (2) the adhesive and the rubber foil; including the material interfaces. As fracture softening is important for common adhesives while negligible for rubber materials, two separate approaches were used to model the bond line.

The load carrying capacity of the conventional stiff adhesive bond line is highly dependent on the softening behaviour (Serrano and Gustafsson 2006), and was thus modelled with bilinear softening illustrated for pure shear in Fig. 3, as typical for structural adhesives (Wernersson 1990). The initiation of damage was predicted by means of a quadratic Norris criterion (Norris 1962), for which a one parameter damage evolution was defined as a function of the effective shear and normal displacement (Larsson et al. 2016).

Characteristic for the rubber and rubber-like materials used in the resilient bond lines is the brittle failure at large shear displacements, which limits the influence of the softening behaviour (Austrell 1997). The resilient bond line is further simplified to a linear elastic material, as shown in Fig. 3. As shear is the dominant mode in this setup, this approximation is reasonable. In both bond line types, the strength is represented by wood failure while the shear modulus used was according to Sect. 2.1.1 for resilient and non-resilient bond lines, respectively.

The wood body is represented by a linear elastic rectilinear orthotropic material model, for which the 2D parameters are given in Table 2. Wood parameters were used in a stochastic fashion, where normal distribution was found for all parameters except for the stiffness (Berblom Dahl 2009). Fracture softening of wood adhesive bonds has been studied

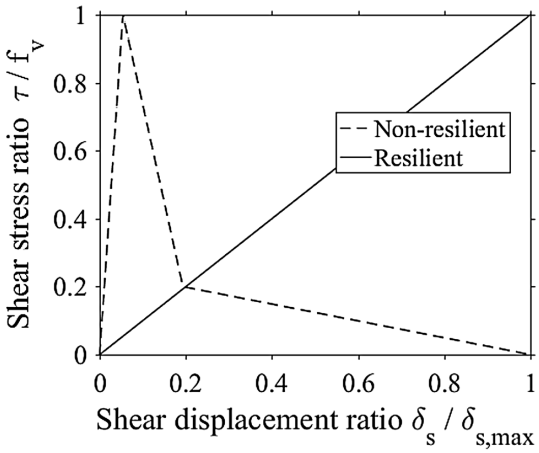

Fig. 3 A linear shear stress-displacement behaviour was used for the resilient bond lines, while a bilinear model was used for the non-resilient

Table 2 Adopted material parameters for wood (Berblom Dahl 2009). Parameters are given in MPa and [-] with corresponding coefficient of variation (CV). Fracture energies are given in Nm/m^2 representing PUR adhesives in wood lap joints (Wernersson 1990)

	Direction	Mean	CV
Young's modulus // grain[a]	E_L	9040	0.38
Young's modulus ⊥ grain	E_R	790	0.28
Shear modulus	G_{TL}	600	0.30
Poisson's ratio	υ_{TL}	0.06	0.07
Shear strength	f_v	4.4	0.38
Tensile strength	$f_{t,90}$	4.9	0.15
Tensile fracture energy	$G_{f,I}$	230	0.14
Shear fracture energy	$G_{f,II}$	850	0.10

[a]Lognormal distribution

by Wernersson (1990), from whom relevant fracture energy values are found.

A load controlled analysis without artificial stabilization was used in the numerical simulations. Symmetry was regarded on the geometry built up by first order plane stress solid elements with 4 nodes and full integration. Cohesive elements were used for the bond line. Failure was evaluated using a stress based Norris failure criterion (Norris 1962) for the resilient bond line while the maximum strength of the propagating fracture was adopted for the non-resilient bond line. Two sets of numerical analyses were conducted:

1. Numerical shear strength comparison between resilient and non-resilient bond lines. The boundary conditions were set in order to achieve a dominant shear action in the lap joint by restricting the horizontal movement of the specimen legs. In comparison to the boundary conditions illustrated in Fig. 1, roller supports are in this set replaced by fixed supports and thus the shackle does not need to be included. A bond line thickness of 1 mm was used regardless of bond line type. The experimental geometry was otherwise reproduced.
2. Detailed comparison to the tests. Comparison to test results are made with the more realistic boundary conditions according to Fig. 1 as presented in Sect. 3.2 using a horizontal linear elastic spring to represent the shackle ($k = 35$ kN/mm).

A screening process for important factors was conducted using a two-level fractional factorial 2^{9-4}_{IV} design for the resilient and non-resilient model individually (Box et al. 1978). The analysis included 9 geometric and material parameters with a variation of ±10% including failure strengths, fracture energies and axial stiffness of the members. A full factorial 3^4 design was then conducted to discover possible non-linear responses and interactions between analysed factors, which is not possible in a common one-factor-at-the-time sensitivity analysis. The four most influential material parameters were then inserted as stochastic variables in order to possibly verify a strength increase of the resilient bond line regardless of the natural variability of wood.

2.3 Analytical study

2.3.1 Shear stress distribution

The analytical expression used for determination of the shear stress distribution and bond line strength is based upon the Volkersen theory (Volkersen 1938) as presented in Gustafsson (2008). For the compression–compression load configuration used in the test, but neglecting bending, the 1D shear stress distribution of the bond line τ_3 is found being

$$\tau_3(x) = C_1 \cosh(\omega x) + C_2 \sinh(\omega x)$$

$$C_1 = \frac{PG_3}{t_3\omega}\left(\frac{1}{E_1A_1\tanh(\omega L)} + \frac{1}{E_2A_2\sinh(\omega L)}\right) \quad (1)$$

$$C_2 = \frac{PG_3}{t_3\omega}\left(\frac{-1}{E_1A_1}\right)$$

$$\omega L = L\sqrt{\frac{G_3b_3(1+\alpha)}{t_3E_1A_1}} \quad \alpha = \frac{E_1A_1}{E_2A_2} \leqslant 1.0$$

The shear stress distribution of the bond line (index 3) is thus governed by the properties of the two adherends (index 1 and 2) and the bond line properties: cross-sectional area A,

longitudinal stiffness E, bond line length L, width b_3, thickness t_3 and shear stiffness G_3.

By identifying the maximum shear stress at $x = 0$ and introducing the material shear strength, the load carrying capacity P_f can be determined by

$$P_f = b_3 L f_v \frac{(1+\alpha)\sinh(\omega L)\tanh(\omega L)}{\omega L(\sinh(\omega L)+\alpha\tanh(\omega L))} \quad (2)$$

As $\tanh(\omega L) \to 1.0$ for large ωL, i.e. for large lap lengths, Eq. (2) can be reduced to

$$P_f \approx b_3 L f_v \frac{(1+\alpha)}{\omega L} \quad (3)$$

The approximation deviates less than 0.5% from the exact solution for $\omega L \geqslant 6$. The Volkersen theory does not include bending, which however does occur in the test setup. Equation (1) is plotted for increasing lap length in Fig. 5.

2.3.2 Definition of a 'long' lap joint

The study presented in this paper argues for the benefits of a resilient bond line in long lap joints. Although the term 'long lap joint' is used in literature, a definition of what can be considered a long lap joint is lacking. As hinted by Volkersen theory above, the definition of a long lap joint must be put into perspective of the adherends and the bond line. To obtain an estimate of the length needed for positive influence of a resilient bond line, the brittleness ratio of lap joints λ can be used. (Gustafsson 1987).

The normalized mean shear stress at failure is governed by the brittleness ratio λ of lap joints. To achieve a high utilization ratio of the bonded area, it is important to have a low brittleness ratio. Using the strength limits of ideal plasticity and linear elastic fracture mechanics (LEFM), it is possible to identify an approximation of the recommended maximum value of λ which allows for a high efficient lap joint as

$$\lambda = \frac{l^2 f_v^2}{t_1 E_1 G_f} \leqslant 2(1+\alpha) \quad (4)$$

where α is defined in Eq. (1) and t_1 is the thickness of element 1. If a resilient bond line is used, then $G_f = f_v^2/2G_3$. The limitations of LEFM should be noted as well as the fact that bending is not included in Eq. (4). To meet the recommended brittleness ratio, a reorganisation of Eq. (4) suggests that a resilient bond line should be used for lap lengths over 420 mm for the geometry used in the experimental study ($\alpha = 0.61$).

3 Test results

The experimental results are presented, starting with the parameter study of the rubber-adhesive bonding. The optimal rubber treatment method was then used for the main study of the influence of lap length on the load carrying capacity of the joint. The section also includes results from the tests of different boundary conditions as well as the different means of achieving a resilient bond line.

3.1 Bonding between rubber and adhesive

Table 3 summarizes the load at failure of the rubber specimens treated by different methods in order to increase the surface energy. The importance of an adequate rubber treatment prior to bonding cannot be underestimated as this simple test suggests a strength increase of up to 60 times by using a combination of 30 s of acid etching after rigorous sanding. In order to achieve a strong bond of the SBR/NR rubber, the initially shiny surface must be sanded until a matt surface is obtained.

3.2 Lap length series

The strengths of the non-resilient PUR-series and the resilient SBR-series were compared for increasing lap lengths and the results are compiled in Table 4, also including the two specimens with smaller steel plates on member ends. It is found that this experimental study shows no significant strength increase by using a low stiffness bond line.

All non-resilient specimens showed a brittle failure in wood close to the bond line. Two types of failure modes

Table 3 The effect of rubber processing steps on tensile strength

Category	Treatment				Average force at failure (N)
	Water	Ethanol	Sanding[a]	Etching[b]	
1	–	–	–	–	0
2	x	–	–	–	5
3	x	x	–	–	5
4	x	x	+	–	15
5	x	x	++	–	50
6	x	x	+	+	140
7	x	x	+	++	130
8	x	x	++	+	310
9	x	x	++	++	90
10	x	x	–	++	30

[a] + Corresponds to 5 s by belt sander while ++ is 30 s (results in a matt surface)

[b] + Corresponds to 30 s submerged in concentrated sulphuric acid while ++ is 3 min

Table 4 Failure load and strength from experimental tests for conventional non-resilient adhesive and the low stiffness resilient SBR/NR with increasing lap length. Strength is the average shear stress at failure and the coefficient of variation of the average is found in parenthesis

Length, mm	Test	Non-resilient (PUR-series)			Resilient (SBR-series)		
		Failure mode[a]	Failure load, kN	Strength, MPa	Failure mode	Failure load, kN	Strength, MPa
200	1	1	359	3.99	1	490	5.45
	2	1	373	4.15	2	420	4.67
	3	1	461	5.12	2	361	4.01
	4	1	441	4.90	1	400	4.44
	Avg		410 (0.12)	4.5		420 (0.13)	4.6
400	1	1	941	5.23	1	687	3.82
	2	1	940	5.22	1	769	4.27
	3	1	716	3.98	1	759	4.22
	4				1	814	4.52
	Avg		870 (0.15)	4.8		760 (0.07)	4.2
700	1	1	1168	3.71	2	911	2.89
	2	1	1285	4.08	2	692	2.20
	3	1	1242	3.94	2	912	2.89
	4	1	1480	4.70	1	1172	3.72
	5				1	1169	3.71
	6				1	1537	4.88
	Avg		1290 (0.10)	4.1		1070 (0.28)	3.4
700 s	1	1	790	2.52	1	1150	3.65

[a]1: Wood failure close to the bond line, 2: Premature failure in glue-rubber interface

were visible in the resilient specimens. Some resilient specimens failed in similar wood bond line failure to the non-resilient specimens, while others failed prematurely in the adhesive-rubber interface as indicated in Table 4. In these cases, visual inspection subsequent to failure indicates poor rubber treatment, in which some rubber areas were of type category 6 instead of the intended category 8 (Table 3) which is believed to initiate the premature failure. Excluding the premature failures from the SBR-700-series results in an average failure load of 1290 kN, the same as for the PUR-700-series.

For a vast majority of the test specimens, a tensile crack perpendicular to grain was formed centrically in the low end of the middle member (prior to final failure due to shear at the bond line) due to perpendicular-to-grain tensile stresses, at the location of the reinforcement screws. The crack did not influence the global behaviour of the lap although an irregularity in the displacement plot was observed, for example at approximately 700 kN for SBR-700-4 in Fig. 4.

A comparison of the deformation of the resilient and non-resilient bond lines are found in Fig. 4. By introducing the 3.5 mm thick SBR/NR sheet, the measured stiffness over the bond line was reduced by a factor of approximately 30. The test results regarding the influence of boundary conditions indicate a greater sensitivity in the non-resilient specimen than in the resilient one.

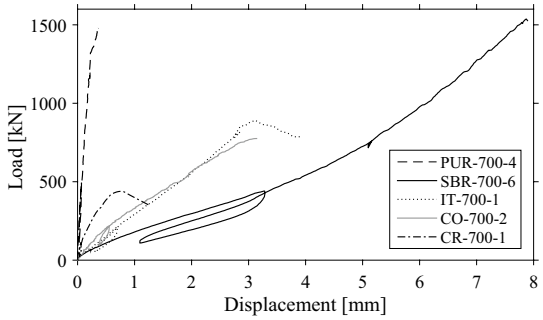

Fig. 4 Load–displacement comparison between the different types of bond lines investigated

3.3 Type of resilient bond line

To investigate the possibility of simplified manufacturing, the SBR/NR was experimentally compared to CR, Move IT and CO, in which the latter was supposedly more easily manufactured than the former.

The results shown in Table 5 suggest that the CR was not as strong as the SBR/NR. The resilient adhesives Move IT and RESA HLP-H enabled very simple production, although

Table 5 Four resilient bond lines compared also to common adhesive using a lap length of 700 mm. Failure load, strength and stiffness with coefficients of variations are presented. *n* is the number of specimens, *t* is the bond line thickness and premature SBR specimens are excluded

Type	n	t, mm	Failure mode[a]	Failure load, kN	Strength, MPa	Stiffness, kN/mm
SBR/NR	3	3.5	1	1290 (0.16)	4.1	230 (0.07)
CR	2	0.5	2	360 (0.30)	1.2	720 (0.11)
IT	2	2	2	760 (0.25)	2.4	270 (0.03)
CO	2	1.5	2	730 (0.09)	2.3	260 (0.18)
PUR	4	0.1	1	1290 (0.10)	4.1	5470 (0.10)

[a]1: Wood failure close to the bond line, 2: Premature failure

it was difficult to obtain a uniform bond line using Move IT due to the high viscosity. Both the CO and IT specimens also showed premature failure, now in the adhesive/wood interface.

The stiffness of the resilient bond lines is to a large extent dependent on the thickness of the layer, which depends on the type of bond method. Figure 4 compares typical load-deformation curves of the different bond lines investigated in this study.

4 Numerical analysis

The results of this study comprise numerical and experimental analyses comparing resilient to non-resilient bond lines, as well as influencing parameters. In this section, two sets of boundary conditions have been used according to Sect. 2.2, presented in the different subsections.

The numerical analyses indicate an increasing strength difference in favour of the resilient bond line as the lap length increases, which however is in disagreement with the presented experimental results. However, it is the authors' belief that the discrepancy between the results is due to possible inadequateness of boundary conditions adopted in the laboratory tests and production difficulties.

4.1 Double lap joints with minimal bending influence

Boundary conditions were set in order to minimize the bending effects in the specimen according to type 1 in Sect. 2.2. For the double lap joint geometry shown in Fig. 1 using deterministically increasing length, independent stochastic material parameters were inserted in a numerical strength analysis. The stochastic material parameters were the shear strength f_v, shear fracture energy G_f, normal stiffness of wood E_L and tensile strength perpendicular to grain $f_{t,90}$. The results of 700 stochastic numerical simulations are shown in Fig. 5 using a 2nd order polynomial fit with corresponding 95% confidence interval. A decreasing average shear stress at failure is visible for both the conventional and the bond

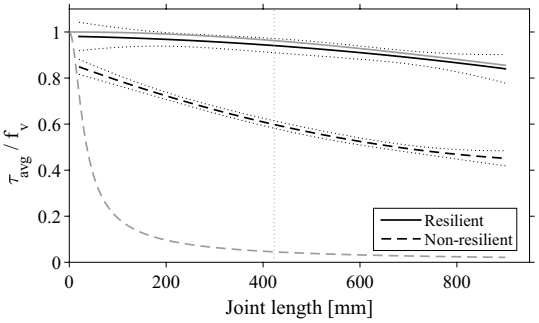

Fig. 5 Normalized shear stress at failure for increasing joint length. Quadratic polynomial fit to numerical stochastic analysis is indicated by black lines according to legend with corresponding 95% confidence dotted adjacent ($R^2_{resi} = 0.034$, $R^2_{n.resi} = 0.498$). Analytical results according to Volkersen theory in grey where a good resemblance is found for the resilient bond line while very poor for the non-resilient. The vertical dotted line represents the suggested lap length limit according to Eq. (4)

lines with low stiffness for increasing lap length, although the effect is less pronounced in the latter case.

To evaluate the applicability of the Volkersen theory on this specific design, a comparison is made to the numerical analysis in Fig. 5. A good agreement is found between analytical and numerical results for a resilient bond line, while very poor agreement for non-resilient bond lines primarily due to the fact that fracture softening is not taken into account in the Volkersen theory.

The numerical analysis indicates that damage is initiated in the non-resilient design at approximately 70% of maximum load, while no damage is modelled for the resilient bond lines.

To obtain a better understanding of the parameters influencing the strength of adhesive lap joints, a factorial design study was conducted. Out of nine material and geometrical parameters analysed, the four most influential were further studied in a full 3^4 factorial design from which the results are presented in Fig. 6. The analysis was conducted for a base bond line length of 500 mm, and all parameters were independently varied ±10% from the reference values discussed in Sect. 2.2. The numerical analysis is based upon an

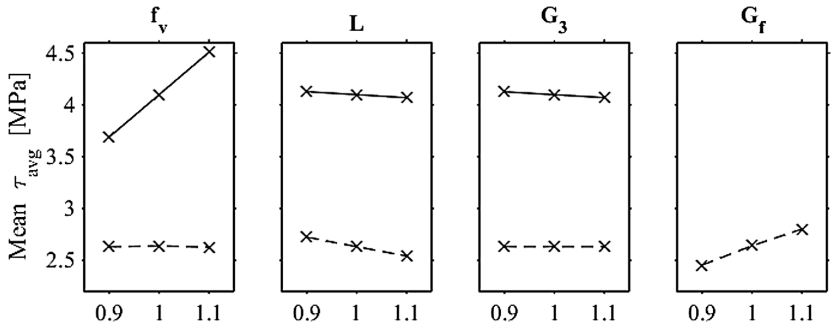

Fig. 6 Parameters that significantly influence the average shear stress at failure according to full factorial 3^4 design using a $\pm$ 10% variation of reference values: shear strength f_v, lap joint length L, stiffness of the bond line G_3 and shear fracture energy G_f. Resilient bond line as solid line while non-resilient as dashed line. Reference values are found in Sect. 2.2

ideal lap joint comparing geometrically similar resilient and non-resilient bond lines.

The factorial design clearly highlights the fundamental differences between resilient and non-resilient bond lines. Due to high stress concentrations in the stiff non-resilient bond line, a shear strength increase does not influence the load carrying capacity, which is more dependent on the fracture energy. Although to some extent proportional, these material properties have been considered individually in this analysis for illustration purposes. Resilient bond lines have a strength advantage when used in long lap joints, as the average shear stress at failure does not drop at the same rate as for non-resilient bond lines for increased lap length as shown in Fig. 6. Low stiffness, by either using a less stiff or thicker bond line, increases the load carrying capacity at the expense of a decreased joint stiffness. As the stiffness of the bond line approaches zero, the strength approaches the theory of perfect plasticity.

The factorial design analysis does not suggest any parameter interaction for the resilient bond line in the analysed parameter region in terms of average shear stress over the lap area. It does however suggest a slight interaction in case of non-resilient bond line between lap length and shear strength, as well as between fracture energy and shear strength.

4.2 Comparison to test results

The numerical results in Fig. 5 indicate a considerably larger difference in load carrying capacity than found in the experimental study. To investigate this discrepancy, additional numerical simulations were conducted with boundary conditions according to the test setup. Roller supports were used, the shackle represented by a linear spring ($k = 35$ kN/mm) and bond line thicknesses of 0.1 and 3.6 mm were used for non-resilient and resilient bond line, respectively. It was found that the resilient SBR specimens were somewhat more sensitive to the shackle stiffness than the non-resilient PUR specimens, while shorter specimens were significantly more sensitive than longer ones. In comparison to the results

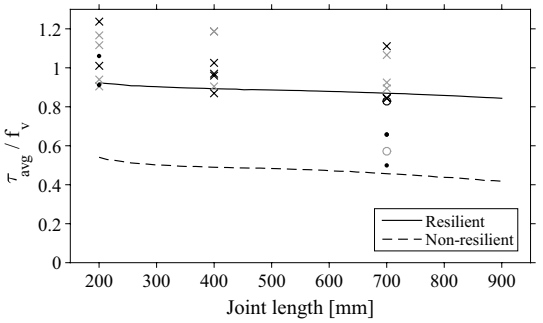

Fig. 7 Numerical results of experimental setup compared to experimental data: resilient in black while non-resilient in grey. Wood close to bondline is marked with "x", dot marks premature failures and results of the test with smaller steel plates are marked with "o"

shown in Fig. 5, the use of the shackle with finite stiffness causes a strength decrease of both types of bond lines as seen in Fig. 7. This is especially relevant for shorter lap lengths as these are subjected to larger bending moments. A general strength increase using a resilient bond line is also found in this analysis, which was however not visible in the tests.

5 Discussion

It is very difficult to achieve a uniform shear stress distribution in a lap joint due to different axial strains in the adherends at a given point of the bonded area. The consequences of this difference can however be minimized by introducing a resilient bond line, which allows the adherends to deform more independently. This conclusion is drawn from the presented numerical analysis as well as previous studies (Gustafsson 2007; Yang et al. 2015). The experimental results are however not as simple to interpret due to different failure modes and unexpected influence of boundary conditions, but the data do not falsify the numerical results.

In comparison to previous experience and the conducted numerical analysis, the high strength of the non-resilient bond lines is found interesting. All GLT specimens were manufactured and delivered at the same time. The test specimens were further produced similarly and also stored together, suggesting that the material parameters are similar for all. The parameters used in the numerical analysis are however based upon literature values rather than measured on the tests themselves. Hence it is possible that the material parameters do not necessarily consider the specific boundary conditions of this test. The load carrying capacity of non-resilient bond lines is also influenced by the fracture energy. The presented shear fracture energy of 0.85 kNm/m^2 was found at a shear failure of 3.56 MPa (Wernersson 1990), which possibly could be higher if a higher shear strength is used. The normal distribution of the shear strength suggests a 95th percentile strength of up to 7.5 MPa, which would increase the numerical load carrying capacities. However, numerical analysis indicates that this effect alone cannot explain the high strength of the non-resilient bond lines.

A large variance in the experimental results of the resilient SBR/NR was found due to premature bond line failure in the rubber/adhesive interface. The results highlight a sensitivity to rubber treatment, in which local differences are likely to initiate failure. However, this problem can be avoided by a simple but detailed visual inspection and does thus not necessarily imply a large variance in the load carrying capacity in an established production method.

A similar double lap joint test setup using resilient bond lines was included in the large resilient bond line test series presented in Gustafsson (2007). Using close to identical production method, an average shear stress at failure of 4.6 MPa was recorded for a lap area of 600×223 mm^2, which is higher than measured in this study. However, the failure also included bending failure of the two outer members of the double lap joints due to their slenderness, possibly influencing the results negatively. The higher strength is probably due to the influence of different boundary conditions.

Comparison between numerical and analytical findings suggests that the Volkersen theory is suitable for hand calculations of lap joints if (1) a resilient bond line is applied and (2) boundary conditions are such that they limit the influence of peel stress interaction in the joint design. The numerical findings of the given geometry also suggest that a strength increase by introducing a resilient bond line can be achieved at shorter lap lengths than the analytical estimate suggests.

The additional testing of smaller steel plates at end grain suggests that the non-resilient bond line is more sensitive to boundary conditions than the resilient one. The same shear stress in the bond line occurs regardless of end plate boundary conditions at a given load, resulting in insignificant influence on the numerical model in which a stress based failure criterion is implemented in the bond line. The fundamental difference is found in the wood body, where the wood volume experiencing a shear stress level close to the shear strength is considerably larger than in the case of smaller end plate. This, in combination with the weakest link theory (volume effect), is a plausible explanation for the decrease in average shear stress at failure from 4.1 to 2.5 MPa for non-resilient joints. The same reasoning is also valid for the insensitivity of the resilient bond line as no significant stress concentrations occur. When the shear stress approaches the strength of the material, nearly simultaneously for the whole lap joint, the weakest link theory predicts failure at some point regardless of end grain support.

Compared to the rubber based resilient bond lines, the manufacturing process of the IT and CO series was considerably more effective. If proper adhesion can be obtained to wood, a resilient adhesive is recommended in wood–wood lap joints. Similar to rubber based resilient bond lines, a low shear stiffness and high shear strength are important parameters for the strength of the joint. Furthermore, manufacturing is more effective if the resilient adhesive also has a high viscosity and only in need of a low curing pressure.

Redundancies should be promoted in structural design. Therefore, not only strength but also the stiffness of the connection is relevant to consider in a design phase in order to ensure the intended load path. The stiffness and slip are also decisive when several types of connectors are used in a single connection, in which simultaneous action requires similar behaviour. By using a resilient bond line, the stiffness can be designed specifically to match other connectors by varying the shear modulus of rubber and/or thickness, thus enabling the addition of strengths for different connectors.

6 Conclusion

The presented research concludes the following findings:

- Resilient bond lines can be achieved by means of adhesives with low stiffness or rubber.
- The experimental study indicates the difficulty of achieving a strong bond between rubber and adhesive, and thus a clear and reliable production method must be established.
- The experimental study shows that a long non-resilient bond line can be stronger than resilient bond line in certain conditions.
- The stiffness of lap joints with resilient bond lines can be designed with great variety.
- Numerical analysis shows that an increased load carrying capacity of lap joints can be achieved by introducing a resilient bond line due to a more uniform shear stress distribution.

- Volkersen theory is applicable to lap joints with resilient bond lines.
- An analytical relation is proposed as definition of a long lap joint.

Despite the somewhat contradictory experimental results, the authors conclude that properly manufactured resilient bond lines do increase the load carrying capacity of long lap joints.

The use of resilient bond lines is not limited to wood–wood configurations. The study is conducted within a project regarding the "Shear plate dowel joint" (SPDJ), which uses the resilient bond line technique in a wood-steel configuration with intended use in heavy timber structures.

Acknowledgements The financial support provided by *Formas* through grant 2012-879 is gratefully acknowledged. The authors would like to thank Thomas Johansson at Moelven Töreboda AB for delivering the GLT as well as Ante Salomonsson at Sika and Steffen Harling at Collano for adhesives and expertise. We would also like to thank Tommy Pettersson at Trelleborg AB for delivering the CR and to Maria Södergren for her expertise in handling strong chemicals. Special thanks also to Per-Olof Rosenkvist and Per-Erik Austrell, LTH.

References

Austrell P-E (1997) Modeling of elasticity and damping for filled elastomers. PhD thesis, Lund: Lund University

Berblom Dahl K (2009) Mechanical properties of clear wood from Norway spruce. PhD thesis ISBN 978–82-471-1911-2 ed. Trondheim, Norway: Norwegian University of Science and Technology

Box GEP, Hunter WG, Hunter JS (1978) Statistics for experimenters. Wiley, New York

Danielsson H, Björnsson P (2005) Strength and creep analysis of glued rubber foil timber joints, s.l.. Master thesis, Lund University

Dillard D, Pocius A (2002) The mechanics of adhesion. s.l.. Elsevier, Amsterdam

Gustafsson PJ (1987) Analysis of generalized Volkersen joints in terms of non-linear fracture mechanics. In: Proc of European Mechanics Colloquium 227 "Mechanical behavior of adhesive joints", pp 323–338

Gustafsson PJ (2007) Tests of full size rubber foil adhesive joints, s.l.: Structural Mechanics, Lund University

Gustafsson PJ (2008) Tests of wooden cleats oriented along fibre, structural mechanics. Lund University, Lund

Larsson G, Gustafsson PJ, Serrano E, Crocetti R (2016) Bond line models of glued wood-to-steel plate joints. Eng Struct 121:160–169

Norris CB (1962) Stength of orthotropic materials subjected to combined stresses. U.S. Department of Agriculture, report No. 1816, Madison

Serrano E, Gustafsson PJ (2006) Fracture mechanics in timber engineering—strength analyses of components and joints. Mater Struct 40:87–96

Sumiyoshi T, Matsui G (1991) Wood joints in classical Japanese architecture. Kajima Institute Publishing, Japan

Volkersen O (1938) Die Nietkraftverteilung in zugbeanspruchten Nietverbindungen mitkonstanten Laschenquerschnitten (The rivet load distribution in lap-joints with members of constant thickness subjected to tension) (In German). Luftfahrtvorschung 15:41–47

Wernersson (1990) Wood adhesive bonds, fracture softening properties in shear and in tension. s.n, Lund

Yang H, Crocetti R, Larsson G, Gustafsson P-J (2015) Experimental study on innovative connections for large span timber truss structures. In: Proceedings of the IASS Working Groups 12 + 18 International Colloquium 2015 International Association for Shell and Spatial Structures (IASS), Tokyo, Japan, s.n

Zwerger K (2000) Wood and wood joints, building traditions of Europe and Japan. Birkhäuser, Berlin

Paper B

Proceedings of the IASS WORKING GROUPS 12 + 18 International Colloquium 2015
"Bio-based and Bio-inspired Environmentally Compatible Structures"
10 to 13 April 2015, Tokyo Denki University, Tokyo, Japan
Andreas FALK, Petr VEGH and John CHILTON (eds.)

Experimental study on innovative connections for large span timber truss structures

Huifeng YANG *, Roberto CROCETTI [a], Gustaf LARSSON [a&b], Per Johan GUSTAFSSON [b]

* College of Civil Engineering, Nanjing Tech University
P.O. Box 80, NO. 30, South Puzhu Rd. Nanjing, China
yhfbloon@163.com

[a] Division of Structural Engineering, Lund University, roberto.crocetti@kstr.lth.se

[a&b] Division of Structural Engineering, and Division of Structural Mechanics, Lund University, gustaf.larsson@construction.lth.se

[b] Division of Structural Mechanics, Lund University, per-johan.gustafsson@construction.lth.se

Abstract

This paper summarizes an experimental investigation on several innovative reinforcing techniques for the "Single Large Diameter Dowel Connection", SLDDC in timber truss structures. Besides lateral reinforcing or prestressing also steel plates glued on two sides of the glulam specimens were used as reinforcing measure. To study the efficiency of these techniques, 15 full-scale quasi-static tensile tests on glulam members with a SLDDC on either ends of each member were performed. It was found that the reinforcing techniques produced significant increase in the bearing capacity of the SLDDCs. All of the reinforcing techniques showed a quite efficiency, in which the splitting of wood can be prevented. Moreover, the residual strength of most of the specimens remains at a high level.

Keywords: timber structure, truss, singe large-diameter dowel connection, reinforcement, improvement, experimental study

1. Introduction

Timber trusses are competitive for relatively large spans, typically larger than 30 m. For such span lengths, however, the magnitude of loads which have to be transferred between truss members becomes significant, often resulting in complex (and expensive) connections.

To find simpler large dowel connections for timber structures, several studies have been carried out. Haller et al. [1] produced and tested some textile reinforcements on the large dowel connections with different textile structures like biaxial weft knitted and stitch bonded. It showed significant increase on the strength, stiffness and also ductility of the connections. The plug shear and splitting failure of the wood are avoided. However, the ultimate fracture is the wood tensile failure because of the stress concentrations and the reduced net cross section. Also, multi inserted reinforcement layer will result in the relative complex and expensive production process.

Kobel [2] conducted an experimental study on the reinforcement of large dowel connections for timber truss structures, in which the dowel has a diameter of 90mm. The study presented several reinforcement methods including reinforcing with self-tapping screws of various configurations and lateral prestressing with threaded rod. It was found that reinforcing screws can effectively impede splitting of the timber and as a result of the remarkable increase of the bearing capacity. By applying lateral prestresses, no splitting occurred and the bearing capacity is even higher.

Pavkovic´ et al. [3] investigate the bearing capacity of reinforced large diameter dowel connections loaded perpendicular to grain of timber with experimental and FEM analytical work. For the glass fiber textile layers reinforcement glued between the timber lamellas, the result demonstrated remarkable enhancement of the strength and ductility of the connections.

In this research, several efficient and relatively inexpensive reinforcement methods of SLDDCs were presented. By means of experimental investigations, the aim of this paper is to study the efficiency of different types of innovative reinforcing techniques for the SLDDC.

2. Material and methods

2.1. Wood materials

Spruce glulam with the strength class of GL30c was used for all of the 15 glulam specimens in the test. The characteristic tensile strength parallel to the grain of $f_{t,0,k}$ = 20 MPa. The average density and the moisture content was 443 kg/m^3 and 11.1%, respectively. And they were measured after testing on samples taken from the part of the specimen where failure had occurred (i.e. from the shear plug). These values varied in the range of 324 ~ 551 kg/m^3 for density and 8.9 ~ 13.4 % for MC.

2.2. Steel

The steel plates and the large diameter dowel were all made of steel quality Q345B, with a nominal yield stress of 345 MPa. The threaded rods, with a diameter of 24 mm, had a nominal yield stress of higher than 800 MPa. The large diameter dowels had a hollow cross section with the outer diameter of 89 mm and the inner one of 38 mm. The yield strength was 320 MPa for the hexagon head wood screws with 6 mm in diameter and 70 mm in length.

2.3. Rubber

The rubber was mixed of natural rubber and SBR (styrene-butadien), of which the density is 1220 kg/m^3, the hardness is 62°, the shear modulus G≈1.2 MPa, the tensile strength is 22.4 MPa, the shear strength is 9.4MPa and the elongation at break is 595 %. The thickness of the rubber layer vulcanized to steel plates was 1.0-1.2 mm. The outer surface of the vulcanized rubber layer was treated by the sulfuric acid in order to get a satisfy bonding between the timber and rubber layer.

2.4. Glue

The glues used in vulcanized steel – glulam interface were Purbond CR 421 (glue+hardener). While the glues used in smooth steel – glulam interface were epoxy (glue+hardener).

2.5. Layout of the reinforcement

The test series were divided into five groups of three specimens each.

The specimens of the group "Non-Pre" and "Pre" had dowel holes with 92 mm diameter in both end of the glulam specimens, implying they were 3 mm larger than those of dowels. The area between the dowel and the loaded end was reinforced using a threaded rod (See Fig. 1(a) and Fig. 1(b)). Meanwhile for the load transmission from the threaded rods to the glulam, a 30 mm thick steel plate was also used. The prestress in the threaded rods of group "Pre" was about 3.8 MPa while applying at about three month before the test. As to group "Non-Pre", it had no prestress inside the threaded rods. The threaded rods acted as the reinforcement of the timber perpendicular to the grain.

The specimens of the group "S2" and "S2+R" presented reinforcement by bonding steel plates to the glulam surfaces around the large dowel holes. The hole diameter of glulam and steel plates was 102 mm and 91.5 mm respectively. It means a 6.5 mm gap between the dowels and the glulam specimens aimed to transfer the applied loads from dowel to timber by bond shear stress of the vulcanized steel – glulam interface. The major difference between these two groups was that the bonding surface of group "S2" was smooth steel, while group "S2+R" was vulcanized rubber layer onto the steel plates (See Fig. 1(c) and Fig. 1(d)).

The specimens in the group named "S1+R" were also reinforced by bonding steel plates but with a doubled glulam elements (See Fig. 1(e)). Furthermore, in all of the bonding steel plates reinforced specimens, each steel plate was anchored by 34 wood screws in order to bear the normal stress at the bonding interface as well as give the pressure while gluing.

The lamellae thickness was 45 mm for glulam specimens. The specimens in the group named "S1+R" (See Fig. 1(e)) had a doubled glulam elements with each had a cross section of 61 mm × 405 mm. And the other groups of specimens had a single cross section of 140 mm × 405 mm. All the glulam specimens were 2, 00 m in length.

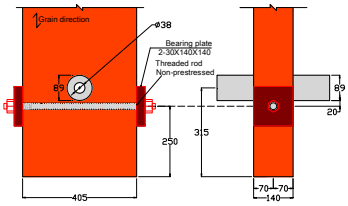

(a) Group "Non-Pre"

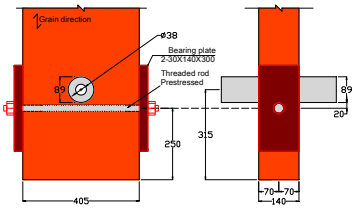

(b) Group "Pre"

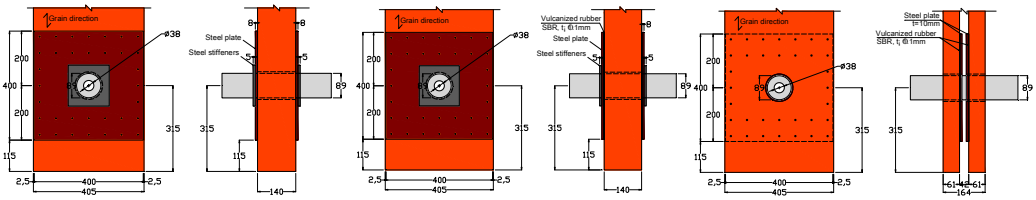

(c) Group "S2" (d) Group "S2+R" (e) Group "S1+R"

Figure 1: Configuration of test specimens. Units: [mm]

2.6. Test setup

All tests were conducted at the Jiangsu Key Laboratory of Civil Engineering, Disaster Prevention and Mitigation, Nanjing Tech University. The general setup for all of the specimens is illustrated in Fig. 2. The tests were quasi-static tensile tests under displacement control and the actuator speed was 0.5 mm/min. Each specimen was equipped with an identical design of reinforced SLDDC on both ends. The loads were applied by the loading rods or loading plates between the dowels and the hydraulic device.

The dowel slip as well as the lateral deformation was continuously measured in both end of the specimens for group "Non-Pre" and "Pre". As to the other three groups, only the steel plate slip was measured.

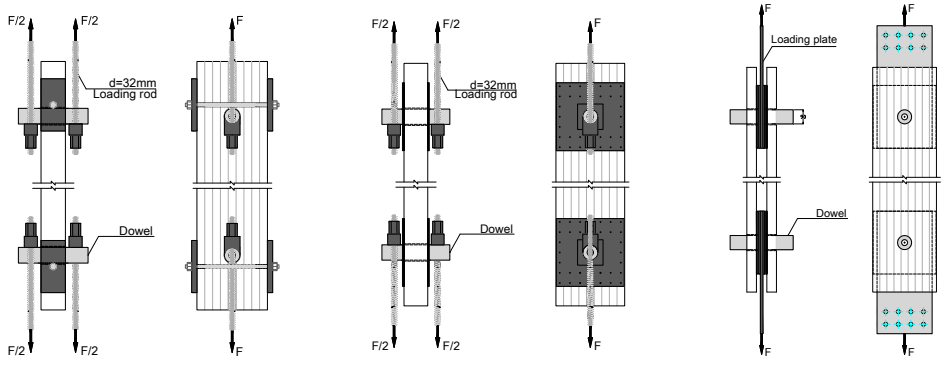

(a) Group "Non-Pre" and "Pre" (b) Group "S2" and "S2+R" (c) Group "S1+R"

Figure 2: General test setup.

3. Results and discussions

3.1. Bearing capacity

Table 1 displays average values of the test results for the specimens. And Fig. 3 gives a comparison on the bearing capacities and the residual strength of different groups. For a comparison, some of the test results of

Kobel [2] are also presented here. From Table 1 and Fig. 3 it can be seen that the bearing capacity of the SLDDCs were significantly increased due to the reinforcements. And the gains in bearing capacity range from 46% to 639%.

For the reinforcement by bonding steel plate with vulcanized rubber layer, e.g. for the specimens in group "S1+R" and "S2+R", the bearing capacities were most greatly improved. It is considered that the introduction of the rubber layer lead to a big decrease of the stress concentration at the bonding interfaces. As a comparison, the bearing capacity of group "S2", in which the reinforcement was by bonding smooth steel plate, the gains in bearing capacity was much less than those of group "S2+R", despite its gains reached to 64%.

Lateral non-prestressing or prestressing is also effective way to improve the load bearing capacities of the SLDDCs. The bearing capacities were 46% and 122% higher than those of non-reinforced "Basic" specimens. As compared to Group "Dywidag" in Kobel [2] (See Fig. 4) with a prestress of about 3.1 MPa, the bearing strength of group "Pre" had no obvious difference. In other words, it can not be seen the notable effects on the bearing capacity by the location of the prestressed rods and the magnitude of the prestress values.

Table 1: Summary statistics of the test results

Specimen group and no.	Bearing capacity F_{max} [kN] Mean (STDV[2])	Residual Strength F_{res} [kN]	$(\frac{F_{res}}{F_{max}})_{mean}$	Density ρ [kg/m^3]	Moisture content MC [%]
Basic[1]	134 (4.1)	0	0	523	12.1
Non-Pre	195 (3.7)	95	49	433	11.0
Pre	298 (7.9)	47	16	456	10.9
S2	220 (22.9)	112	51	423	11.5
S2+R	990 (11.6)	57	6	457	11.4
S1+R	755 (7.4)	347	46	443	10.9
Dywidag[1]	306 (9.4)	90	29	392	9.2

Note: 1. From Kobel [2]; 2. STDV refers to coefficient of variation. Hereby the bearing capacity of another end which stayed intact was conservatively taken as the same as that of failure end. So the sample size was six for each group.

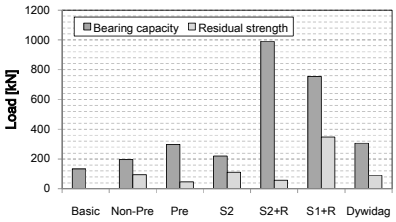

Figure 3: Bearing capacities and residual strength

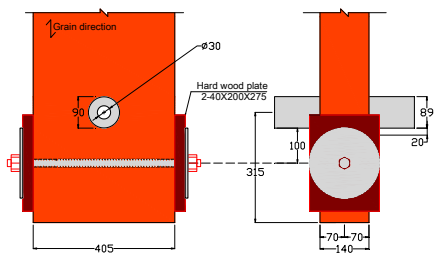

Figure 4: Configuration of "Dywidag" from Kobel [2]

The residual strength was defined here as the minimum load just after the first failure of the specimen. The values of the residual strength for group "Non-Pre", "S2" and "S1+R" were about 50% of the maximum load. For group "S2+R" and "Pre" the value was only 6% and 16%, respectively. The maximum residual strength of 347kN was recorded by group "S1+R" and it was due to the failure just occurred in one side of the specimen (It is considered of the effect of the loading eccentricity by the test arrangement). After this first failure, another side was also able to bear a high load. For group "S2+R", F_{res} to F_{max} ratio was only 6% because of the high load and the sudden failure. And the specimen would bear a big impact load from the fracture and thus result to a very small residual strength.

Another interesting phenomenon occurred in the load-displacement curves recorded by the test machine for group "S2". After the first failure and the recorded residual strength, the load increased to a higher level

compared to the F_{max}. And then the load dropped and again increased to a high level, so back and forth several times (See Fig. 5). This observation indicates that this kind of specimen failed gradually in the last load stage. This may due to the fracture of the bonding surface near the load end caused by the stress concentration, and then some load was transferred to the wood screws nearby. While the second bonding fracture occurred with the increasing load, growing number of wood screws participated in the work. As a result, the ultimate load was usually higher than that at the first failure.

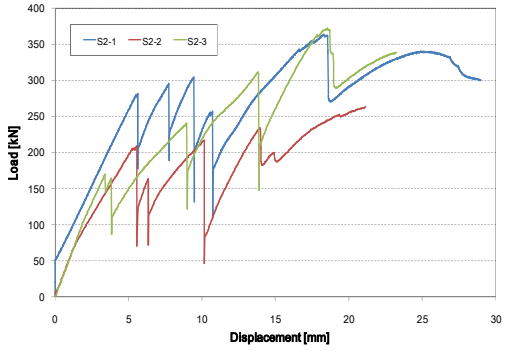

Figure 5: Load-displacement curves of group "S2"

3.2. Failure mode

For the SLDDCs with lateral reinforcement, the ultimate failure mode was a shear plug fracture (See Fig. 6). For a comparison, giving a prestress in the lateral reinforcement would generally lead to a larger shear plug and so as to reach a higher bearing capacity. It showed that even when there was no prestress in the rods, not any splitting appeared in the glulam specimen.

(a) Group "Non-Pre" (b) Group "Pre"

Figure 6: Failure modes of SLDDCs with lateral reinforcement

For the bonding smooth steel plate reinforced specimens, the failure caused by the first bonding shear fracture between the steel plate and glulam. And then the rest of the bonding layer combined with some of the wood screws worked together to bear the applied load, till to the failure of the whole bonding surfaces (See Fig. 7(a)). While for the group "S2+R", with a rubber layer, the ultimate failure showed a fully wood shear failure around the bonding area (See Fig. 7(b)). The average value of the shear stress at ultimate load reached to 3.1 MPa. As to group "S1+R", with a double glulam specimens, the failure mode was combined the wood shear failure and tensile failure (caused by the load eccentricity for the glulam), see Fig. 7(c).

Another observation was that there was also the shear plug failure for the SLDDCs reinforced with bonding steel plates. However, it did not mean that it is a failure mode of this kind of specimens. For the reason of that this shear plug was just caused by the large impact load while the wood shear failure, i.e. the shear plug occurred just after the failure.

(a) Group "S2" (b) Group "S2+R" (c) Group "S1+R"

Figure 7: Failure modes of SLDDCs reinforced with bonding steel plates

3.3. Stiffness

The Load-slip stiffness is steel plate slip for the group "S2", "S2+R" and "S1+R". While it is dowel slip for the other groups, groups in Kobel [2] is also included. And it was determined as the rate of dowel or steel plate slip in load direction between 0.4 F_{max} and 0.7 F_{max}.

Due to the test arrangement error, the dowel slip values were unfortunately not valid. But it can be seen from the test result of Kobel [2] that the lateral reinforcement has no contribution to the stiffness. For group "S2", there was quite little slip before the first failure, implying quite high slip stiffness. And due to the load eccentricity of the glulam in group "S1+R", the slip value was also invalid. So only the slip value of group "S2+R" was recorded. According to the sip value of this group, the stiffness (484 kN/mm) was obtained and gave a comparison with group "Basic" (308 kN/mm) and "Dywidag" (311 kN/mm) from Kobel [2]. So the gains of the stiffness was about 57% for group "S2+R" to group "Basic" and "Dywidag".

The load-slip behaviour of group "S2+R" was given in Fig. 8. There was a quite small variation in the stiffness and the bearing capacity. The relative smaller bearing capacity of S2+R-1 was due to the eccentricity caused by the big load to the test equipment. And then an update was provided to the other two specimens in this group. It could also be observed from Fig. 8 that there was an increasing stiffness during the late loading stage due to the strain hardening of the rubber layer.

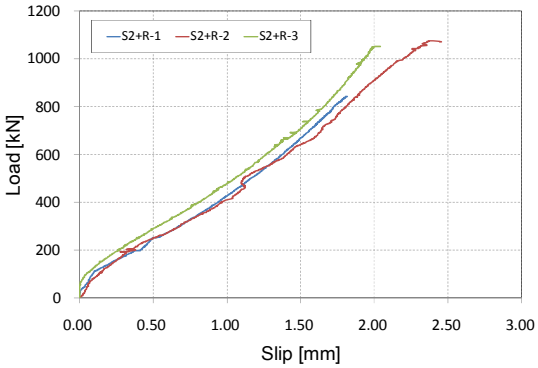

Figure 8: Load-slip behaviour in group "S2+R"

4. Conclusions and future work

From the results of the full-scale test series for SLDDCs the following conclusions can be drawn:

- Lateral reinforcing or prestressing are both able to prevent the splitting, but lateral prestressing will lead to a larger bearing capacity.
- The location of the prestressed rods around the dowel hole in glulam specimen appears to has little effect on the bearing capacity.

- The prestress may be reduced to some level since it is so close in the bearing strength between the groups "Dywidag" (prestress was about 3.1 MPa) and "Pre" (prestress was about 3.8 MPa).
- The reinforcement with bonding steel plates to the glulam is a quiet efficient way to the SLDDCs, especially while a rubber layer is vulcanized to the steel plates. The gains in bearing capacity reached to 639%. The main reason is the considerably reduced stress concentration and therefore come into a quite uniform shear stress distribution on the bonding surfaces.
- The slip stiffness of the group with a rubber layer on the steel plate can also be increased into a high level compared to the control "Basic" group.
- For a bonding smooth steel plate reinforcing, the gains in bearing capacity was much less than that had a rubber layer. But even so, its gains reached to 64%.

From the test and the observation, further studies should be carried out including:

- The lateral prestressing with a lower level should be taken into consideration.
- In order to further improve the efficiency of the bonding steel plate reinforcement, different kinds of shapes and placement of steel plate need to be studied.
- Since the wood screws can prevent the sudden fracture of the bonding smooth steel plate reinforcement, it is noteworthy that the arrangement of the wood screws should also an important factor on the bearing capacity as well as the slip stiffness.
- For the group with bonding steel plate vulcanized a rubber layer, some measures should be taken so as to endure the sudden impact load on the glulam specimen caused by the fracture at a very high load level.
- Numerical model is a more efficient and economical way to carry out some parametric analysis and also the stress distribution study.

Acknowledgement

The cooperation received from Moelven Töreboda AB (http://www.moelven.com) for the supply of glulam and Henkel for the Purbond CR 421 glue. Also we would like to thank master students Wenxiang Zhu and Wei Xu from Nanjing Tech University for the hard and valuable test work.

References

[1] Haller P., Birk T., Offermann P. and Cebulla H., Fully fashioned biaxial weft knitted and stitch bonded textile reinforcements for wood connection. *Composites: Part B*, 2006; 37; 278-285.

[2] Kobel P., Modelling of strengthened connections for large span truss structures. *Master's Thesis*, Department of Structural Engineering, Lund Institute of Technology, Sweden; 2011.

[3] Pavkovic´ K., Rajčić V. and Haiman M., Large diameter fastener in locally reinforced and non-reinforced timber loaded perpendicular to grain. *Engineering Structures*, 2014; 74; 256–265.

Paper C

Engineering Structures 121 (2016) 160–169

Contents lists available at ScienceDirect

Engineering Structures

journal homepage: www.elsevier.com/locate/engstruct

Bond line models of glued wood-to-steel plate joints

Gustaf Larsson [a,*], Per Johan Gustafsson [a], Erik Serrano [a], Roberto Crocetti [b]

[a] Division of Structural Mechanics, Lund University, P.O. Box 118, SE-221 00 Lund, Sweden
[b] Division of Structural Engineering, Lund University, P.O. Box 118, SE-221 00 Lund, Sweden

ARTICLE INFO

Article history:
Received 10 September 2015
Revised 22 February 2016
Accepted 25 April 2016

Keywords:
Timber structure
Wood-to-steel plate joints
Shear plate dowel joint
Rubber foil connection
Numerical analysis
Numerical model

ABSTRACT

The competitiveness of timber as structural material in large structures is often governed by the cost of structural joints. Tests indicate that the new joint concept presented herein using glued wood-to-steel plate joints can possibly reduce the cost by matching joint strength to member strength. The design is inspired by two previously proposed designs using a single large dowel and using a rubber foil interlayer in adhesive joints. Analytical 1D and numerical 3D models of the bond line are proposed in order to further develop the concept, both in the case of a traditional adhesive joint and for the innovative rubber foil adhesive joint.

The glued wood-to-steel plate joints studied are lap joints with a load bearing capacity assumed to be governed by failure within or along the bond line. In the 1D and 3D structural models both linear elastic and non-linear fracture mechanics were applied, with the non-linear fracture mechanics model taking into account the gradual damage fracture softening in a fracture zone. For the conventional type of bond line it was found that bond line softening needs to be considered for adequate strength analysis while it was not needed for a bond line with a rubber foil.

The computational results are compared to previous full scale test results. The numerical results show good agreement and the analytical results reasonable agreement. When using a high strength adhesive, the strength of the wood along the bond line is governing joint failure. For this case, the analyses predict a 150% load bearing capacity increase by the introduction of a rubber foil as compared to a traditional design. The test results indicated an even higher increase.

1. Introduction

1.1. Background

The properties and cost of structural joints often govern the competitiveness of timber as main structural material in large structures. Ideally, a joint should be able to withstand the same forces as the main members, something which however seldom is the case due to joint detailing (leading to e.g. stress concentrations and large stresses perpendicular to the bond line).

Glued wood-to-steel joints can be designed to obtain promising properties. The high stiffness of conventional adhesives does however result in a limited active load transfer area for lap joints. As stress concentrations arise, the material strength of the adherents is reached prematurely for a small section and fracture is initiated. In order to significantly reduce the stress concentrations thus generating a more uniform stress distribution, Gustafsson [1] proposed adding an intermediate rubber layer, see Fig. 1.

1.2. The shear plate dowel connection

The shear plate dowel connection is an applied example of a glued wood-to-steel joint. It is a new design concept developed to increase connection strength while maintaining easy assembly thanks to the use of a single large diameter dowel. Fig. 2 shows the connection which is based on the concept of the "Single Large Diameter Dowel Connection" (SLDDC) design proposed by Crocetti et al. [2]. The use of externally glued steel plates minimizes the impact on the wood, for which a pure shear action is accomplished by using a larger hole in the glulam than in the steel plate. The connection type has been tested by Yang et al. [3], with and without a rubber interlayer.

Abbreviations: SLDDC, Single Large Diameter Dowel Connection; LEFM, linear elastic fracture mechanics; NLFM, non-linear fracture mechanics; EELA, equivalent elastic layer approach.

* Corresponding author.
E-mail addresses: gustaf.larsson@construction.lth.se (G. Larsson), per-johan.gustafsson@construction.lth.se (P.J. Gustafsson), erik.serrano@construction.lth.se (E. Serrano), roberto.crocetti@kstr.lth.se (R. Crocetti).

http://dx.doi.org/10.1016/j.engstruct.2016.04.053
0141-0296/

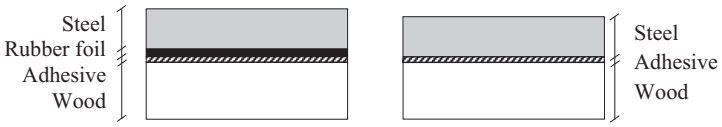

Fig. 1. Rubber foil adhesive joint (left) in comparison to conventional adhesive joint (right).

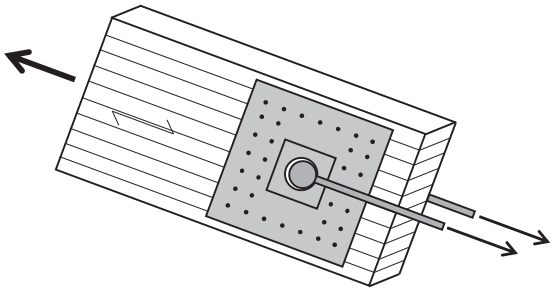

Fig. 2. Glued shear plate dowel connection.

As the steel plates of the connection reduce the risk of both splitting and shear plug failure of the loaded member end, the dowel to element end distance can be reduced from the minimum of 7d suggested by Eurocode 5 [4] thus enabling more compact connections. The connection was originally intended as a truss joint but can also be used in other applications, e.g. as hinges at arch springing points or tension ties. By combining several dowels moment stiff connections are also made possible. The rubber foil bond line can typically be used whenever a higher static or shock load bearing capacity of a glued joint is needed.

1.3. Previous work

The type of glued wood-to-steel plate joint studied herein is a new design concept and it does seem that it has not been studied in terms of detailed strength analyses previously. However, Yang et al. [3] and Gustafsson [1] have conducted tests on the connection type whereas the SLDDC has been tested in full scale tests by Kobel [5] with joints of the same type as those described by Crocetti et al. [2].

For simple lap joint geometries, such as glued wood-to-steel plate joints, the Volkersen theory [6] may be used to obtain an analytical solution by assuming pure shear action, c.f. Section 3. Adhesive bonds with more complex geometries are commonly solved using stress analysis or linear elastic fracture mechanics (LEFM) [7]. Stress or strain discontinuities occur when using continuum mechanics in design situations were adjacent materials have different stiffnesses, for which edge elements also are mesh dependent. Thus it is not trivial how to perform e.g. finite element analysis of such model. On the one hand, as the existence of a singular stress field is one of the assumptions in LEFM, such approach should in principle be appropriate. On the other hand, LEFM is only valid when the fracture process region is small compared to other dimensions of the structure, which is again seldom the case. The limitation of a small fracture process region can however be overcome using non-linear fracture mechanics (NLFM), e.g. softening plasticity [8], damage mechanics [9] or plasticity-damage models [10].

NLFM is computationally comprehensive, and thus several so-called extended LEFM models have been developed in order to reduce the number of limitations in LEFM without using stepwise or iterative numerical calculations. In this study, the extended LEFM model called the equivalent elastic layer approach (EELA) as proposed by Gustafsson [11] is used. It can been used for strength analyses of glued joints and for solid materials for which the location of the fracture plane is known in advance. The approach has been used in 2D applications by Gustafsson and Serrano [12], Coureau et al. [13] and extensively by Jensen in e.g. [14,15], but extended to 3D analysis in this paper.

1.4. Failure modes

Glued wood-to-steel plate joints can fail in the wood, in the steel or in the bond line. Here, the term bond line includes the adhesive, possible rubber foil, a thin wood layer along the glue and the material interfaces. Test results presented in [1,3] indicate, both for joints with and without a rubber foil, typically a dominant mode of shear failure in the bond line; either in the wood/adhesive interface or in the wood close to the bond line. If properly manufactured, wood failure close to bond line should be the governing failure mode. In the test series of the shear plate dowel connection [3] also shear plug failure occurred in the wood part of the joint. Reportedly the plug failure was a secondary failure occurring after bond line failure.

1.5. Present study

The present paper relates to one analytical and various numerical models for glued wood-to-steel plate joints as limited in strength by fracture in the bond line. Both joints with and without a rubber foil are studied. Using Volkersen theory [6], an analytical 1D shear stress distribution is derived. Furthermore, numerical linear and non-linear 3D analyses are conducted in order to investigate the influence of the interaction between shear and peel stresses in the bond line and also to investigate the choice of fracture model. The choice of material parameter values corresponds to failure in wood close to the bond line.

The aim of the present paper is to present an efficient and rational computational bond line strength analysis model and to indicate which factors may be of interest to include in a possible design model.

1.6. Limitations

The following main limitations apply to the models:

- Quasi-static analysis of short term strength.
- Only failure in the wood close to the bond line is considered.
- Linear elastic material model of wood (orthotropic) and steel (isotropic).

2. Calculation methods

In the calculation methods studied, steel and wood adherends are throughout modelled as isotropic and orthotropic linear elastic materials, respectively. Failure is assumed to develop in the bond line and not in the adherends. The adherends are in the 1D analysis assumed to act as bars which can be stretched in their longitudinal

direction, thus bending is not included. In the 3D analysis the adherends are modelled by 3D solid finite elements.

The bond line, with its different material layers and material interfaces as described above, is modelled as a single homogeneous layer. This layer is in the 1D analysis assumed to act as a shear–slip interface with a linear relation between the shear stress τ and the shear slip δ. In this study, two different choices regarding this linear relation, i.e. the shear stiffness of the interface, are investigated: (a) a stiffness representing the actual elastic bond line shear stiffness or (b) a stiffness chosen in order to represent correctly the strength and fracture energy of the bond line (in the sense that at the instant when the bond line strength is reached, the elastic energy stored equals the fracture energy of the bond line) [11]. These two alternatives give similar shear stiffness value for a bond line with a rubber foil. However, for a conventionally glued bond line there is commonly a very large difference between the two stiffness values, typically about one or two orders of magnitude. This is because the elastic strain capacity commonly is very small compared to the strains during plastic deformation and fracture. If the purpose of the modelling is joint strength analysis, then the shear stiffness should be chosen such that bond line strength and fracture energy are correctly represented, for details see Sections 3 and 4.

In the 3D analyses, the homogeneous layer that models the bond line is assigned a non-zero thickness equal to its physical thickness. The state of stress in the layer is defined by three stress components. Taking the 1-direction as the bond surface normal, the normal stress σ_{11} and the shear stresses τ_{12} and τ_{13} define these bond layer stress components. The corresponding strain components are denoted $\varepsilon_{11}, \gamma_{12}$ and γ_{13}. These strains are formally forced to be constant across the thickness of the layer and accordingly, the corresponding relative displacements across the bond line thickness are $\delta_{11} = t\varepsilon_{11}, \delta_{12} = t\gamma_{12}$ and $\delta_{13} = t\gamma_{13}$, where t is the bond layer thickness. Influence of in-plane stresses σ_{22}, σ_{33} and τ_{23} is not considered and these stresses are in the calculations assumed equal to zero.

In the 3D finite element analyses, the bond layer is modelled by the use of cohesive elements. The mechanical response of these elements is defined by traction-separation laws, i.e. relations between stresses $(\sigma_{11}, \tau_{12}, \tau_{13})$ and the relative displacements $(\delta_{11}, \delta_{12}, \delta_{13})$. The traction separation laws can be linear or non-linear and coupled or uncoupled. Non-linear relations for the bond layer are defined in terms of a damage model that enable analysis taking into account gradual fracture softening as described in Section 4.1. The properties are in the case of a linear relation obtained from the strength and the fracture energy parameters of the bond line under consideration. A special feature for bond lines with a rubber layer is that the effective normal stiffness is affected by edge distance. For an inner point of the bond layer, the in-plane normal strain is close to zero entailing high normal stiffness due to Poisson's ratio of rubber being close to 0.5, c.f. Section 4.2.

3. 1D analytical method

An analytical expression for the shear stress distribution of the centrically loaded shear plate dowel connection based on the Volkersen theory [6] is presented. The failure load is then derived by identifying the maximum stress and introducing a stress based failure criterion. The failure criterion accounts for the fracture energy according to the equivalent elastic layer approach.

3.1. Shear stress distribution according to Volkersen theory

Glued wood-to-steel plate joints are characterised by shear action, for which a non-uniform shear stress distribution is obtained due to the large overlap length. Volkersen [6] presents a second order homogeneous ordinary linear differential equation for the shear stress according to Eq. (1).

$$\tau_3'' - \omega\tau_3 = 0 \quad \text{where} \quad \omega^2 = \frac{G_3 b_3}{t_3}\left(\frac{1}{A_1E_1} + \frac{1}{A_2E_2}\right) \tag{1}$$

Indices 1 and 2 indicate the adherents while index 3 indicates the adhesive layer, c.f. Fig. 3.

The adhesive lap joint under consideration is schematically shown in Fig. 3. All elements are assumed to behave linear elastically, the adherents act as centrically loaded bars and the adhesive layer acts only in shear with constant shear strain across the thickness. Bending is not included.

Eq. (1) is solved individually for the two parts A and B shown in Fig. 3b. The mid length normal forces $N_1(L/2)$ and $N_2(L/2)$ at the load application point are determined using shear stress continuity and force equilibrium according to Eq. (2).

$$\begin{cases} \tau_3^A(L/2) = \tau_3^B(L/2) \\ P = N_1(L/2) + N_2(L/2) \end{cases} \tag{2}$$

By the presented boundary conditions in Fig. 3 and Eq. (2), the shear force distribution on a centrically loaded lap joint is found to be:

$$\begin{aligned} \tau_3(x) &= \begin{cases} \tau_3^A & for \quad 0 \leqslant x < L/2 \\ \tau_3^B & for \quad L/2 \leqslant x \leqslant L \end{cases} \\ \tau_3^A &= \frac{PG_3}{t_3\omega E_1A_1}\left[\left(\frac{1}{\tanh(\beta)} + \frac{\alpha - \operatorname{sech}(\beta)}{2\sinh(\beta)}\right)\cosh(\omega x) - \sinh(\omega x)\right] \\ \tau_3^B &= \frac{PG_3}{t_3\omega E_1A_1}\left[\left(\frac{\cosh(2\beta)}{2\sinh(\beta)}(\alpha + \operatorname{sech}(\beta))\right)\cosh(\omega x)\right. \\ &\quad \left. -\cosh(\beta)(\alpha + \operatorname{sech}(\beta))\sinh(\omega x)\right] \end{aligned} \tag{3}$$

where

$$\omega L = L\sqrt{\frac{G_3 b_3(1+\alpha)}{t_3E_1A_1}} \quad \alpha = \frac{E_1A_1}{E_2A_2} < 1 \quad \beta = \frac{\omega L}{2} \tag{4}$$

Fig. 11 shows the analytical variation of the shear plate dowel connection with rubber.

3.2. Choice of bond line stiffness

Slender lap joints which fail in an elastic brittle failure can be analysed using Volkersen theory. However, the non-elastic strain capacity is typically very significant for adhesive joint strength and should therefore be considered e.g. by the equivalent elastic layer approach (EELA) [11], see Fig. 4. Depending on what type of analysis is conducted, a choice of bond line stiffness thus can be made.

EELA presents a characteristic linear relation of the bond line obtained by respecting the bond line strength and fracture energy. By using a fictitious stiffness, the fracture-softening capabilities of the bond line can be included in the constitutive relations. For mode II fracture this is achieved by replacing the bond line shear stiffness with an equivalent stiffness defined according to Eq. (5).

$$\frac{G_3}{t_3} = \frac{f_v^2}{2G_f} \tag{5}$$

where

G_3: Shear modulus of bond line; f_v: Bond line shear strength.
t_3: Bond line thickness; G_f: Fracture energy of bond line.

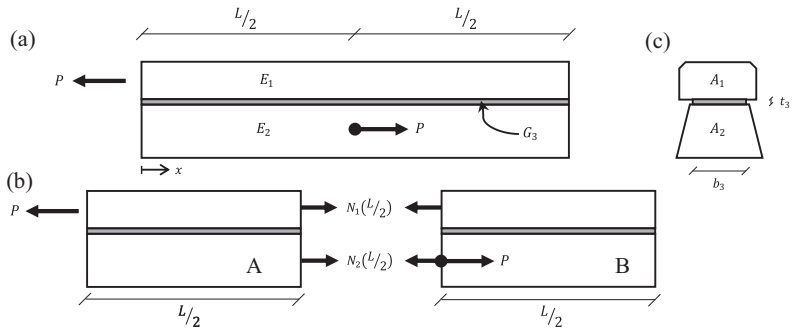

Fig. 3. Nomenclature of the theoretical analysis using Volkersen theory. Young's modulus E_i and shear stiffness of the bond line as G_3. The geometry is divided into part A and B at load application point.

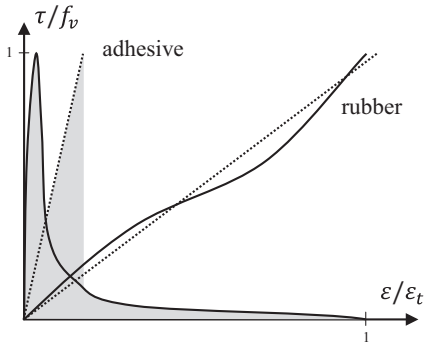

Fig. 4. A schematic comparison between normalized fracture-softening behaviour and EELA for common adhesives (two left curves) and rubber (right). Note that EELA correctly represents material strength and fracture energy, as indicated by shaded areas.

See also Fig. 4. As the shear modulus is replaced by a fictitious value, the initial elastic stiffness of the bond line is in general not represented correctly. However, as rubber behaves similar to the model in hand, the approach can for rubber foil bond lines be considered accurate also regarding deformations. For fracture in mode I, a linear elastic normal stress versus normal slip curve is defined analogously, thus enabling full 3D modelling capabilities.

Stresses are given by means of linear elastic stress analysis. Due to the special choice of properties of the elastic layer, either $\tau_{max} = f_v$ or $G = G_f$ can be used as a failure criterion. In case of mixed mode loading some mixed mode failure criterion should be used.

3.3. Failure load

A generalized Volkersen theory is obtained by applying EELA together with the Volkersen stress analysis. A failure load is then calculated by applying a stress based failure criterion: $\tau_{max} = f_v$. Maximum stress occurs at $\tau(x = 0)$ which yields the failure load according to Eq. (6).

$$P_f = f_v b_3 \frac{(1+\alpha)L}{\omega_g L} \frac{\sinh(\omega_g L)}{\alpha \cosh\left(\frac{\omega_g L}{2}\right) + \cosh(\omega_g L)} \tag{6}$$

For Volkersen theory, $\omega_g = \omega$ as defined in Eq. (4) while for the generalized Volkersen theory the normalized joint length ω_g is defined in Eq. (7).

$$\omega_g L = L\sqrt{\frac{f_v^2 b_3 (1+\alpha)}{2 G_f E_1 A_1}} \tag{7}$$

The Volkersen theory and the generalized Volkersen theory will yield the same results if rubber is present as discussed in Section 2. Shear fracture in the wood in vicinity of the bond line is the expected failure mode, thus f_v is determined by wood material strength.

As bending is not included in the Volkersen model, the presence of peel stresses due to loading eccentricity is neglected. The model should in general thus not be used for prediction of the load carrying capacity of the studied connection. However, reinforcement can be introduced in order to reduce such stresses, e.g. by means of screws. Provided that the shear stiffness of the reinforcement is either negligible or taken into account, the model should give a realistic estimation of the capacity and Eq. (6) could be used to develop a simple design criterion.

4. 3D numerical stress and strength analyses methods

Possible interaction between shear and peel stress in the joint is evaluated by means of finite element modelling in a commercial general purpose software. The simulations have been performed in 3D using a model consisting of wood, steel and a bond line. The bond line is represented by a cohesive layer with a single element in the thickness direction. The bond line thus represents the adhesive or, alternatively, the adhesive and the rubber foil if applied. The bond line also represents the material interfaces. The specimens will henceforth be called S-R and S-nR for the rubber and non-rubber specimen respectively.

4.1. S-nR – Joint without rubber layer

In order to evaluate the applicability of EELA in 3D, comparisons were made with non-linear fracture mechanics analyses where linear and bilinear fracture softening behaviours were used, see Fig. 5. The bilinear softening behaviour is a good approximation for several types of common adhesives [16], but also linear softening was studied in order to investigate whether the softening shape would influence the failure load. As EELA does not account for the true shape of the softening curve, different results of the linear and bilinear non-linear analyses would imply that EELA is not suitable for the joint type.

As depicted in Fig. 5, all three fracture models consider both the bond line strengths and its fracture energies, but by different means. When fracture softening is used, a single scalar damage

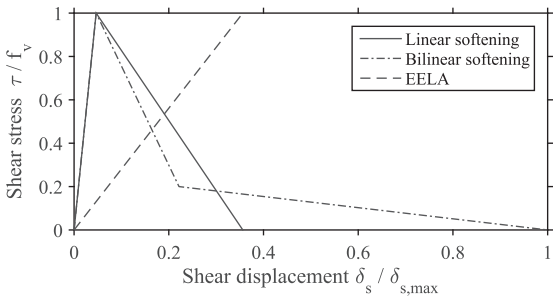

Fig. 5. Normalized stress–displacement plot illustrating the three numerical models used for the numerical analysis of the S-nR specimen. Note that material strength and fracture energy is the same for all models.

variable D is initiated after material failure which represents the material stiffness degradation. For linear softening, damage is defined as

$$D = \frac{\delta_m^f(\delta_m^{max} - \delta_m^0)}{\delta_m^{max}(\delta_m^f - \delta_m^0)} \tag{8}$$

where $\delta_m^f = 2G^C/T_{eff}^0$ with T_{eff}^0 being the effective traction at damage initiation. The maximum value of the effective displacement attained during the loading history is referred as δ_m^{max}, which can be determined using the fracture energy G^C. During analysis, D is determined for the different modes respectively but the minimum is used for all.

For the case of bilinear softening curves for normal and shear modes, see Fig. 5, damage was back-calculated from experimental data [17] and then used as tabular input to the software. Mixed mode is defined in terms of tractions and is expressed by

$$\begin{aligned} \phi_1 &= \frac{2}{\pi}\text{atan}\frac{\tau}{\langle t_n \rangle} \\ \phi_2 &= \frac{2}{\pi}\text{atan}\frac{t_t}{t_s} \end{aligned} \tag{9}$$

where $\tau = \sqrt{t_s^2 + t_t^2}$ is the vector sum of the two shear components. Using this nomenclature, $\phi_1 = 0$ corresponds to mode I, $\phi_2 = 0$ to mode II in the first shear direction and $\phi_2 = 1$ to mode II in the second shear direction.

4.2. S-R – Joint with rubber layer

When rubber foil is applied, its flexible behaviour will dominate the deformations and the bond line is thus represented by rubber properties. In comparison to adhesives, the bond line has for this case close to zero fracture-softening capability.

In dominant shear action rubber can be modelled as being linear elastic with fairly good accuracy, c.f. Fig. 4 and [18]. The incompressible behaviour of rubber will, however, to a large extent affect the normal stiffness. Given an isotropic linear elastic material in plane strain, one can theoretically identify the normal stiffness k_n as a function of Poisson's ratio ν, modulus of elasticity E, and layer thickness t, for an edge point and inner point of the rubber layer respectively, see Fig. 7 and Eq. (10).

$$k_{n,edge} = \frac{E}{t(1-\nu^2)} \quad k_{n,inner} = \frac{E(1-\nu)}{t(1+\nu)(1-2\nu)} \tag{10}$$

As the rubber properties are to be modelled using cohesive elements, the size of a transition region close to the free edge of the rubber was investigated using linear finite element analysis. A plane strain tensile test of a wide specimen made of a rubberlike linear elastic material perfectly bonded to stiff plates was analysed, see Figs. 6 and 7.

The equivalent normal stiffness of the rubber shows a variation along the width due to the pronounced Poisson's effect, which is obvious from inspection of Fig. 6 showing the normal stress distribution for a state of uniform normal strain of the rubber layer. It is further clear from Fig. 7 that the inner stiffness is well represented by the theoretical results. However, stress concentrations arise at the ends due to the sudden change in stiffness. Further investigations reveal a mesh size dependence of the peak stress value at the ends of the specimen but also that extrapolating the stress curve from values coincide with the theoretical values of Eq. (10). These findings make it plausible to exclude the concentration as a numerical artefact, and at the same time the findings provide a mean of disregarding this very local phenomenon. A transition length is defined as the distance from the edge to the point where 99% of the plateau value is reached. Linear simulations of a rubberlike material indicate an influence of Poisson's ratio and bond line thickness on this transition length. For rubber (low stiffness and Poisson's ratio close to 0.5) this is approximated by Eq. (11).

$$l_{transition} = 9t \tag{11}$$

The transition length has a positive effect in the applied analyses of the connection as the position of maximum peel stress does not coincide with the position where maximum shear stress is found, the latter typically being located at the bond line edge.

Similar simulations were conducted to verify the shear stress distribution. As the theory predicts, analyses indicate zero shear stress at the specimen ends and an effective shear stiffness being equal to the shear modulus, i.e. $G = E/2(1+\nu)$. The transition length and variation of equivalent shear stiffness is negligible and thus considered constant along the bond line.

For the joint design in hand, this linear modelling approach has been verified by comparing the obtained stress distribution to the one obtained from non-linear, third order analyses using both neo-Hookean [19] and Yeoh [20] material models. As seen in Section 5.4, reasonable agreement with conducted tests is also obtained.

The strength of the bond line is found using a stress based failure criterion, for which a Norris criterion [21] is deemed suitable for the 2D bond line. Compressive normal stress will not cause failure and is thus not included in the criterion, see Eq. (12).

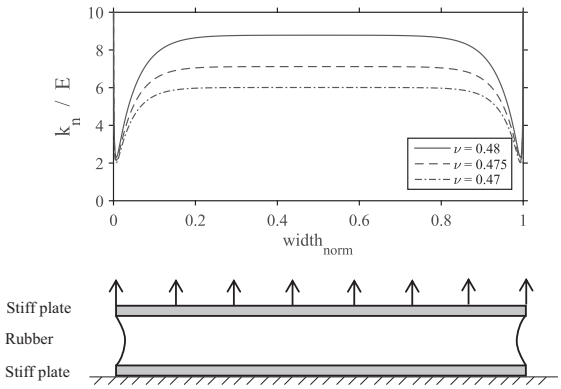

Fig. 6. Stiffness variation determined by numerical tension simulation of a rubberlike material. The specimen width is 30 times the rubber layer thickness. The rubber layer is modelled using an isotropic linear elastic material with $E = 3.6$ MPa.

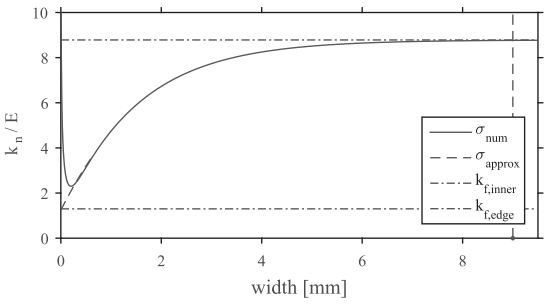

Fig. 7. Normal stress distribution plotted over the transition length. By excluding the stress concentration at the end, data fitting validates the theoretical edge stiffness. The transition length according to Eq. (11) indicated by the vertical dashed line.

$$\left(\frac{\sigma_{11}}{f_{t90}}\right)^2 + \left(\frac{\tau_{12}}{f_v}\right)^2 + \left(\frac{\tau_{13}}{f_{v90}}\right)^2 - 1 = 0 \tag{12}$$

Index t indicates tension, index v indicates shear and index 90 is used for the perpendicular to grain direction. Stress directions are defined in Section 2.

5. Calculation results and comparison to tests

5.1. Test series

The calculation results will be compared to tests conducted by Yang et al. [3]. The shear plate dowel connections was subjected to quasi-static displacement controlled tensile test according to Fig. 8. Each specimen had a length of 2 m with identical connections in each end. Three nominally equal specimens were tested in each series, i.e. 6 tested joints in total. However, the non-failing joint is disregarded in this work. The size of the steel plates was 400 × 400 mm^2 with a thickness of 8 mm. The plates were 13 mm thick in the area close to the dowel in order to avoid yielding and possible buckling. It should be noted that the plates were not only glued, but also 34 screws (70 × 6 mm) were inserted to keep the plates in position during curing. Two similar test series were conducted with the only difference being the presence of a rubber layer.

The glulam used was of strength class GL30c while the steel was of grade Q345B with a nominal yield stress of 345 MPa. The rubber was a mix of natural rubber and SBR (styrene-butadiene) with a hardness of 62° Shore A, which is approximately equivalent to a shear modulus 1.2 MPa [18]. The tensile strength of the rubber is 22.4 MPa while its shear strength is 9.4 MPa. The failure elongation in tension is 595% [3] and the rubber layer had a thickness of 1.0–1.2 mm. The rubber was vulcanized to the steel plate which ensures a steel–rubber interface strength similar to the rubber itself. A 2-component polyurethane (Purbond CR421, glue + hardener) was used to adhere the rubber to the glulam while epoxy (SHB) was used to adhere the steel directly to the glulam for the connections without any rubber layer.

The displacement of the steel plate relative the side of the beam was recorded, see Fig. 8. The failure load P_f and average shear stress at failure τ_f of the specimens are found in Table 1.

The test results suggest a considerable strength increase in the connection by introducing a rubber foil. Failure examination of the S-nR specimen does however indicate premature failure at the steel–adhesive interface rather than in the wood, c.f. [3]. Furthermore, a mistake in the test set-up design of the first S-R specimen

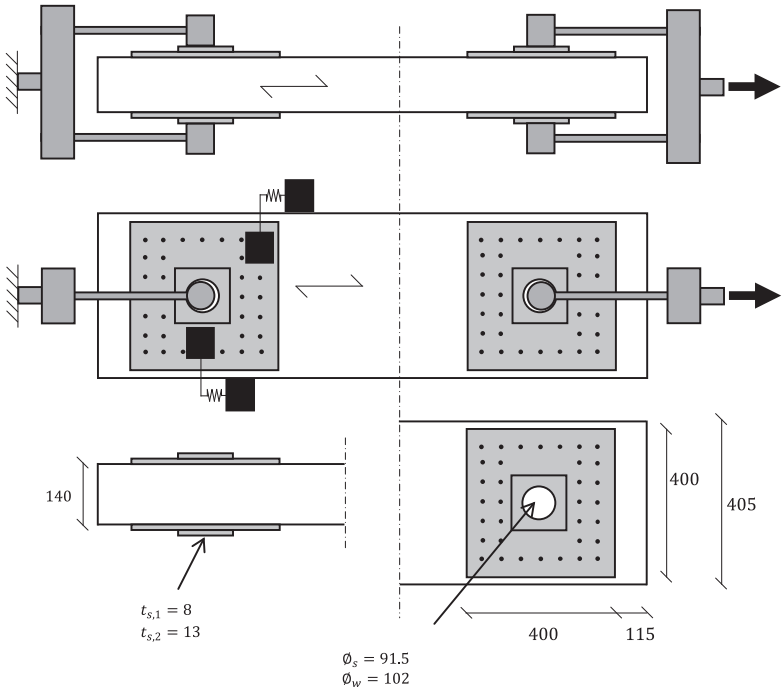

Fig. 8. Geometry and test setup used by Yang et al. [3]. Subscript s for steel, w for wood. All dimensions are in mm and the typical arrangement of displacement gauges is shown in the lower part of the middle figure.

Table 1
Failure loads and mean shear stress at failure of laboratory test series with (S-R) and without rubber (S-nR).

S-nR	P_f (kN)	$\overline{\tau_f}$ (MPa)	S-R	P_f (kN)	$\overline{\tau_f}$ (MPa)
I	281	0.93	I	843	2.78
II	209	0.69	II	1076	3.54
III	165	0.54	III	1052	3.46
AVG	218	0.7	AVG	990	3.3

Table 2
Adopted elastic material parameters for wood [7]. Parameters are given in MPa and (–).

Young's modulus (MPa)		Shear modulus (MPa)		Poisson's ratio	
E_L	14,000	G_{TR}	60	υ_{TR}	0.3
E_T	500	G_{TL}	700	υ_{TL}	0.02
E_R	800	G_{RL}	600	υ_{RL}	0.02

Table 3
Bond line parameters. Units: MPa and J/m^2.

	σ_{perp}	τ_0	τ_{90}
S-nR	$E = 3000$	$G = 1000$	$G = 1000$
	$G_{f,I} = 470$	$G_{f,II} = 740$	$G_{f,II} = 300$
	$f_{t90} = 4.9$	$f_v = 4.4$	$f_{v90} = 1.6$
S-R	$E = 3.6$	$G = 1.2$	$G = 1.2$
	$f_{t90} = 4.9$	$f_v = 4.4$	$f_{v90} = 1.6$
	c.f. Eqs. (10) and (11)		

resulted in bending of the glulam which lowered its capacity. This bending was prevented in the later S-R tests.

5.2. Numerical analysis parameters

A linear elastic rectilinear orthotropic material model was chosen for the wood using the elastic parameters given in Table 2, no identification experiments were conducted. The steel plate is modelled as a linear elastic isotropic material with Young's modulus $E = 210$ GPa and a Poisson's ratio, $\nu = 0.3$.

The bond line is modelled according to Section 4, thus dependent on the presence of rubber. As the prominent failure mode is wood shear failure close to the bond line, wood properties are used for strengths and fracture energies. The values shown in Table 3 are those given by Berblom Dahl [22] and Serrano [7] respectively for clear wood specimens. The effective normal stiffness for S-R was applied to a perimeter zone according to Section 4.2 assuming a Poisson's ratio of 0.497. This value was found by comparing stress levels from simulations using a linear elastic rubber layer with those from simulations using a hyperelastic (Neo-Hookean) material model for the rubber. Bond line stiffness for the adhesive in the S-nR joints is also found in Table 3.

Table 4
Failure load comparison of full-sized S-nR test specimens. The variation of the results indicates the importance of fracture analysis on adhesive connections. The bilinear model is considered realistic, which further indicates the premature failure of the test series.

Type of analysis	Failure load (kN)	Average shear stress (MPa)
1D Analytical, linear	92	0.30
3D Numerical, linear	128	0.42
Test	**218**	**0.72**
3D Numerical, NLFM Bilinear softening	**562**	**1.85**
3D Numerical, NLFM Linear softening	795	2.62
3D Numerical, EELA	803	2.64
1D Analytical, EELA	863	2.84

For simplicity, the simulations were run in load control. By doing so there was no need to model the dowel itself, nor its interaction with the steel plate which would call for detailed contact modelling. Instead a non-uniform pressure load was prescribed on the hole edges to simulate pin pressure. The simulations were run without introducing artificial stabilization (viscous damping) and using the built-in automatic incrementation features of the software. The minimum step length was expressed as ratio of total load and was set to $5 \cdot 10^{-3}$. Double symmetry was used and the load was applied horizontally to the right, see Figs. 8 and 9.

The element mesh commonly used is shown in Fig. 9. First order solid elements with full integration over 8 nodes were used for the glulam and steel while cohesive elements were used for the bond line with one element in the thickness direction. With the presented modelling approach stress concentrations at the edges are substantially reduced thus enabling the use of a simple stress failure criterion.

5.3. Results for S-nR – Joint without rubber layer

The predicted failure load of the S-nR specimen varies greatly depending on the calculation method used, see Table 4. The test results are also presented for which the premature failure should be kept in mind, c.f. Section 5.1. As the stiffness of the adhesive is considerably larger than for the screws, the latter are excluded from the analysis as they only have a minor influence on the joint strength. In comparison to the linear 1D analysis according to Eq. (3), the joint geometry causes a more uniform shear stress distribution in the linear 3D, and thus yields a higher failure load even though the 3D analysis considers stress interaction. Due to the high adhesive stiffness, the linear 3D analysis is sensitive to discretization in comparison to fracture softening analysis.

EELA shows good resemblance between analytical 1D and numerical 3D results, but also with the linear fracture softening model. The bilinear model does however imply that the failure loads found by EELA are unreasonably high, which indicates a frac-

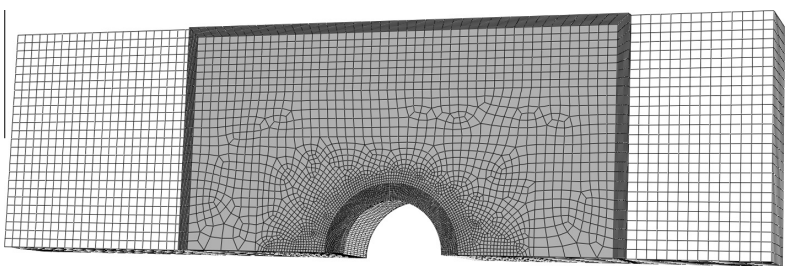

Fig. 9. Typical FE-mesh used in the analyses (double symmetry used). Approximately 80,000 elements in total. Wood elements shown in white, steel plate in grey.

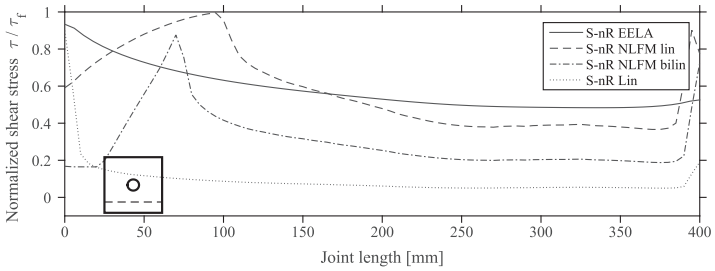

Fig. 10. Shear stress distribution comparison between presented models in Section 2 at failure load. The distribution is along a line at 60 mm distance from the plate edge, see lower left corner. Conventional linear stress analysis 'S-nR Lin' underestimates the capacity significantly. The load is directed right.

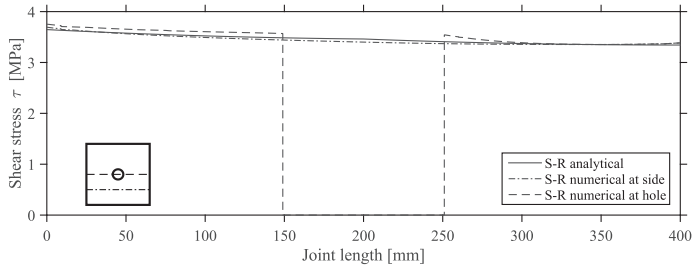

Fig. 11. Shear stress distribution of the S-R specimen; 1D analytical and 3D numerical EELA for a total connection load of 1050 kN directed right. The numerical stress paths are taken in the middle (hole) and at 60 mm distance from the plate edge (side), see lower left corner.

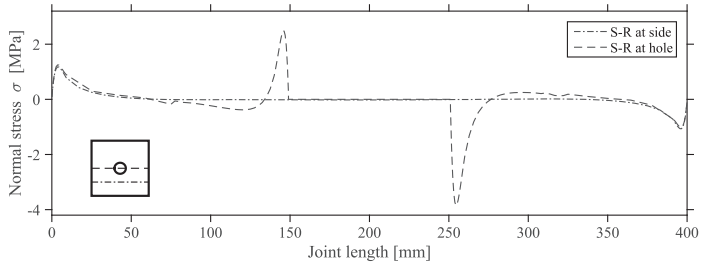

Fig. 12. Normal stress distribution by numerical EELA analysis of the S-R specimen. Total load is 1050 kN directed right. The peel stress (positive) peak at $x \approx 150$ mm governs the failure region.

ture softening behaviour dependency of the failure load. This indication makes the use of EELA not suitable for the connection in hand as it disregards the shape of the softening curve as well as assumes that all fracture energy can be activated during the propagating failure. Since no detailed knowledge about the exact shape of the softening curve is available for the bond line studied, no further analyses of the joint without rubber foil were performed. As a comparison, the shear stress distribution at failure is illustrated in Fig. 10. The bilinear model verifies the premature failure in the test series discussed in Section 5.1.

5.4. Results for S-R – Joint with rubber layer

In comparison to the S-nR specimen, a self-similar stress distribution throughout the load application is obtained for the S-R specimen due to the linear analysis. A good resemblance between the analytical 1D expressions and the numerical 3D models is found for which a close to uniform distribution is obtained, shown in Fig. 11.

The higher load capacity in combination with a slightly larger eccentricity due to increased bond line thickness results in higher normal stresses in the S-R specimen in comparison to the S-nR. The numerical results are shown in Fig. 12.

The combined state of stress is evaluated using the Norris stress criterion according to Section 4.2, and applying a single point maximum stress failure criterion. A comparison of the load bearing capacity of the connection is presented in Table 5. For the geometry at hand, the linear numerical analysis shows a reasonable agreement with the test results, especially if the first test result is disregarded, c.f. Section 5.1. The analysis further indicates that including peel stress reduces the failure load by 20% as compared

Table 5
Failure load comparison of the S-R specimen.

Type of analysis	Failure load (kN)	Average shear stress (MPa)
Test	990	3.26
3D Numerical	1050	3.46
1D Analytical	1270	4.18

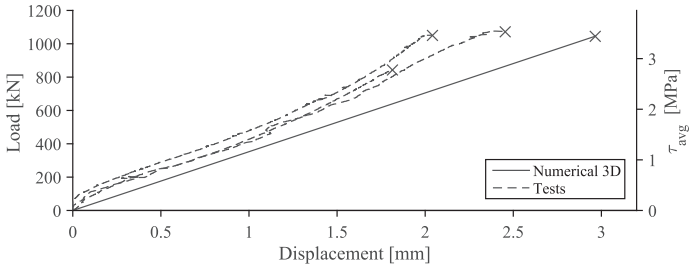

Fig. 13. Load–slip comparison of the rubber plate connection between tests and numerical analysis.

to the analytical 1D-solution and also predicts the failure region to be close to the hole instead of being located at the outer perimeter of the steel plate.

In order to evaluate the linear elastic representation of rubber, a load–slip comparison to test data is of interest, see Fig. 13. The deformation measure used for the numerical results in this plot is chosen so as to represent the measurement points used in the tests. It can be concluded that the numerical analysis underestimates the joint stiffness, which is possibly due to the large amount of screws used but not modelled.

6. Discussion

A large increase in load bearing capacity of the shear plate connection by using a rubber foil between the steel plate and the wood was recorded in the tests, partly due to premature failure discussed in Section 5.1. If the steel–adhesive interface can be made sufficiently strong and failure in the wood close to the bond line is made the governing factor, the numerical results for the S-nR specimen reported herein predicts a failure strength increase of 150% when the rubber foil is applied. In addition, the *elastic* behaviour of the relatively soft rubber foil also suggests a considerably higher capacity in cyclic loading since the response is reversible up to load levels very close to the failure load.

The shear stress distribution is close to uniform for a 1 mm rubber foil thickness, hence no significant strength increase is possible by using a thicker foil. However, a thicker foil would most probably increase the joint's impact resistance and, of course, reduce joint stiffness. Such characteristics can be of interest in shock loading situations or when mechanical fasteners are needed to interact with a glued bond line.

A full analysis of a rubber layer requires a non-linear material model, non-linear geometry (due to high straining) and a considerable amount of elements in the thickness direction in order to accurately capture the deformation pattern. By using the suggested method of analysis with cohesive elements, a considerably faster analysis run time is attained.

Peel stresses in the bond line can be reduced by fastening the plate also with screws. The same screws can also be used to obtain curing pressure for the adhesive. The failure load comparison presented in Table 5 suggests a good resemblance between the numerical 3D analysis and the test results. However, the numerical model does not include the screws shown in Fig. 8 which should increase the load carrying capacity of the joint as the rubber enables screw-adhesive interaction [1]. The numerical analysis indicates a failure region just behind the hole, thus it can be of interest to insert screws also there. Note that the failure region differs between the presented models, from the outer perimeter of the bond line behind the load in the Volkersen analysis to the hole perimeter behind the load in the numerical analysis. This shift is due to the inclusion of peel stresses in the FE-analyses and the use of the Norris failure criterion based on the multi-axial stress state.

Even though strength analyses of the rubber foil adhesive joints are promising, additional efforts are needed in order to account for long term effects, dynamic loading and fire safety before structural application.

7. Conclusions

- An analytical expression of the 1D shear stress distribution, based on Volkersen theory, was developed for centrically loaded glued lap joints. The analysis indicates that the generalized Volkersen theory can be used to determine the load bearing capacity of the joint with reasonable agreement when an intermediate layer with a rubber foil is applied. The predicted load is higher than can be expected due to the neglected bending.
- Numerical bond line models of glued wood-to-steel plate joints are presented for which a bilinear fracture softening model is suggested for traditional wood-to-steel plate adhesive joints and a linear elastic model is suggested if an intermediate rubber foil layer is used.
- If only failure of wood close to the bond line is considered, the suggested models indicate a 150% increase of the load bearing capacity by introducing a rubber foil. The increase is lower than experimental experience, indicating difficulties in properly bonding the steel plate to wood. Compared to a traditional adhesive bond, the numerical results indicate that the failure load is reached without early damage initiation and evolution in the bond line when a rubber foil is used.

Acknowledgements

The financial support provided by *Formas* through grant 2012-879 is gratefully acknowledged. The authors would also like to thank associate professor Huifeng Yang and others at Nanjing Tech University for a pleasant stay and for providing information on the experimental work.

Appendix A. Supplementary material

Supplementary data associated with this article can be found, in the online version, at http://dx.doi.org/10.1016/j.engstruct.2016.04.053.

References

[1] Gustafsson PJ. Tests of full size rubber foil adhesive joints. Lund University; 2007.
[2] Crocetti R, Axelson M, Sartori T. Strengthening of large diameter single dowel joints. SP Technical Research Institute of Sweden; 2010.

[3] Yang H, Crocetti R, Larsson G, Gustafsson P-J. Experimental study on innovative connections for large span timber truss structures. In: IASS working groups 12 + 18 International Colloquium 2015, Tokyo, Japan; 2015.
[4] Swedish Standards Institute. SS-EN 1995-1-1:2004: Eurocode 5: design of timber structures. Stockholm, Sweden: SSI; 2009.
[5] Kobel P. Modelling of strengthened connections for large span truss structures. Master thesis. Lund University; 2011.
[6] Volkersen O. Die Nietkraftverteilung in zugbeanspruchten Nietverbindungen mit. Luftfahrtvorschung 1938;15:41–7.
[7] E. Serrano. Adhesive joints in timber engineering, modelling and testing of fracture properties. PhD thesis. Lund; 2000.
[8] Ottosen NS, Olsson K-G. Hardening/softening plastic analysis of adhesive joint. J Eng Mech 1988;114(1):97–116.
[9] Krajcinovic D. Damage mechanics. Mech Mater 1989;8:117–97.
[10] Edlund U. Mechanical analysis of adhesive joints: models and computational methods. PhD thesis. Linköping, Sweden; 1992.
[11] PJ Gustafsson. Analysis of generalized Volkersen joints in terms of non-linear fracture mechanics. In: Proc of European mechanics colloquium 227 "Mechanical behavior of adhesive joints"; 1987. p. 323–38.
[12] Gustafsson PJ, Serrano E. Glued truss joints analysed by fracture mechanics. In: 5th World conference on timber engineering, Montreux, Switzerland; 1998.
[13] Coureau J-L, Gustafsson PJ, Persson K. Elastic layer model for application to crack propagation problems in timber engineering. Wood Sci Technol 2006;40:275–90.
[14] Jensen JL. Quasi-non-linear fracture mechanics analysis of the double cantilever beam specimen. J Wood Sci 2005;51:566–71.
[15] Jensen JL, Gustafsson PJ. Shear strength of beam splice joints with glued-in rods. J Wood Sci 2004;50:123–9.
[16] Wernersson H, Gustafsson PJ. The complete stress–slip curve of wood–adhesives in pure shear. Mech Behav Adhes Joints 1987:139–50.
[17] Wernersson H. Wood adhesive bonds – fracture softening properties in shear and in tension. PhD thesis. Lund: Lund University; 1990.
[18] Austrell P-E. Modelling of elasticity and damping for filled elastomers. PhD thesis. Lund: Lund University; 1997.
[19] Treloar LRG. The physics of rubber elasticity. 3rd ed. Oxford: Clarendon Press; 1975.
[20] Yeoh OH. Some forms of the strain energy function for rubber. Rubber Chem Technol 1993;66:754–71.
[21] Norris CB. Strength of orthotropic materials subjected to combined stresses. Report no. 1816. Madison: U.S. Department of Agriculture; 1962.
[22] Berblom Dahl K. Mechanical properties of clear wood from Norway spruce. PhD thesis. Trondheim, Norway: Norwegian University of Science and Technology; 2009. ISBN 978-82-471-1911-2.

Paper D

WCTE 2016
World Conference on Timber Engineering
August 22-25, 2016 | Vienna, Austria

ANALYSIS OF THE SHEAR PLATE DOWEL JOINT AND PARAMETER STUDIES

Gustaf Larsson[1], Per Johan Gustafsson[2], Erik Serrano[3], Roberto Crocetti[4]

ABSTRACT: The shear plate dowel joint is a single large dowel joint with rubber-glued steel plates. The design has shown promising results in terms of strength in experimental work. The paper presents results from theoretical models that have been developed to enable further studies of the joint. The failure load obtained through a numerical 3D analysis is in good agreement with test results. Parameter studies and design alterations are presented, which concludes that the joint design is efficient and that the shear slip stiffness can be designed to match commonly used fasteners.

KEYWORDS: Shear plate dowel joint, rubber foil adhesive joint, single dowel, numerical model, timber, connection, joint

1 INTRODUCTION

The properties and cost of structural joints often govern the competitiveness of timber as main structural material in large structures. Mechanical fasteners such as dowels, screws and nails are typically used as they provide strength and ductility to the timber joint. However, in order to avoid splitting, proper distances are required to member edges as well as between different fasteners as described in the European design code Eurocode [1]. These distances entail an increase of member dimensions, which subsequently reduces the utilisation factor of the member in span and thus causes excessive material use.

Several types of timber reinforcements have been studied in order to enhance the brittle properties of wood. Early research focused on global element reinforcements [2] [3] of which textiles were proposed suitable also as local reinforcement in e.g. joints [4]. Several studies have since been aimed specifically at minimizing the required distances between mechanical fasteners and end distance by e.g. self-tapping screws [5] and fibre textile [6] [7]. The shear plate dowel joint (SPDJ) distinguishes itself from previous joint proposals by combining high strength with efficient on and off site production, while maintaining a short end distance. The design also enables easy joint-to-member strength matching.

1.1 THE SHEAR PLATE DOWEL JOINT

The favourable properties of the SPDJ design is achieved by combining the strength of a flexible lap joint with the simplicity of a single dowel design.

A limiting factor in design of lap joints is shear stress concentrations at the joint ends, which grow significantly for large lap lengths. These concentrations reduce the active load transfer region of the joint and thus limit the total load bearing capacity. This premature failure is further deprived due to the high stiffness of commonly used structural adhesives.

In order to minimize the stress concentrations by softening the bond line, Gustafsson [8] suggested adding an intermediate rubber layer as see Figure 1. A close to uniform shear stress distribution over the lap joint length is found even for thin rubber layers, dramatically increasing the elastic load bearing capacity. The stiffness of a rubber foil adhesive joint is typically comparable to, if not stiffer than, bolted joints [8].

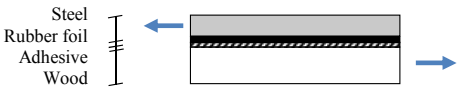

Figure 1: *Pull-pull adhesive lap joint with intermediate rubber layer*

[1] Gustaf Larsson, Lund University, Sweden, gustaf.larsson@construction.lth.se, P.O. Box 118, SE-221 00 Lund, Sweden
[2] Per Johan Gustafsson, Lund University, Sweden, per-johan.gustafsson@construction.lth.se
[3] Erik Serrano, Lund University, Sweden, erik.serrano@construction.lth.se
[4] Roberto Crocetti, Lund University, Sweden, roberto.crocetti@kstr.lth.se

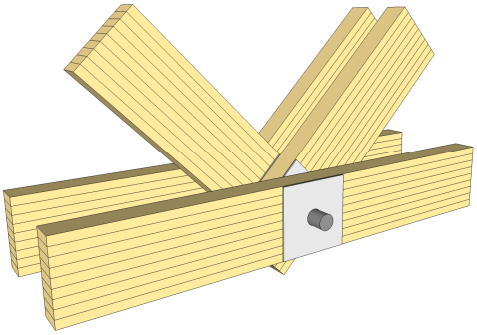

Figure 2: *The shear plate dowel joint used in a truss node*

A high degree of prefabrication and easy on site assembly can be achieved by a using a single dowel joint design, see Figure 2. However, a single dowel would be very prone to splitting failure and is thus in need of a large end distance, if no type of reinforcement is used.

Several types of reinforcements have been tested for large diameter dowels, such as self-tapping screws [9] [10] and fibre textile [11], but none of these techniques efficiently reduce the possibility of shear plug failure. However, by combining the concepts of a single large dowel and the rubber foil adhesive joint, the premature shear plug failure is avoided.

The rubber foil adhesive technique is used to externally glue large metal plates with vulcanized rubber to the timber member, see Figure 2. Shear action between timber and rubber is then assured by using a larger hole diameter in the timber than in the steel plates. As the rubber foil enables the use of the bonded area, the member strength can simply be matched by an appropriate choice of plate size. Screws can be used to apply curing pressure, minimize steel plate bending due to eccentricity, and increase joint bearing capacity as the rubber foil can be designed to match the slip of the screws.

The SPDJ was first tested in [8], but later in full scale by Yang et al. [12] along with comparative tests without a rubber foil. For a steel plate size of 400x400 mm^2 and dowel diameter of 91 mm, the average failure load was found being 218 kN without rubber foil, compared to 990 kN with rubber foil. The dominant failure mode was shear failure in the bond line, but indications of wood failure also exist [8] [12]. Even though a premature failure in the steel-adhesive interface was found for the specimens without rubber, the benefit of the rubber layer on load bearing capacity is clear.

1.2 PRESENT STUDY

The purpose of this paper is to establish validated and efficient strength analysis procedures of the SPDJ as limited in strength by fracture in the bond line or the timber member. Here, the term bond line includes the adhesive, rubber foil, a thin wood layer along the glue and the material interfaces.

Analytical 1D expressions and a numerical 3D approach are presented to determine the failure load of the joint. The 1D analysis is based upon the Volkersen theory [13], which considers the shear stress distribution, while the numerical 3D approach is needed to also consider peel stress interaction. The analytical expressions can be used to develop design procedures of the joint.

2 1D ANALYTICAL ANALYSIS

The SPDJ is characterised by lap shear action between the steel plate and timber element. A non-uniform shear stress distribution is obtained for large overlap lengths due to the various stiffnesses of the joint materials. Based on studies on large riveted overlap connections in steel, Volkersen [13] presented a differential equation for the shear distribution as Equation (1).

$$\tau_3'' - \omega\tau_3 = 0$$
$$\omega^2 = \frac{G_3 b_3}{t_3}\left(\frac{1}{A_1E_1} + \frac{1}{A_2E_2}\right) \tag{1}$$

Indices 1 and 2 indicate the adherents while 3 indicates the adhesive layer, see further Figure 3. In the Volkersen theory, the adherends are assumed to act as centrically loaded bars and the adhesive layer can only transfer shear stress, which is constant over the thickness. Bending is thus not included and all materials are modelled as linear elastic.

Using stress continuity and force equilibrium over the centric load application point, the analytical shear force distribution for the SPDJ is governed by (2).

$$\tau_3(x) = \begin{cases} \tau_3^A & for \quad 0 \le x < L/2 \\ \tau_3^B & for \quad L/2 \le x \le L \end{cases}$$

$$\tau_3^A = \frac{PG_3}{t_3\omega E_1A_1}\left[\left(\frac{1}{\tanh(\beta)} + \frac{\alpha - \operatorname{sech}(\beta)}{2\sinh(\beta)}\right)\cosh(\omega x) - \sinh(\omega x)\right] \tag{2}$$

$$\tau_3^B = \frac{PG_3}{t_3\omega E_1A_1}\left[\left(\frac{\cosh(2\beta)}{2\sinh(\beta)}\left(\alpha + \operatorname{sech}(\beta)\right)\right)\cosh(\omega x) - \cosh(\beta)\left(\alpha + \operatorname{sech}(\beta)\right)\sinh(\omega x)\right]$$

in which

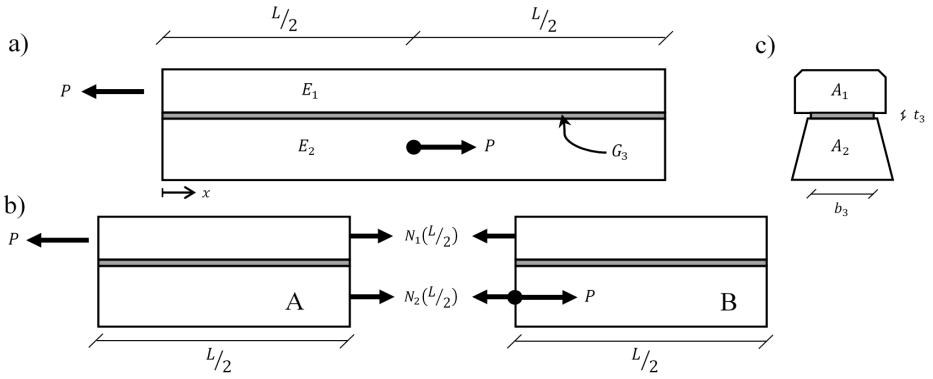

Figure 3. *Nomenclature of the theoretical analysis using Volkersen theory. Young's modulus is denoted E_i for wood and steel respectively, and shear stiffness of the bond line is denoted G_3. The geometry is divided into part A and B at the load application point.*

$$\omega L = L\sqrt{\frac{G_3 b_3(1+\alpha)}{t_3 E_1 A_1}}$$

$$\alpha = \frac{E_1 A_1}{E_2 A_2} < 1 \qquad (3)$$

$$\beta = \frac{\omega L}{2}$$

This analytical shear stress distribution is shown in Figure 7.

For a given a shear strength f_v, the maximum load bearing capacity, P_f, is limited by the shear stress behind the applied load at $x = 0$ in Equation (2). Thus, the failure load can be expressed as

$$P_f = f_v b_3 \frac{(1+\alpha)L}{\omega L} \frac{\sinh(\omega L)}{\alpha \cosh\left(\frac{\omega L}{2}\right) + \cosh(\omega L)} \qquad (4)$$

Among the simplifications made in the Volkersen theory, disregarding bending is of special concern for the SPDJ design. Due to the eccentricity between the system lines of the steel plate and timber member, bending will occur and thus it is expected than Equation (4) will overestimate the load carrying capacity of the joint.

However, the bond line peel stresses can be reduced if adequate reinforcement is introduced, e.g. by means of screws. The model could then probably be used to obtain a realistic estimation of the capacity, provided also that the shear stiffness of the screws are either negligible or taken into account.

3 3D NUMERICAL ANALYSIS

3.1 GENERAL

Numerical 3D analysis can be used in order to consider the stress interaction between shear and peel stresses in the bond line. For this, the general-purpose finite element software ABAQUS was used. The simulations were performed in 3D using a model consisting of wood, steel and a bond line.

3.2 STEEL AND WOOD MATERIAL MODELS

Wood is modelled using a linear elastic material formulation. Orthotropic parameters are used in both rectilinear and polar manner, see Table 1 and Figure 4. Failure in the wood member is evaluated by a Tsai-Wu failure criterion [14], in which the strength interaction coefficients are set to zero. Strength parameters are found in Table 2.

The steel is modelled as an isotropic linear elastic material using Young's modulus of 210 GPa and Poisson's ratio of 0.3.

Table 1: *Elastic material properties for wood* **[15]**. *Units are given in MPa and [-].*

Young's modulus		Shear modulus		Poisson's ratio	
E_L	13700	G_{TR}	60	υ_{TR}	0.3
E_T	500	G_{TL}	700	υ_{TL}	0.02
E_R	800	G_{RL}	600	υ_{RL}	0.02

Table 2: *Wood strength parameters in MPa* **[16]**.

	Tensile	*Compression*		
f_L	63	29	f_{TL}	4.4
f_R	4.9	3.6	f_{RL}	6.1
f_T	2.8	3.8	f_{RT}	1.6

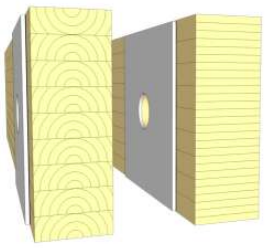

Figure 4: *Polar and rectilinear material model used in wood stress analysis.*

3.3 BOND LINE MODEL

The bond line represents the rubber and the adjacent interfaces between rubber-wood and rubber-steel. An efficient bond line model is of interest and thus a linear analysis with a minimum amount of elements is favoured even though a non-linear elastic behaviour is characteristic for rubber. However, shear action can be modelled with a linear behaviour with a reasonable accuracy, and as it is the main action of the joint, a reasonable agreement is found with non-linear material models.

Special consideration is needed in order to model the incompressibility of rubber as the Poisson's ratio approaches 0.5, which highly affects the normal stiffness of the bond line. Based upon a linear elastic material formulation, one can identify a difference in normal stiffness between edge and inner points of the material due to strain boundary conditions. The stiffness is a function of Young's modulus E, Poisson's ratio ν and the rubber thickness t according to Equation (5).

$$k_{n,edge} = \frac{E}{t(1-\nu^2)}$$
$$k_{n,inner} = \frac{E(1-\nu)}{t(1+\nu)(1-2\nu)} \quad (5)$$

A transition region with an increasing normal stiffness from $k_{n,edge}$ to $k_{n,inner}$ is thus expected. The region is defined as the distance from the edge to a point at which a stiffness of 99% of $k_{n,inner}$ is found, which was investigated using linear finite element analysis. There, a rubberlike linear elastic material was perfectly bonded to stiff plates and subjected to tensile forces in plain strain conditions. The normal stiffness variation is plotted over the specimen width in Figure 5, which indicates that the inner stiffness is well represented by the theoretical results. Parameter studies indicate a linear relation between the transition length and the rubber thickness according to Equation (6) for Poisson's ratio close to $\nu = 0.5$.

$$l_{transition} = 9t \quad (6)$$

However, stress peaks arise at the ends due to sudden stiffness change. These peaks are mesh dependent, but data extrapolation suggests that the theoretical edge stiffness is accurate. These findings make it plausible to exclude the edge stress concentration as a numerical artefact, and at the same time provide a mean of disregarding this local phenomenon.

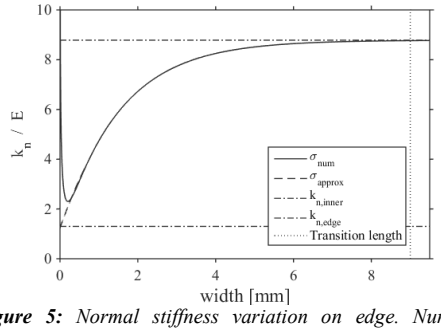

Figure 5: *Normal stiffness variation on edge. Numerical stiffness σ_{num} compared to theoretical values k_n from Equation (5) with the approximated distribution in dashed curve. The transition length, as given in Equation (6), is indicated as a vertical line.*

Conducted test series [12] indicated that wood failure close to the bond line was the governing failure mode, and thus wood strength parameters were used in a Norris strength criterion [17]. It was found that good model characteristics were achieved using a single cohesive element in the thickness direction, for which the normal stiffness variation as described above was applied. The material properties of the bond line are found in Table 3, representing the elastic properties of rubber for normal (σ_{perp}), principal shear (τ_0) and transverse shear direction (τ_{90}) [18] while using wood strength characteristics [16]. The stiffness was then determined using Eq (5), in which Poisson's ratio was set to 0.497.

Table 3: *Material properties for the cohesive model of the bond line. Units are given in MPa.*

σ_{perp}		τ_0		τ_{90}	
E	3.6	G	1.2	G_{90}	1.2
$f_{t,90}$	4.9	f_v	4.4	$f_{v,90}$	1.6

4 MODEL EVALUATION

4.1 EXPERIMENTAL WORK

In order to validate the presented models, comparison is made to conducted test series by Yang et al. [12]. The presented material properties are chosen to represent the used materials, while the test setup and geometry is given in Figure 6.

Two identical SPDJ were prepared in each end of a 2 m long glulam element. The 400x400 mm^2 steel plates were thicker around the hole to prevent local buckling. The steel plates were fastened by 34 screws during curing. Three nominally equal specimens were included in the test series, with a resulting average failure load of 990 kN [12].

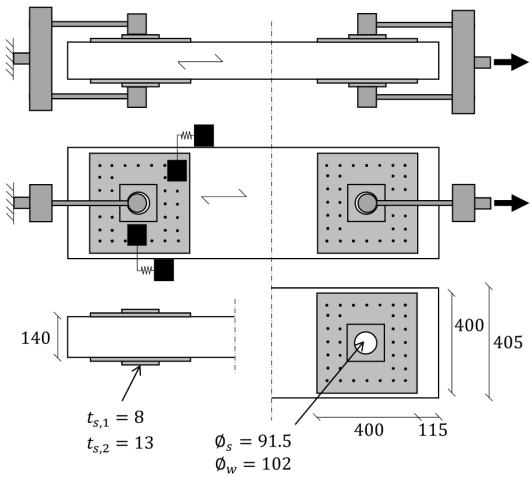

Figure 6: *Test setup and geometry used by Yang et al.* **[12]**, *with displacement gauges indicated by black solids. Dimensions are given in millimetres.*

4.2 BOND LINE STRESS DISTRIBUTION

The bond line shear stress distribution is given by both the analytical 1D and the numerical 3D model. The distributions show good agreement as shown in Figure 7, which also reveals the close to uniform stress distribution needed for good load carrying capacity of the joint.

The normal stresses in the bond line are only evaluated in the numerical 3D analysis, and the results are found in Figure 8. Stress peaks occur on the hole perimeter due to the load application eccentricity, but a bending of the entire steel plate can also be seen. The lower bond line normal stiffness at the edges, discussed in Section 3.3, results in reduced normal stresses at the ends.

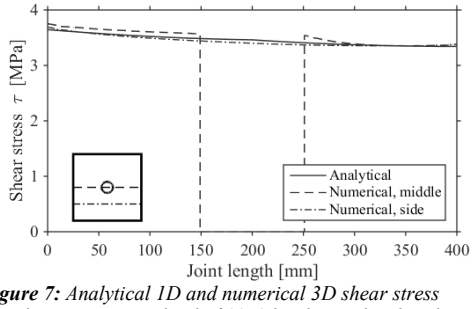

Figure 7: *Analytical 1D and numerical 3D shear stress distribution at a joint load of 1050 kN directed right. The numerical middle and side path are indicated by left legend.*

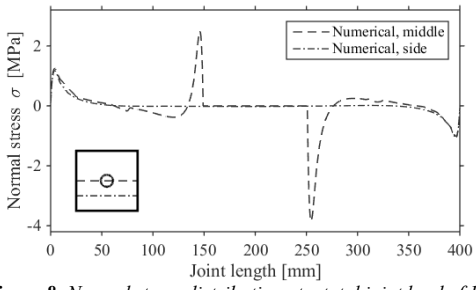

Figure 8: *Normal stress distribution at a total joint load of 1050 kN directed right (c.f. Figure 6).*

The critical peel stresses are found in Figure 8 as positive normal stresses. By introducing the peel stress component in the failure analysis, the failure region is moved from the edge behind the load (maximum shear stress) to the hole perimeter (maximum peel stress).

4.3 STRENGTH AND STIFFNESS

Table 4 provides a failure load comparison of the presented 1D- and 3D calculation methods, as well as the average failure load from tests [12]. As expected, the analytically determined failure load according to Eq (4) is found to be higher by disregarding peel-shear stress interaction. Deviating 6% from experimental values, the 3D numerical analysis shows reasonable agreement. Yang [12] describes a test setup error, which resulted in a low failure strength of the first specimen (see also Figure 9). If excluded from the average, the 3D analysis deviates 4% from test results, independent of polar or rectilinear wood model was used.

The stress state evaluation of the 3D model was conducted according to a Norris failure criterion, which concludes that bond line failure is reduced by 20% by regarding peel stresses. By such, the bond line failure region is also changed from the outer perimeter of the plate to the vicinity of the hole.

Table 4: *Bond line failure load and corresponding average shear stress according Eq (4) and FEM.*

Type of analysis	Failure load	Avg shear stress
Test [12]	990 kN	3.26 MPa
3D Numerical	1020 kN	3.35 MPa
1D Analytical	1270 kN	4.18 MPa

The numerical model also enables stiffness comparison between model and tests, which is found in Figure 9. The typical S-shaped curve of the non-linear elastic behaviour of rubber is seen in the test results, while it is assumed linear in the bond line model. It can further be seen that the numerical model indicates a softer joint than the test series, which is possibly due to the large amount of screws used but not modelled.

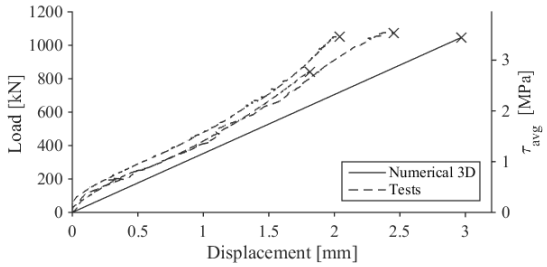

Figure 9: *Load-displacement curve comparison between tests and numerical 3D model. Average shear stress is found on the right y-axis.*

4.4 WOOD STRESS ANALYSIS

Using the presented bond line model, a good strength agreement was found with tests. However, as indications of timber failure were found in the tests [12] the stress situation in the timber member was also investigated, see Table 5.

The linear stress analysis indicates large tensile stresses parallel to grain in the upper and lower hole perimeter. Evaluating the stress tensor at this point by a Tsai-Wu failure criterion [14] indicates a failure already at a load level of 660 kN, which is 35% lower than the test results indicate. However, this concentration is possibly a crack initiation point, which could explain the combined bond line and shear plug failure seen in the tests. Previously assumed as a secondary failure, these findings make it plausible that the shear plug occurred simultaneously, if not prior, to the bond line failure.

The failure load is further decreased using polar coordinates for the wood representation (Figure 4). The Tsai-Wu criterion indicates failure at 560 kN, with a new failure region at the outer bond line perimeter in front of the applied load.

In comparison to the estimated bond line failure according to Norris, the Tsai-Wu criterion of the wood identifies more localized peak values for both the rectilinear and polar material models. This local behaviour lowers the capacity of the joint by acting as possible fracture initiation points. Even so, by comparing the numerical results to the tests indicates that the bond line failure is the ultimate failure.

Table 5: *Bond line failure load from numerical 3D analyses.*

Type of analysis	Failure load
Test [12]	990 kN
Bond line	1020 kN
Rectilinear wood	660 kN
Polar wood	560 kN

5 SPDJ DESIGN EVALUATION

5.1 RUBBER PARAMETER ANALYSIS

A large variety of rubber materials can be found on the market today, typically used as seals or to reduce vibrations. As such, the resistance to chemicals, effective temperature range and the hardness are the relevant design aspects. However, high shear strain capacity, high shear strength and low creep are needed for the implementation of the SPDJ. A thin rubber layer is also favourable, along with a suitable shear stiffness.

The shear stiffness and the rubber thickness are intimately related as they affect the bond line flexibility. The flexibility is needed to allow different elongation of the adherends and thus increase the joint strength. However, normal stresses have a negative impact on the joint, as seen in Section 4.3, which are increased for thicker rubber layers.

In Figure 10, the joint failure strength is shown as a function of rubber hardness for different thicknesses. The hardness is given in shear modulus as well as the industry standard degrees Shore A, which is non-linear in comparison to the shear modulus [18]. It is of little surprise that the load capacity increases for a decreasing hardness, assuming the wood failure is governing. However, as shown in Figure 11 the joint slip also increases for decreased hardness, which is often undesirable. A good balance must thus be found between joint slip and load carrying capacity, which is dependent on the application and possible interaction with other types of fasteners. Note that the strength capacity is, however, predominantly determined by the size of the plate.

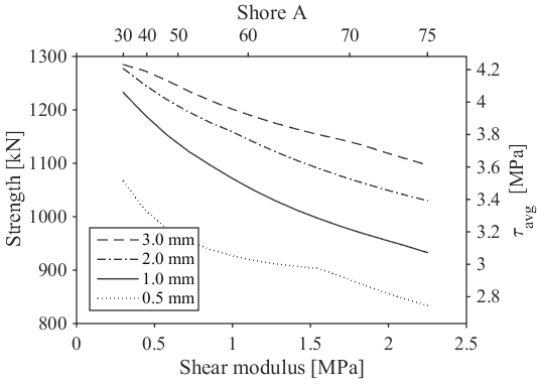

Figure 10: *Failure strength of the SPDJ reference design for increasing stiffness using different rubber layer thicknesses. Stiffness is given in Pascal (lower x-axis) and Shore A (upper x-axis).*

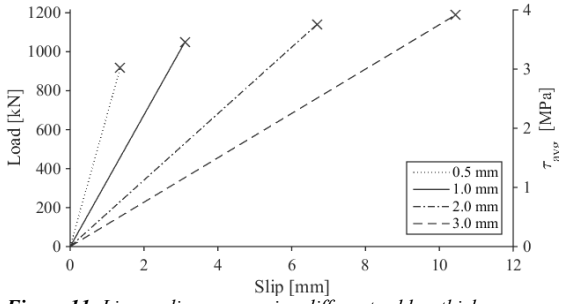

Figure 11: *Linear slip curves using different rubber thicknesses with a shear modulus $G = 1.1\ MPa$.*

5.2 ALTERNATIVE DESIGNS

Two alternative designs were analysed in order to potentially reduce the stress concentrations in the wood presented in Section 4.4. Both designs in Figure 12 reduce the bonded area in vicinity of the hole, with the aim of minimizing stress transfer around the hole.

In the first design, elliptical cut-outs are removed from the steel plate (elliptical design), while an area in the middle is left unbonded in the second (strip design). The steel plates are, in both cases, made longer in order to have the same effective area as the reference square design. The failure loads are compared to the original design in

Table 6. It is evident that, for capacity reasons alone, a given bond area is better used in the strip design than the other tested.

Peel stress concentration arose at the hole perimeter in the original design as was presented in Figure 8. Similar concentrations are found for the elliptical design, but are eliminated in the strip design due to the lack of bonded area at the hole perimeter. The only peel stresses acting on the strip design are at the ends due to global plate bending, similar to what was also found for the original design. However, due to the longer plate in the strip design, the peel stresses are lower even though a stress concentration arises at the inner corner.

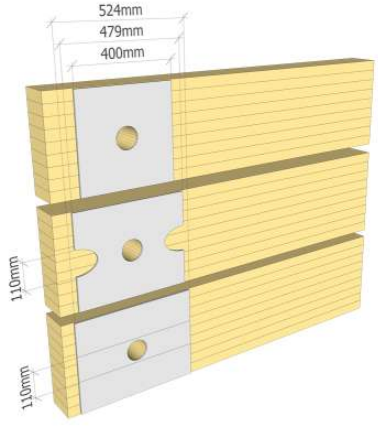

Figure 12: *Alternative designs investigated to possibly minimize stress concentrations around the hole.*

The intermediate rubber layer distributes the shear stress close to uniform for the three overlap areas. However, as also the Volkersen theory identifies, the distribution is more non-uniform for longer overlap areas. The peak shear stress in the strip design now coincides with the considerably lower peak peel stress, resulting in a bond line failure of 1100 kN.

The strip design is again promising when looking at the wood. Removing the bond line stress concentrations around the hole also lowers the corresponding stresses in the wood. The tensile stress parallel to grain is reduced by approximately 25% while the shear stress concentration is removed entirely.

All the designs are similar in terms of joint slip, but the strip design is the better choice in terms of strength at the cost of a larger joint. The strength increase is not necessarily worth the increased size, showing that the original square plate design is indeed efficient.

Table 6: *Failure load comparison of different geometries. Rectilinear wood model was used.*

Geometry	Bond line failure load	Wood failure load
Original	1020 kN	660 kN
Reduced elliptical	950 kN	660 kN
Reduced strip	1100 kN	990 kN

Ductility is also of interest in timber joints, especially in areas with seismic activity. The work presented here has had the aim of finding the ultimate strength of the SPDJ design, which has resulted in the characteristic brittle wood failure. However, ductility can be achieved by careful designing of the steel parts to enable yielding and/or buckling within the joint. Either the plate can be made thin to obtain a deformation zone in the unbonded region of the hole, or the steel dowel can be designed to deform in the contact zone. The latter has been studied by e.g. Pavković et al. [11], and is considered the best alternative.

6 CONCLUSIONS

The presented research has shown that the SPDJ can efficiently withstand large forces using a simple design with a high degree of prefabrication. Failure modes commonly found for dowel connections are prevented, and the joint strength can with ease be designed to match member strength.

Calculation models have been presented in order to allow numerical investigations, while an analytical equation preferably can be used to suggest a design code procedure. By disregarding stress interaction, the analytical failure load is found being approximately 30% too high, while the numerical model shows a reasonable agreement.

Analysis of alternative designs indicate that the original square plate design is not only simple to manufacture, but also an efficient shape. However, the ratio between load bearing capacity and bonded area can be increased if the presented strip design is used.

The rubber foil adhesive joint can typically be used whenever a strong adhesive bond line is required. The SPDJ is one interesting application that the technique enables, but many more are possible. Ongoing studies aim to determine fundamental properties of the rubber foil adhesive joint, such as strength characteristics and long-term behaviour.

ACKNOWLEDGEMENT

We gratefully acknowledge the financial support provided by the Swedish research council *Formas* through grant 2012-879.

REFERENCES

[1] European Committee for Standardization (CEN), EN 1995-1-1:2004: Eurocode 5: Design of Timber structures, Brussels, Belgium, 2004.

[2] B. Bohannon, "Prestressed laminated wood beams," Forest products lab, Madison, Wisconsin, 1964.

[3] K. B. Borgin, G. F. Loedolff and G. R. Saunders, "Laminated wood beams reinforced with steel strips," *Structural Divison,* vol. 94, no. 7, pp. 1681-1706, 1968.

[4] R. E. Rowlands, R. P. Van Deweghe, T. L. Laufenberg and G. P. Kreuger, "Fiber-reinforced wood composites," *Wood abd Fiver Science,* vol. 18, no. 1, pp. 39-57, 1986.

[5] H. Min-juan and L. Hui-fen, "Comparison of glulam post-to-beam connections reinforced by two different dowel-type fasteners," *Construction and Building Materials,* vol. 99, pp. 99-108, 2015.

[6] D. F. Windorski, L. A. Soltis and R. J. Ross, "Feasibility of fiberglass-reinforced bolted wood connections," Forest Products Laboratory, Madison, Wisconsin, 1997.

[7] P. Haller, T. Birk, P. Offermann and H. Cebulla, "Fully fashioned biaxial weft knitted and stitch bonded textile reinforcements for wood connections," *Composites: Part B ,* vol. 37, pp. 278-285, 2006.

[8] P. J. Gustafsson, "Tests of Full Size Rubber Foil Adhesive Joints," Lund University, 2007.

[9] R. Crocetti, M. Axelson and T. Sartori, "Strengthening of large diameter single dowel joints," SP Technical Research Institute of Sweden, 2010.

[10] P. Kobel, "Modelling of Strengthened Connections for Large Span Truss Structures," Master Thesis, Lund University, 2011.

[11] K. Pavkovic, V. Rajcic and M. Haiman, "Large diameter fastener in locally reinforced and non-reinforced timber loaded perpendicular to grain," *Engineering Structures,* vol. 74, pp. 256-265, 2014.

[12] H. Yang, R. Crocetti, G. Larsson and P.-J. Gustafsson, "Experimental study on innovative connections for large span timber truss structures," in *IASS working groups 12 + 18 International Colloquium 2015*, Tokyo, Japan, 2015.

[13] O. Volkersen, "Die Nietkraftverteilung in zugbeanspruchten Nietverbindungen mit konstanten Laschenquerschnitten," *Luftfahrtvorschung,* vol. 15, pp. 41-47, 1938.

[14] S. Tsai and E. Wu, "A general theory of the strength of anisotropic materials," *Journal of Composite Materials,* vol. 5, pp. 58-80, 1971.

[15] E. Serrano, Adhesive Joints in Timber Engineering, modelling and testing of fracture properties, Lund, 2000.

[16] K. Berblom Dahl, Mechanical properties of clear wood from Norway spruce, ISBN 978-82-471-1911-2 ed., Trondheim, Norway: Norwegian University of Science and Technology, 2009.

[17] C. B. Norris, Stength of orthotropic materials subjected to combined stresses, Madison: U.S. Department of Agriculture, 1962.

[18] P.-E. Austrell, "Modelling of elasticity and damping for filled elastomers," Lund University, Lund, 1997.

Paper E

Dowel design of the shear plate dowel joint

G. Larsson[a,*], E. Serrano[a], P.J. Gustafsson[a], H. Danielsson[a]

[a]*Division of Structural Mechanics, Lund University, P.O. Box 118, SE-221 00 Lund, Sweden*

Abstract

The shear plate dowel joint (SPDJ) is a novel connection design for heavy timber structures. The connection uses a single large diameter dowel and glued-on steel plates to transfer loads between members. Consequently, the design of the dowel is of great influence for the global performance of the connection. This paper presents an experimental and numerical investigation of the influence of the geometry and the material parameters of the dowel, focusing on the possibility to design the joint for ductile failure modes.

The study is conducted for a single-member node configuration as well as a three-member node configuration. Testing was conducted on dowels made of steel, aluminium, birch and laminated densified wood, and shear plates of steel and plywood. It is shown that ductile deformations of the SPDJ can be increased by 30–80% using thin-walled metal dowels. The results show that most of the tested wood-based materials are inadequate for such detailing, except laminated densified wood.

The numerical study is focused on the ductile response obtained when using steel tubes as the load transferring dowel. The optimal ratio of dowel outer diameter D_o to steel plate size is found to be 0.35, with a tube wall thickness of approximately $0.075D_o$. Using this geometry, a good balance between load carrying capacity and ductile failure modes is obtained.

Keywords: timber connection, shear plate dowel joint, rubber foil, ductility

1. Introduction

Adequate strength is the single most important functional requirement of a structural connection, but also the stiffness and its predictability is of importance in order to determine the load paths within a structure. However, the orthotropic behaviour and natural variability of timber increases the complexity of stiffness predictions and, consequently, considerable research efforts have been spent on the topic of predicting load-slip behaviour of timber connections in the last decade.

This study concerns the influence of dowel design (material and geometry) on the load-deformation behaviour of the novel shear plate dowel joint (SPDJ) [1]. The SPDJ is designed for heavy timber structures typically made from glued laminated timber (GLT) and utilizes a single large diameter dowel to transfer forces between members. The risk of premature shear plug failure, typical for single large diameter dowels with short end distance, is significantly reduced by the use of externally bonded steel plates as shown in Figure 1. The external plates combined with an oversized hole in the timber member substitutes the shear plug failure caused by direct dowel-timber contact by shear failure of the plate bond line.

The steel plates are bonded to the timber using a flexible bond line, in this study comprised of a vulcanised rubber layer and structural adhesives. The design has shown impressive strength in full-scale short-term tests by achieving a close to uniform shear stress distribution over the bonded area [2]. Another appealing feature is the designable stiffness [3]. These preferable characteristics are made possible by the use of a bond line with low elastic shear stiffness yet with high strength and fracture energy, here also denoted a resilient bond line [4]. However, the bond line does not prevent the typical brittle wood failure in shear, which is the loading mode ensured by the oversized hole in the timber member.

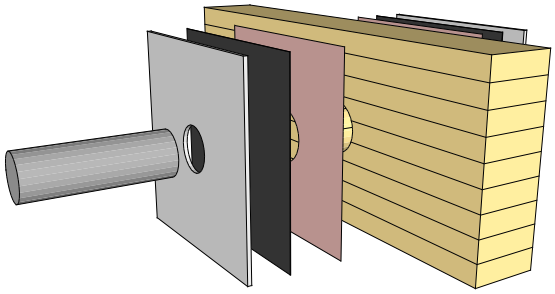

Figure 1: Exploded view of the shear plate dowel joint (SPDJ). From left: A large diameter dowel; plate with hole diameter matching the dowel; rubber foil vulcanized to the steel plate; structural adhesive; and the GLT member.

Using a solid steel dowel, the elastic load-slip behaviour

*Corresponding author
Email address: gustaf.larsson@construction.lth.se (G. Larsson)

of the SPDJ will to a great extent be governed by the characteristics of the rubber layer, while the joint load bearing capacity will be governed by the strength (and its variability) of the timber [2]. Suitable commercial rubbers typically have a coefficient of variation for shear stiffness of 5% (if expressed in Pascal) [5]. The prediction of the load-slip behaviour of the SPDJ can thus be considered enough well-defined for practical applications. However, the strength of the SPDJ is governed by two brittle failure modes of the timber, namely shear and tension perpendicular to the grain. Such brittle failure is undesired in practical application.

The ductile behaviour of steel can be utilized in order to increase the ductility of the SPDJ by allowing plastic deformations to occur in either the dowel or the plate. In addition, this would also reduce the strength variability of the joint as compared to allowing for the brittle wood failures discussed above, see also the discussion of Jockwer [6]. Plate deformation at the location of dowel-to-plate contact is made possible by the oversized hole in the timber, but analyses suggest that the clearance between the dowel and wood must be unreasonably large to facilitate both plate and bond line deformations [7]. The studied means to achieve a ductile failure with high prediction accuracy is thus by allowing deformation of the dowel in shape of a tube, a system previously studied in other configurations such as the expanded tube fasteners [8] or as reinforcement [9]. In addition to the dowels used to increase connection ductility, wood-based dowels and plates are also tested in order to investigate the possibilities of a connection without metal components.

The study aims to experimentally investigate the global connection response using different types of dowels in different joint configurations. The tests also serve as a reference for numerical studies of the geometry, which aim to identify a suitable relation between the size of the dowel and the size of the plate, as well as a suitable ratio between the inner and outer diameter of a tubular dowel for improved ductility. The tests also serve as a reference for numerical studies of the geometry, which aim to identify a suitable relation between the size of the dowel and the size of the plate, as well as a suitable ratio between the inner and outer diameter of a tubular dowel for improved ductility.

The study comprises:

- Experimental tests of small scale SPDJs in short-term quasi-static loading. Six different dowel types were tested in a single-member node configuration, while four dowel types in a three-member node configuration.
- Numerical analysis of geometrical aspects of steel dowels in the joint.

2. Method

The nomenclature used in describing the geometry of the joint components is given in Figure 2. The tests are conducted for two different test configurations: a single-member setup was used to analyse dowel deformations primarily in shear,

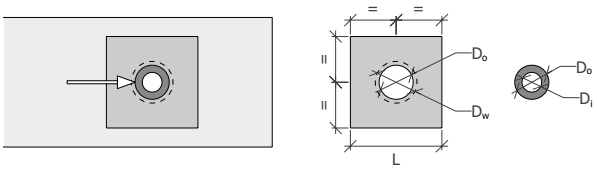

Figure 2: Nomenclature of the plate and dowel geometries of the shear plate dowel joint.

whereas a three-member node set-up was used to also include possible bending of the dowel. Solid dowels or thick-walled steel tubes were used as references to be compared to thin-walled tubes. Additional tests were also conducted using aluminium dowels as well as wood-based dowels and plywood plates.

2.1. Experimental setup

The experimental setups are illustrated in Figure 3. A plate size of 65×65 mm^2 with a 20 mm dowel was used for the single-member nodes, while larger 120×120 mm^2 plates with 45 mm dowels were used for the three-member nodes to facilitate the bending moment. The thicknesses of the steel plates were 5 and 8 mm, respectively.

A 1.0–1.2 mm thick rubber layer was vulcanized to the steel plates to achieve a bond line with low stiffness yet high fracture energy. The rubber was a mix of natural rubber and styrene-butadien rubber (SBR) with a hardness of 62° Shore A. According to data from the rubber supplier, the tensile strength was 22.4 MPa, the shear strength was 9.4 MPa and the elongation at break was 595%. After vulcanization, the rubber was sanded and etched in acid in order to lower the surface energy and making it possible to adhere to the timber, see Gustafsson [10]. The plates were then glued externally to the GLT members using SikaForce 7710 and hardener 7020. Curing pressure was applied using four screws for each plate. The screws were removed prior to testing. The steel used for the plates was of quality Q345B [11], with a yield strength of 345 MPa.

The GLT was of strength class GL30c with a cross section of 80×170 mm^2. To allow dowel movement, the hole diameter D_w was made 15 and 10 mm larger in the GLT than the dowel radius for the smaller and larger SPDJ respectively. The hole was placed at the centre of the member height and with an end distance in the parallel to grain direction of 3.5 times the dowel diameter, i.e. half of the Eurocode 5 requirement for dowel type connections. Average density and moisture content (MC) were measured at the time of plate bonding to 480 kg/m^3 at 9.1% respectively. At the time of the test, MC had reduced to an average of 8.7%, with a coefficient of variation of 3%.

Dowel diameters and wall thicknesses varied for the different tests and are specified in Tables 1 and 2. The number of nominally equal specimens of each type are specified. The steel dowels were of type E470, which according to standards [12] have a yield strength and ultimate strength of 470

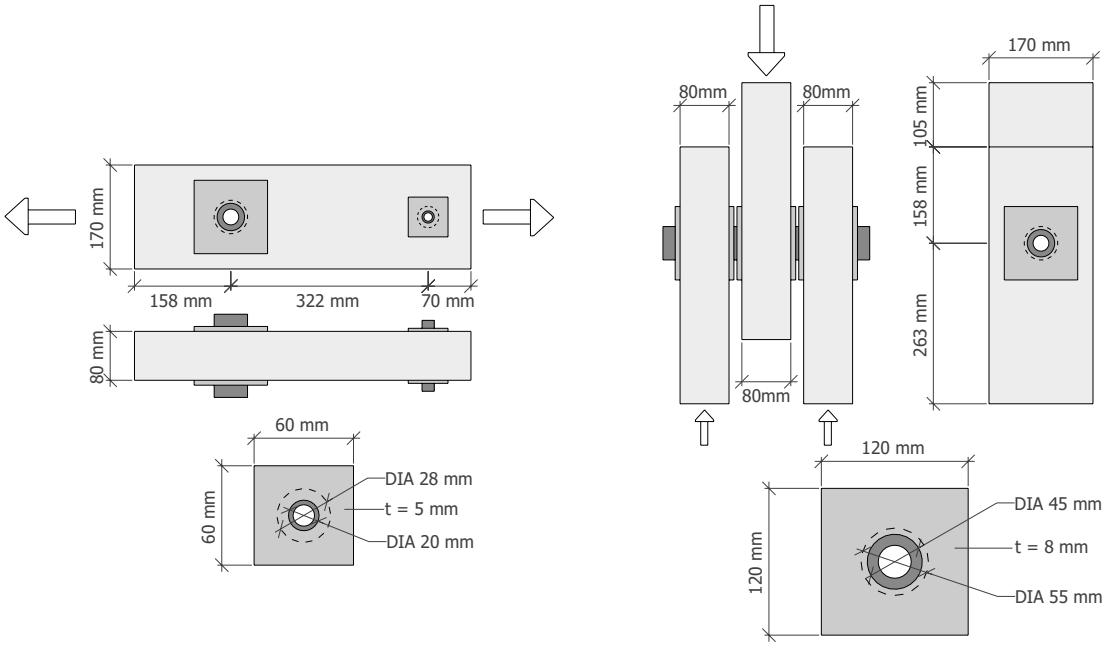

Figure 3: Geometries of tested single-member and three-member nodes.

Table 1: Dowel types tested in three-member node configuration. Series name after configuration type – dowel material – outer diameter – inner diameter.

Series	Dowel $D_o - D_i$	Plate $L \times t$	Number of specimens
T−Ref−45	Steel tube 45−20	Steel 120×8	3
T−Alu−45−i	Aluminium tube 45−i; i = 35, 41	Steel 120×8	2
T−St−45−i	Steel tube 45−i; i = 37, 41	Steel 120×8	2
T−W−40	Birch rod 40−0	Steel 120×30	1

Table 2: Dowel types tested in single-member node configuration. Series name after configuration type – dowel material – outer diameter – inner diameter.

Series	Dowel $D_o - D_i$	Plate $L \times t$	Number of specimens
S−Ref−20	Steel dowel 20−0	Steel 65×5	3
S−Alu−20−i	Aluminium tube 20−i; i = 12, 16, 18	Steel 65×5	3
S−St−20−i	Steel tube 20−i; i = 15, 17	Steel 65×5	3
S−DW−20−S	Densified wood 20−0	Steel 65×5	3
S−DW−20−W	Densified wood 20−0	Plywood 65×30	3
S−W−20	Birch rod 20−0	Plywood 65×15	3
S−W−40	Birch rod 40−0	Plywood 75×15	1

MPa and 650 MPa, respectively. Despite the same steel quality, the tests indicated different strengths for different tube dimensions, c.f. Section 2.2. Yield and ultimate strength for the AW-6060 T6 aluminium dowels [13] were tested on the actual dowels by tensile tests, and found being 180 MPa and 215 MPa, respectively.

Testing commenced with the single member nodes, which were subjected to a displacement controlled quasi-static tensile load at a rate of 1.8 mm/min. The larger SPDJ were here used as support. Once the smaller specimen had failed, the larger SPDJ acting as support was refitted and tested in the three-member node configuration. The difference in size between the dowels at the two ends was chosen large enough not to result in any damage of the larger plate during the single-member tests. The relative shear displacements between the timber member and the loading plates were recorded using linear potentiometers placed centrically on the plate edge. In case of the three-member node, the relative displacement of the inner and outer member was recorded as well as the shear movement of the outermost plates.

Additional tests were conducted on wooden SPDJ using dowels of birch and laminated densified wood, as well as shear plates of beech plywood. The shear strength of the birch dowel was determined in separate tests involving a loading similar to the load experienced in the SPDJ. The average shear stress at failure was found to be 10.5 MPa. As an even stronger wood dowel alternative, laminated densified wood of type Lignostone© Transformerwood© was used. This material has a flexural strength of 140 MPa according to the manufacturer [14].

Beech plywood plates with a thickness of 15 and 30 mm for the 1- and 3-member nodes, respectively, were also tested as an alternative to steel. The rubber used in this configuration was a 3.5 mm thick mixture of SBR and natural rubber with a hardness of 60° Shore A (shear stiffness of 1.2 MPa), tensile strength $f_t \geq$17.5 MPa and an elongation at failure of 400%, according to the supplier of the rubber. The rubber was glued to the GLT and the plywood using SikaForce 7710 and hardener 7020.

A larger diameter dowel was used for the S−W−40 specimen, and thus a larger plate size was used to have approximately the same effective shear area as for the other single member specimens with smaller dowels.

2.2. Numerical analysis

Numerical 3D-modelling of single- and three-member nodes was conducted using a commercial general-purpose FE software [15]. Modelling was only conducted for joints made from steel dowels and steel plates, verified by the tests of steel components presented in Tables 1 and 2. The model was then used to conduct geometrical parameter studies in order to identify suitable dowel characteristics to promote ductile a failure mode.

A typical mesh of the three-member configuration is shown in Figure 8, also showing that double symmetry is used. Load was applied in the same manner as in the tests, using an algorithm with displacement control and contact formulation.

Table 3: Adopted parameters for wood [16]. Parameters are given in MPa and [–].

E_L	9040	G_{TR}	30	υ_{TR}	0.59
E_T	340	G_{TL}	580	υ_{TL}	0.36
E_R	790	G_{RL}	640	υ_{RL}	0.31

Connection deformations were measured between the same points as used in the tests, i.e. the shear displacement of the plate. The GLT was modelled as a homogeneous and rectilinear orthotropic timber material with elastic material parameters according to Table 3.

The bond line was modelled using the hyperelastic Yeoh material model. The material parameters of that model were found by least square fitting of the elastic response of the series S−Ref−20, in which dowel deformations are assumed negligible. The Yeoh model can be described as in Equation 1 [17] relating shear stress τ to the shear strain κ using three material parameters C_{i0}, which enable the characteristic S-shaped stress vs. strain curve of rubber. The shear stiffness of the adhesive is not explicitly taken into consideration as it is considerably stiffer than the rubber layer [18].

$$\tau = 2C_{10}\kappa + 4C_{20}\kappa^3 + 6C_{30}\kappa^5 \quad (1)$$

The steel plates were modelled as isotropic material and perfectly plastic. Yielding properties of the steel dowels were input as tabulated data. Although all dowels were specified as being made from the same material, additional tension tests showed a variation with dowel diameter. Thus in order to verify the model using the experimental data, the yield strength for the 20 mm dowels was set to 220 MPa (f_u = 490 MPa), while 350 MPa (f_u = 650 MPa) was used for the 45 mm dowels according to the tensile tests performed on the actual dowels. Once the model was verified, the material parameters for the dowels were held constant during the parametric study for clarity, as presented in Table 4.

Linear elements with full integration were used for all materials but the rubber, for which a hybrid formulation was used, as is commonly recommended for incompressible or nearly incompressible materials.

Failure was defined either by excessive dowel deformation to the extent that the displacement controlled numerical analysis was aborted, or by timber failure close to the bond

Table 4: Adopted parameters for steel and rubber, MPa and [–].

Steel		Yeoh[1]	
E	210 000	C_{10}	0.5488
f_y	250	C_{20}	0.0009
f_u	470	C_{30}	0.0006
υ	0.31		

1) Experimental values based upon conducted tests.

line. No maximum applied displacement was prescribed. Timber failure was assessed using Weibull weakest link theory [19] assuming the potential failure zone being restricted to the timber area bonded to the plate. This bonded area was modelled using cohesive elements. The multiaxial stress state in the timber close to the bond line was used to formulate an effective dimensionless stress measure based on a Norris criterion [20]. This criterion includes the dominant shear strength f_v and the tension perpendicular to the bonded area (peel strength), $f_{t,90}$ for each integration point. The ratio between the peel strength and shear strength $f_{t,90}/f_v$ was set to 0.6 [21], by which values f_v = 8.5 MPa and $f_{t,90}$ = 5.1 MPa were determined by fitting to the experimental data of the S−Ref−20 test. The strength values 8.5 and 5.1 MPa refer to the reference strength of a 2-parameter Weibull model, with the associated reference area of 1000 mm^2. The Weibull shape parameter m was determined by fitting the numerical results of the three-member node reference test specimen T−Ref−45, identifying $m = 10$. This shape parameter value corresponds to a coefficient of variation of 12%. Thus it was assumed that the 2-parameter Weibull distribution can be expressed through the following cumulative probability density function:

$$F = 1 - e^{-\left(\frac{\bar{\sigma}}{f_v}\right)^m} \tag{2}$$

with

$$\bar{\sigma} = \sqrt{\left(f_v/f_{t,90}\right)^2 \sigma^2 + \tau^2} \tag{3}$$

The parameter studies performed are primarily conducted for a steel plate size of 200×200 mm^2 for the single-member nodes, while 300×300 mm^2 was used for the three-member nodes.

3. Single-member nodes results

3.1. Tests

The test specimens were loaded until failure for which three failure modes were present: (a) plate bond line failure by a combination of adhesive and shallow timber rupture; (b) ductile dowel failure; and (c) plate failure by inadequate strength between plywood veneers. The bond line failure by a shallow wood failure (a) is the ultimate limit to the total load carrying capacity of the connection. The reference test series aimed at identifying the response for this failure mode in terms of capacity and load vs. displacement behaviour.

The results for single-member nodes are compiled in Table 5 and Figure 4, with an upper bound of the load-carrying capacity identified from the reference tests being 35 kN (COV 7%), corresponding to 5.4 MPa in average shear. A ductile failure was found for the thin-walled tube dowels at the expense of total load carrying capacity. As expected, the behaviour of the thick-walled tubes approaches the behaviour of solid dowel reference case, see Figure 4. The curves illustrated in the figure are measured data from one of two attached linear potentiometers for one specimen of each type.

The joint stiffness is in Table 5 defined as the relative deformation between the GLT element and the load application plate between $0.4F_{el}$ and $0.7F_{el}$, where F_{el} is the limit of proportionality as marked by × in Figures 4 and 7. In case of brittle behaviour, then $F_{el} = F_{ultimate}$. The residual capacity ratio, expressed in percent, is defined as the ratio between the residual capacity and the elastic limit as $F_{res} = (F_u - F_{el})/F_{el}$.

The low strength of the specimens using a plywood plate is due to low inter-veneer bonding strength. Despite the high embedment strength in comparison to solid timber products, plywood is clearly not adequate to be used for this type of shear action. This is evident from the results given in Table 5, with specimen types S−DW−20−W and S−W−20 showing plate failure at very low load levels. Note that the dowel of specimen S−W−40 came in direct contact with the GLT and thus the high load level obtained should not be compared with the other specimen types. The significantly lower stiffness of the plywood plate joints compared to the stiffness of the steel plate joints is primarily due to the thicker rubber used for the plywood plate case, 3.5 mm as opposed to the 1.0 mm thickness used for the steel plate case.

Impressive characteristics were obtained both in terms of embedment strength and shear strength by the laminated densified wood dowel of specimen S−DW−20−S (Table 5). Only minimal permanent deformations were visible after steel plate failure, comparable to the thicker steel dowels.

In terms of residual capacity, again the all-wood S−W−40 configuration stands out due to the direct contact. The SPDJ is normally designed to avoid this secondary contact, but such an action could possibly also be utilized to increase the residual capacity. The point of contact is clearly visible in Figure 4 (subplot 4) at a deformation of approximately 8 mm. After contact, the primary deformation mode was extensive embedment deformation of the load application plate consisting of 15 mm beech plywood, as well as shear deformations of the dowel. This test was cancelled prior to failure.

3.2. Numerical

The numerical model is verified by comparison of the load-displacement behaviour of the joint with steel dowels, see Figure 5. The joints with thick-walled dowels display an elastic response with a capacity that is limited by brittle bond line failure as predicted by the Weibull analysis. The initial S-shaped elastic response is clearly visibly in all tests but is less pronounced in the numerical analysis. It is possible that the discrepancy is due to the use of fillers in the rubber, which are used to increase stiffness but also accentuate the natural nonlinearities of the stress-strain curve. This is not fully captured by the Yeoh material model, which instead can be considered to entail an average stiffness in an elliptic hysteresis curve [17].

Once verified by tests, the numerical model was used to conduct a parametric study involving different dowel geometries, with results presented in Figure 6. The load carrying capacity of the connection vs. dowels of increasing size relative to the plate side length is plotted for different dowel thicknesses. The load carrying capacity F_{max} is normalized by shear

Table 5: Test results of the single member node with coefficient of variation within parenthesis. Residual capacity is presented in the cases in which the connection showed a ductile behaviour.

Specimen	Load capacity [kN]	Residual capacity ratio [%]	Shear at failure[1] [MPa]	Stiffness [kN/mm]	Failure mode[2]
S−Ref−20	35.4 (7%)	–	5.4	11.2 (13%)	*a*
S−Alu−20−18	14.8 (3%)	54 (22%)	2.3	3.5 (7%)	*b*
S−Alu−20−16	27.6 (0.3%)	34 (26%)	4.2	5.7 (8%)	*a (b)*
S−Alu−20−12	35.1 (5%)	–	5.4	9.9 (1%)	*a*
S−St−20−17	29.6 (6%)	36 (38%)	4.5	5.3 (3%)	*a (b)*
S−St−20−15	33.1 (8%)	–	5.1	9.9 (12%)	*a*
S−DW−20−S	31.4 (10%)	–	4.8	8.6 (6%)	*a*
S−DW−20−W	13.2 (4%)	–	2.0	1.9 (7%)	*c*
S−W−20	10.7 (11%)	–	1.6	1.5 (5%)	*b*
S−W−40[3]	41.1	101	–	2.7	–

1) Average shear stress at failure assuming uniformly distributed shear stress over the bonded area.
2) *a* indicates bond line failure; *b* indicates dowel failure; *c* indicates plywood failure. Parenthesis indicates a significant dowel deformation limited by plate failure.
3) Direct contact between dowel and timber element.

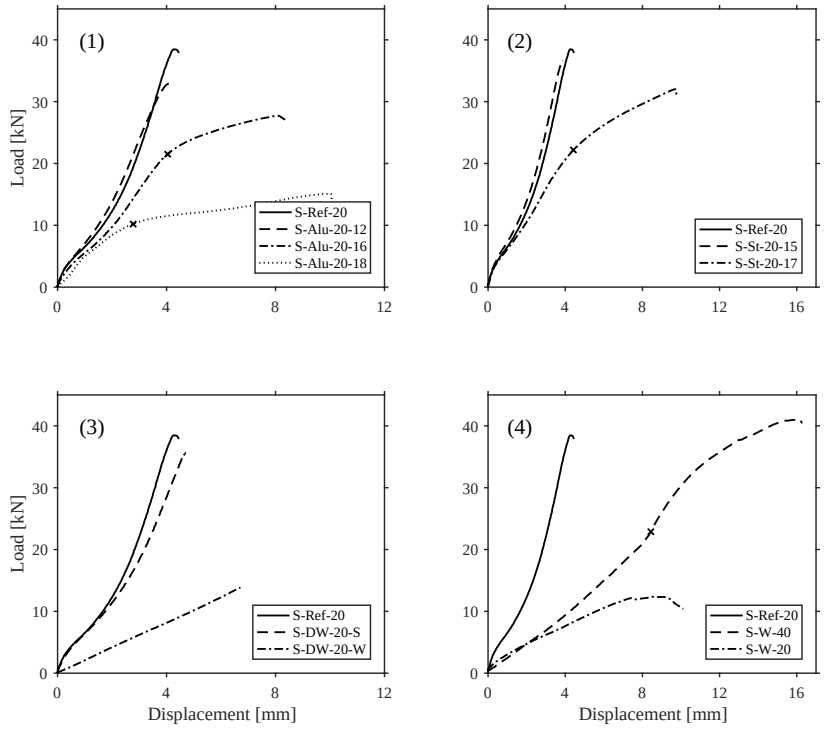

Figure 4: Load vs. displacement response of the single-member nodes for dowels made of aluminium (1), steel (2), laminated densified wood (3) and wood dowels (4). Elastic limit load marked by × when different from maximum load.

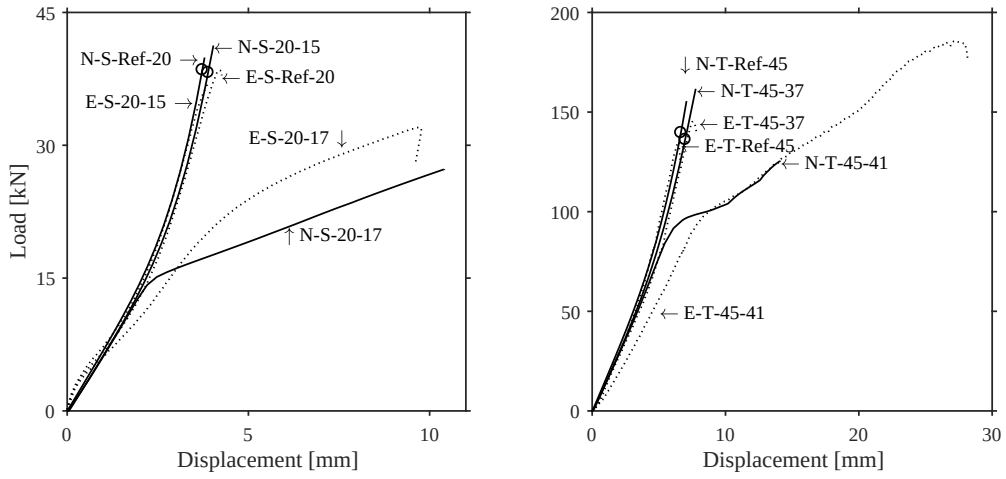

Figure 5: Comparison between numerical predictions (lines) and test results (dotted) for steel dowel joints in single-member and three-member node configurations. Timber failure as predicted in the numerical analysis is marked by ∘.

strength parallel to grain f_v and the total square plate area $2L^2$. The area differs from the effective area $A_{eff} = 2(L^2 - A_{hole})$ with A_{hole} being the hole area.

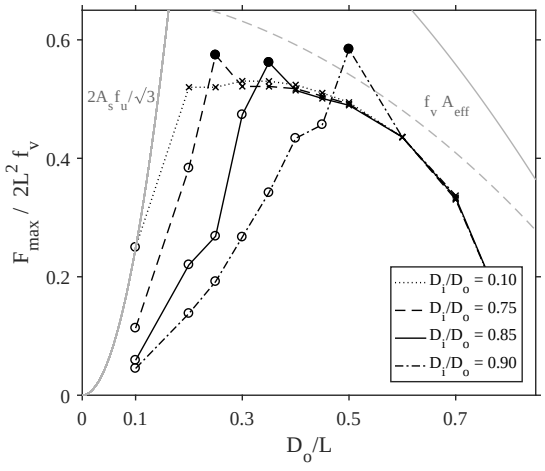

Figure 6: Investigation of dowel outer diameter D_o in relation to plate side length L for different dowel thicknesses in single-member node configuration. See Figure 2 for nomenclature. Ductile dowel failure is marked by ∘, brittle timber failure by × and • marks failure subsequent a direct dowel-timber contact. Analytical maximum load limits in terms of plastic dowel shear strength and effective shear strength of wood, including Weibull size effect as dashed line, are also shown.

To provide context for the results presented in Figure 6, analytical limitations are also plotted. Smaller dowels (low values of D_o/L) are limited by the shear capacity of the steel, while joints with larger dowels are instead limited by shear failure of timber close to the bond line. Two analytical curves are plotted for the bond line failure: one assuming perfect plasticity (and no peel stress interaction) where the capacity is proportional to the shear strength and effective area as $F = f_v A_{eff}$; and a second identical analysis where Weibull size effects are considered as presented in Section 2.2.

In this study, the plate size was kept constant for the different joint configurations of the parametric study. Thus, the effective timber shear area A_{eff} is identical for any given ratio between dowel diameter and plate side length, D_o/L. It is thus reasonable for bond line failures of a given D_o/L ratio to be of similar magnitude for the different D_i/D_o ratios, as is also the case for the failures marked with × in Figure 6. However, direct contact between the dowel and hole inner perimeter did occur prior to bond line failure for three geometries, causing increased load carrying capacity. These cases are indicated by solid dots in Figure 6. This phenomenon was also seen during the experimental testing.

From the results it is concluded that an outer dowel diameter of 30–35% of the plate side length is appropriate, since this ratio gives the highest capacity while still resulting in a ductile failure mode, as shown in Figure 6. The use of other plate sizes has a limited influence on the results.

4. Three-member nodes results

4.1. Tests

The test results of the three-member nodes in terms of load capacity, stiffness and failure modes are presented in Table 6.

Table 6: Test results of the three-member node with coefficient of variation in parenthesis. Residual capacity is presented in the cases in which the connection showed a ductile behaviour.

Specimen	Load capacity [kN]	Residual capacity ratio [%]	Shear at failure[1] [MPa]	Stiffness [kN/mm]	Failure mode[2]
T−Ref−45	130.2 (5%)	–	5.4	23.2 (7%)	*a*
T−Alu−45−41	58.0 (5%)	76 (2%)	2.4	9.6 (7%)	*b*
T−Alu−45−35	142.7 (8%)	12 (113%)	5.9	15.5 (2%)	*a*
T−St−45−41[3]	177.8 (8%)	84 (18%)	–	13.5 (1%)	*a (b)*
T−St−45−37	141.8 (5%)	–	5.9	20.9 (5%)	*a*
T−W−40	50.2	25	2.1	3.3	*c (b)*

1) Average shear stress at failure assuming uniformly distributed shear stress over the bonded area.
2) *a* indicates bond line failure; *b* indicates dowel failure; *c* indicates plywood failure. Parenthesis indicates a significant dowel deformation limited by plate failure. See further Section 3.1.
3) Direct contact between dowel and timber element.

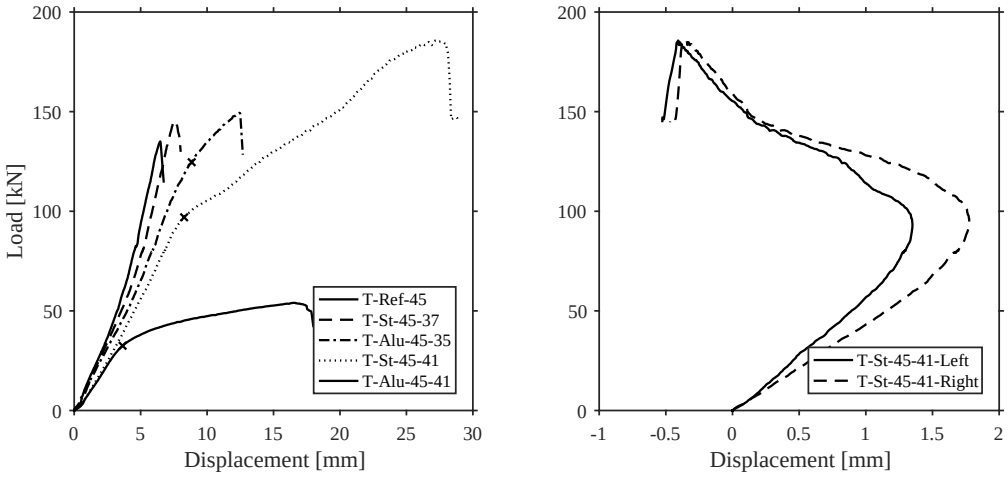

Figure 7: Left: Load displacement curves for the three-member nodes. Elastic limit load marked by × when different from maximum load. Right: The displacement of the outermost plates of specimen T−St−45−41, indicating change of direction of the load carried by the outermost plates on either side of the specimen due to dowel deformations. The negative value suggests large enough displacement to add extra load to the innermost plates.

It was found that the average shear stress at failure of the reference three-member node was similar to average shear stress of the single member specimen. However, the S-shaped load–displacement curve is less pronounced since dowel bending and crushing are more prominent deformation modes in this configuration, as shown in Figure 7. It is also noticeable that the reference case with the thickest dowel is not the strongest, although the stronger plate failures do correspond to the expected range of nominal shear strength of Norway spruce [16].

Significant dowel deformations and residual strength were present in T−Alu−45−41 and T−St−45−41. The aluminium specimen showed residual strength but at the expense of total load carrying capacity, which is a typical behaviour for the SPDJ design. However, the load carrying capacity of specimen T−St−45−41 was higher than the reference capacity of the plate bonding as indicated in Table 6. Similar to the single-member specimen S−W−40, this was made possible by considerable dowel deformations which enabled direct contact between dowel and timber. Thus, the average shear stress between the plate and the GLT at failure is not possible to determine with the available measuring system.

Initially, both plates of an outer member share the applied load. However, as bending deformations in the dowel increases, the inner plate of the outer member carries a larger share of the load. This phenomenon is present in all cases but minimized in the reference case (T−Ref−45) due to the larger

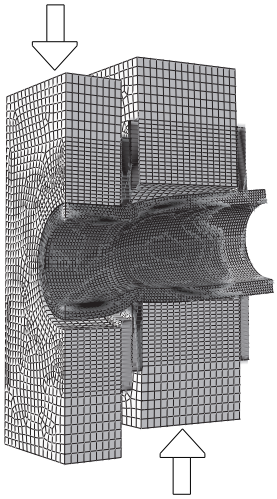

Figure 8: Deformed three-member node configuration from numerical analysis. Double symmetry was used, and a typical mesh is shown. The presented deformation illustrates the secondary contact between the dowel and the wood, as well as the reversed contact between dowel and outermost steel plate of the outer member (far right).

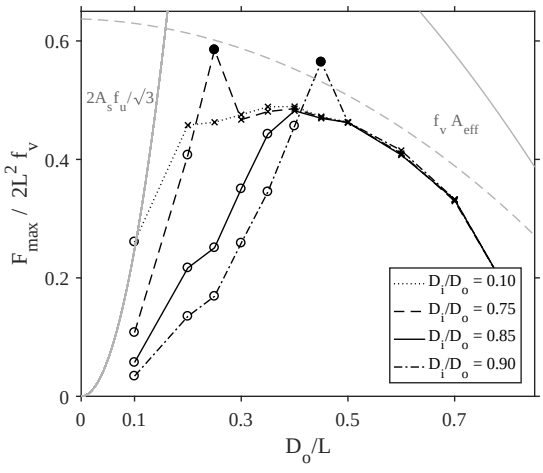

Figure 9: Investigation of dowel outer diameter D_o in relation to plate side length L for different dowel thicknesses in three-member node configuration. See Figure 2 for nomenclature. Ductile dowel failure is marked by ∘, brittle timber failure by × and • marks failure subsequent a direct dowel-timber contact. Analytical maximum load limits in terms of plastic dowel shear strength and effective shear strength of wood, including Weibull size effect as dashed line, are also shown.

bending stiffness of the dowel. However, the thinner metal dowels as well as the wooden dowel of the T−W−40 specimen were all bent to such a degree that the load from the dowel on the outermost plates of the outer members changed direction during the course of the test, as shown in Figure 7 (right). This dowel bending increases the loading on the inner plate.

4.2. Numerical

A comparison between experimental and numerical results in terms of load-displacement response of the three-member node is shown in Figure 5. Similar outcomes as previously discussed for the single node specimens remain, but here the plastic response predictions are more accurate. A typical deformed shape of the specimen can be seen in Figure 8. This type of deformation was also seen in the tests.

A parametric study on dowel geometries was performed also for the three-member node configuration. The results are shown in Figure 9. The increased dowel bending moment in the three-member joint suggests a slightly higher optimal ratio D_o/L, which to some extent is traceable in Figure 9, where the highest capacity is found for a ratio of 0.35–0.40.

One reason for the limited increase of optimum ratio D_o/L of the three-member node is the combination of pipe crushing and bending deformations, which causes the innermost plate of the outer member to take a majority of the load. For $D_o/L = 0.45$ and $D_i/D_o = 0.90$, the contact force ratio at failure between the two plates of the outermost member, F_{out}/F_{in}, was 0.5. Due to the combination of pipe crushing and bending deformations, the behaviour three-member node configurations with thin-walled dowels is similar to the behaviour of the single-member nodes.

5. Fibre orientation of outer members of a three-member node

The similar behaviours of the single and three-member nodes shown in Figures 6 and 9 are to some extent due to the fact that all plates have the same shear capacity. For the three-member node, when bending of the dowel becomes substantial, the inner plate of the outer member will indeed carry all load transferred to the outer member, and thus the configuration behaves similar to the single-member load case. However, if the SPDJ is used in a beam-column connection, the fibre direction of the outer members is rotated 90 degrees. The load will then be introduced into the member by shear perpendicular to grain, engaging the weaker rolling shear action.

A simplified analysis of such a case involving a different orientation of the material in the outer members was analysed numerically. The material directions of the outer members were rotated by 90 degrees but keeping the geometries identical. In order to account for the rolling shear loading in the transfer from the plate to the timber, the ratio between the peel strength and shear strength perpendicular to grain $f_{t,90}/f_{v,\perp}$ was set to 1.2, based upon the previous assumption $f_{t,90}/f_v = 0.6$ [21] and $f_{v,\perp} = f_v/2$ [22]. Fitting was here made

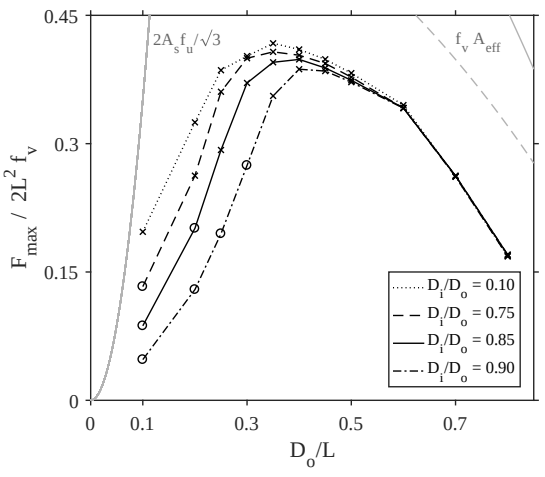

Figure 10: Investigation of dowel outer diameter D_o in relation to plate side length L for different ratios of inner and outer diameters in three-member node configuration with material orientations being rotated 90 degrees between inner and outer member. The load carrying capacity F_{max} is normalized by shear strength parallel to grain f_v and the total square area (not regarding the increasing hole size in timber). Ductile dowel failure is marked by ∘, brittle timber failure by × and • marks failure subsequent a direct dowel–timber contact. Analytical maximum load limits in terms of plastic dowel shear strength and effective shear strength of wood, including Weibull size effect as dashed line, are also shown.

to unpublished experimental data for the same SPDJ geometry as for S−Ref−20 but loaded perpendicular to grain. The fitting resulted in $f_{v,\perp}$ = 3.6 MPa and $f_{t,90}$ = 4.3 MPa.

As can be seen in Figure 10, only a marginal increase in optimal ratio D_o/L was found compared to the parallel three-member node configuration, assuming the same width of the jointed timber elements. The study indicates that it is difficult to fully utilize the outermost plates even for larger dowels, as the effective shear area of the timber is then reduced. A consequence is that it might be difficult to achieve a ductile behaviour even for the thinnest tubes in this configuration.

6. Discussion

The highest possible load carrying capacity of the shear plate dowel joint is limited by the timber element in brittle shear failure close to the bond line. Such brittleness can however be avoided by designing the failure to occur in a ductile material. In case of the SPDJ and using a tubular dowel, pipe crushing is a failure mode that can be designed for, as shown in the present study for both the tested single- and three-member test setups. Thus it is concluded that a ductile behaviour of this type of joint is possible to obtain. The fundamental difference between the two test configurations is the bending of the dowel during loading. The increased bending moment in the three-member node configuration increases the elastic deformation of the connection, but also provides a means to further improve the ductility of the joint. In comparison to ductility, the test results of two configurations (S−W−40 and T−St−45−41) show a possibility for increased residual strength by means of direct contact between the dowel and the GLT member at higher load levels. Although it might prove difficult to accurately predict at what load level this interaction will be activated, such an activation could still be valuable in terms of added safety.

Aluminium dowels were added to the test series to investigate possible differences in ductile behaviour as compared to steel dowels. Although a direct comparison was difficult due to different dowel dimensions and due to different failure modes during testing, the results at least indicate that the tested steel and aluminium alloys both have sufficient ductile behaviour for the SPDJ.

The screws used in order to apply curing pressure between the plates and the GLT members were removed prior to testing to eliminate the possibility of load sharing. However, the resilient bond line used in the shear plate dowel joint can indeed be used to enable interaction with screws by careful design of the stiffness, which is not possible with conventional stiff bond lines. Making use of such a combination of screws and a resilient bond line would result in an even stronger design and would be a preferred design in practise.

The laminated densified wood showed impressive performance when used as a dowel in the single member node configuration. However, the material should also be suitable to use as plates in order to create a connection without any metal parts. Apart from possible environmental benefits also lower weight and more coherent aesthetics could be used as motivation for such a joint, although at a higher cost and with less ductility. A design without metal detailing could possibly also be more efficient in case of fire.

A numerical 3D finite element model was verified by the experimental work and was used in parameter studies in order to size up the connection and find suitable geometry guidelines for the design phase. Suitable geometric parameters are shown in Table 7. Similar recommendations for the single- and three-member node are made due to large dowel deformations. It should also be noted that the suitable geometries are to some extent dependent on the yield strength of the dowel, where thinner tubes typically can be used for higher steel grades.

The dowel deformations cause the outermost plate of the three-member setup to be utilized to a low degree, even negatively affect the performance of the connection in some cases as shown in Figure reffig:Tests3. The merit of the outermost plate is connection symmetry, while an exclusion could enhance the fire performance by embedding the connection in timber, and possibly increase the aesthetics. Exclusion of the outermost plates are suggested in a similar design presented

by Herzog et al. [23].

Ductility is often referred to as the only valid option to dissipate energy during seismic events. However, the type of resilient bond line used for the shear plate dowel joint can prove useful by allowing large displacements. Nevertheless, ductility is a beneficial connection characteristic as it provides means to indicate imminent failure. As also shown in the test series, the possibility of large deformations can, in some cases, introduce additional load paths within the joint which increase the load carrying capacity at high load levels, i.e. adding residual strength when needed most.

7. Conclusion

The study has shown that

- Ductility can be introduced in the shear plate dowel joint by using metal tubes as the load transferring dowel, but typically at the expense of total load bearing capacity.
- Low shear strength of plywood renders it unsuitable as plate material.
- Laminated densified wood is a highly capable product for large load transfers. It is a suitable material for dowels and possibly even plates, although the latter was not tested in this study.
- The numerical analyses suggest the geometrical ratios found in Table 7 to be suitable for a shear plate dowel joint with high load-carrying capacity yet with a ductile failure mode.

Table 7: Suggested geometrical parameters for single and three-member nodes for a given plate side length L.

	Single member	Three-member
Dowel diameter D_o/L	0.30–0.35	0.35–0.40
Dowel thickness D_i/D_o	0.85	0.85–0.9

8. Acknowledgements

The financial support provided by *Stiftelsen Nils och Dorthi Troëdssons forskningsfond* through grant 893-16 is gratefully acknowledged. The authors would like to thank Thomas Johansson at Moelven Töreboda AB for the GLT, Ante Salomonsson at Sika for adhesives and Niels Wösten at Röchling for the laminated densified wood. Special thanks also to Per-Olof Rosenkvist, Lund University for help in the lab.

References

1. Larsson G. High capacity timber joints - proposal of the shear plate dowel joint. Licentiate thesis; Lund University; 2017.
2. Yang H, Crocetti R, Larsson G, Gustafsson PJ. Experimental study on innovative connections for large span timber truss structures. *Proceedings of the IASS Working Groups* 2015;12(18).
3. Larsson G, Gustafsson PJ, Serrano E, Crocetti R. Analysis of the shear plate dowel joint and parameter studies. In: *World conference on timber engineering 2016*. 2016:.
4. Larsson G, Gustafsson PJ, Crocetti R. Use of a resilient bond line to increase strength of long adhesive lap joints. *European journal of wood and wood products* 2018;76(2):401–11.
5. Sheeting & Matting - Industrial & Wear resistant. Trelleborg; 2015.
6. Jockwer R. Impact of varying material properties and geometrical parameters on the reliability of shear connections with dowel type fasteners. International Network on Timber Engineering Research (INTER 2016); 2016:49–7.
7. Lefèvre C. Reinforcement of a large diameter single dowel joint. Master's thesis; University of Mons; 2015.
8. Leijten A. Densified veneer wood reinforced timber joints with expanded tube fasteners. Ph.D. thesis; TU Delft; 1998.
9. Pavković K, Rajčić V, Haiman M. Large diameter fastener in locally reinforced and non-reinforced timber loaded perpendicular to grain. *Engineering structures* 2014;74:256–65.
10. Gustafsson P. Tests of full size rubber foil adhesive joints. Tech. Rep. TVSM-7149; Div. of Struct. Mech., Lund University; 2007.
11. National standards of the People's Republic of China . Steel plates for boilers and pressure vessels, GB 713-2008. 2008.
12. EN 10297-1:2003 . Seamless circular steel tubes for mechanical and general engineering purposes - Technical delivery conditions. 2003.
13. EN 12020-1:2008 . Aluminium and aluminium alloys - Extruded precision profiles in alloys EN AW-6060 and EN AW-6063 - Part 1: Technical conditions for inspection and delivery. 2008.
14. Röchling Engineering Plastics . Lignostone Transformerwood - High-performance insulation components for oil filled power transformers. 2017.
15. Dassault Systèmes . Abaqus Analysis User's manual; 2017.
16. Dahl KB. Mechanical properties of clear wood from norway spruce. Ph.D. thesis; NTNU Trondheim; 2009.
17. Austrell PE. Modeling of elasticity and damping for filled elastomers. Ph.D. thesis; Lund University; 1997.
18. Alexandre R, Sandra J, da Silva VD, Dulce R, Carlos L, Bedon C. Structural adhesive sikaforce 7710 l100-experimental characterization. In: *ne-xt facades-COST Action TU1403 Adaptive Facades Network Mid Term Conference*. 2017:.
19. Weibull W. A statistical theory of the strength of materials. 151; Generalstabens litografiska anstalts förlag; 1939.
20. Norris CB. Strength of orthotropic materials subjected to combined stresses. *FPL-1816 Madison, Wis : US Dept of Agriculture, Forest Service, Forest Products Laboratory* 1962;.
21. Eberhardsteiner J. Mechanical Behavior of Spruce Wood: Experimental Determination of Biaxial Strength Properties. Springer-Verlag; 2013.
22. Swedish national board of housing, building and planning . BKR 94 - BFS 1993:58 med ändringar BFS 1995:18. 1995.
23. Herzog T, Natterer J, Schweitzer R, Volz M, Winter W. Holzbau atlas. Walter de Gruyter; 2003.

Paper F

Duration of load behaviour of a glued shear plate dowel joint

G. Larsson[a,*], P.J. Gustafsson[a], E. Serrano[a], R. Crocetti[b]

[a] *Division of Structural Mechanics, Lund University, P.O. Box 118, SE-221 00 Lund, Sweden*
[b] *KTH, School of Architecture and the Built Environment (ABE), Civil and Architectural Engineering, Building Materials*

Abstract

An experimental study of the duration of load effects in a glued shear plate dowel joint is conducted. The joint design features a single large diameter dowel for load transfers between members, via external steel plates which are bonded to the timber with a low stiffness bond line. Due to the low bond line stiffness, the timber element is subjected to a close to uniform shear stress distribution over the bond area.

The study comprises a total of 80 test specimens loaded in shear, both parallel and perpendicular to grain, at three load levels in the range of 50–80% of the short-term failure load. All specimens failed within approximately 110 days in outdoor sheltered conditions during which time deformations were recorded for one specimen of each type and load level.

The study finds a significantly larger influence of duration of load for this dominant shear action than what is reported in literature for bending tests. The method of ranked stress was used to determine a suggested reduction factor k_{mod} for the shear plate dowel joint to 0.10 and 0.30 for parallel and perpendicular loading respectively. This is a rough estimate based upon a 50-year extrapolation of 4-month data. It must thus be concluded that the studied shear plate dowel joint is not efficient in terms of long-duration loads in outdoor sheltered climate, and that further studies are needed in order to verify the use in other climate classes. It is also evident in this study that there is a lack of knowledge and empirical evidence on duration of load effects in timber for shear loading.

Keywords: shear plate dowel joint, duration of load, shear strength, resilient bond line, rubber foil, timber connection, wood

1. Introduction

This paper investigates the duration of load effects in a glued shear plate dowel joint (SPDJ), a novel connection designed for use in heavy timber systems. An efficient on-site assembly is ensured using a single large diameter dowel [1, 2, 3]. A premature shear plug failure is avoided using an externally bonded steel plate which is attached to the timber with a bond line of low stiffness yet high fracture energy [4, 5]. This is realised by the use of a rubber foil which is vulcanised to the steel plate and adhesively bonded to the timber. Such a resilient bond line enables a close to uniform shear stress distribution over the entire bond area, thus increasing the load carrying capacity considerably. An exploded illustration of the SPDJ is found in Figure 1.

The rubber foil is thus necessary for the strength of the connection, but also enables the possibility to design the connection stiffness [6] by choosing specific rubber mixtures and/or thickness of the foil. However, introducing a rubber foil in the load carrying system poses a new set of challenges, including duration of load (DOL) effects especially regarding rubber creep [7] and timber subjected to shear loading.

While well documented in bending [8, 9, 10, 11], the DOL behaviour of timber subjected to shear loading is considerably less investigated. Shear blocks have been studied by Leont'ev [12] in a comprehensive 10-year indoor study of clear wood specimens loaded parallel to grain, without climate control. His findings suggest that timber in shear is more affected by DOL than bending, suggesting a reduction factor for a 50-year loading of 0.3 compared to 0.5 for bending [9].

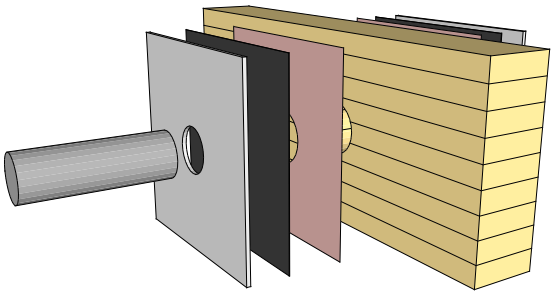

Figure 1: Exploded view of the Shear plate dowel joint. From left: A single steel dowel; steel plate with hole size matching the dowel; rubber foil vulcanized to the steel plate; structural adhesive and then the GLT member with oversized hole to ensure no direct contact between dowel and timber.

The findings of Leont'ev are in conflict with the results

* Corresponding author
Email address: gustaf.larsson@construction.lth.se (G. Larsson)

from a study conducted by Spencer and Madsen [13] on wooden torque tubes in close to controlled climate, who found the Madison curve [8] conservative for normal levels of applied stress. Furthermore, the study indicates that strong material is more affected of duration of load effects. Similar conclusions were drawn in a previous torsion test by Madsen, in which identical test specimens were subjected to accelerated DOL testing by stepwise ramp loading regime [14]. See Gerhards [15] for a comprehensive summary of conducted DOL studies. For this study, also the work of van de Kuilen [16] who investigated DOL effects on three types of timber joints, some of which with dominant shear action, is of interest and will be used for comparing results.

The present paper aims to evaluate the structural behaviour of the shear plate dowel joint when subjected to long term static loading. This DOL study comprises a comprehensive experimental test program of small scale SPDJ subjected to long term static loading in outdoor sheltered conditions, both parallel and perpendicular to grain. The reliability of the connection will be determined in terms of a reduction factor for duration of load effects, k_{mod}, similar to European standards.

2. SPDJ specimens and test conditions

The study is conducted on a 65×65−20 shear plate dowel joint, indicating a plate size of 65×65 mm^2 and a single dowel of 20 mm in diameter. The connection is tested both parallel and perpendicular to grain, achieved using a tensile and a bending test setup, respectively, see Figures 2 and 3. Considerably larger 120×120−45 SPDJ are mounted as supports in the tensile tests, which are designed not to fail during testing.

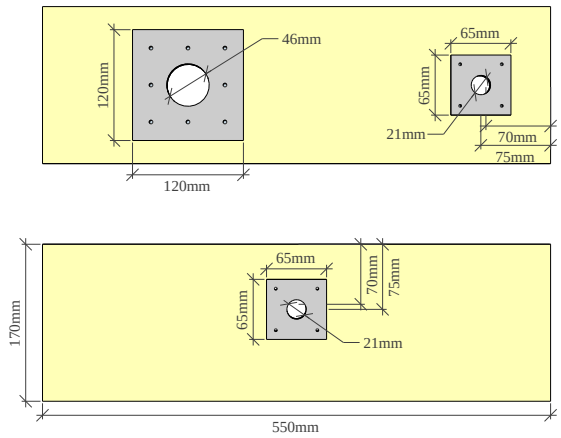

Figure 2: Tensile and bending test specimen dimensions, to scale. The measurement system required eccentric hole placement, thus the centre of the steel plate is 75 mm from edge, while the hole in the GLT is 70 mm from edge.

The joints are mounted on 550 mm long GLT elements with a cross-section of 80×170 mm^2 of strength class GL30c, manufactured in Töreboda, Sweden. The average moisture content of the GLT at the time of SPDJ production was 9.1%, measured using a resistance type hand-held moisture meter. The average density was 480 kg/m^3.

The steel plates with vulcanized rubber were produced in China by Wuxi Fuyo Tech. A mix of natural and SBR rubber with a thickness of 1.0–1.2 mm was vulcanized to the steel plates. In order to achieve a strong adhesive bond of the rubber to the GLT, the surface energy of the rubber was lowered by grinding and acid etching [4]. The rubber foil, vulcanised to the steel plate, was then bonded to the GLT using SikaForce 7710 + hardener 7010, a 2-component polyurethane adhesive. Curing pressure was applied using four 3.5×35 mm screws which were all removed from the plates prior to testing. For structural application it would be plausible to keep the screws inserted in order to increase the strength of the resilient bond line [5], but in this study, aiming at investigating the glued joint, the screws were removed.

In order to ensure force transfer through the joint by shear action of the plate rather than by contact between the dowel and the GLT element, a 35 mm hole was made in the timber at an end distance of 3.5d, where d is the dowel diameter. A 21 mm hole was made in the steel plate, neatly fitting the 20 mm dowel. It should be noted that the steel plate is not centrically aligned over the hole in the GLT. This misalignment is not of general use in the SPDJ design, but necessary in this test series to ensure enough movement in the rig for failure registration by the logging system. This misalignment is visible in the failed specimen shown in Figure 5. The thickness of the GLT element was 80 mm, for which the end grain was covered by acrylic paint to reduce moisture transport.

All specimens were conditioned to outdoor sheltered conditions for at least one month prior to testing or mounting. The short-term testing of the connection strength was thereafter conducted in indoor climate in February, but with min-

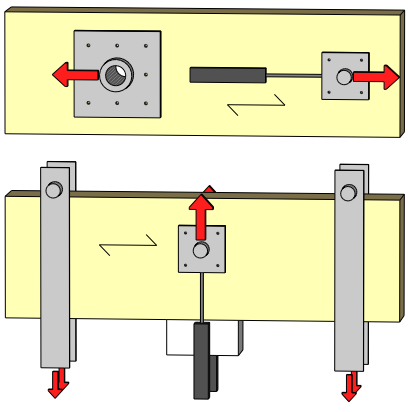

Figure 3: Test setup including placement of the linear potentiometers as shown in black.

imal time to acclimatise in order to represent the DOL tests which were conducted in the outdoor sheltered climate. The outdoor sheltered climate was characterized by a well-ventilated, unheated and uninsulated timber barn located in southern Sweden, about 100 km from the sea at an altitude of 180 m (57°09'N 14°46'E). During January-March the RH was typically about 90% at an average temperature of -2°C, while during May-July the RH was about 65% at an average temperature of 15°C. Relative humidity data is plotted in Figure 8. The tests were all conducted or initiated in February 2018.

The long-term loading was achieved using rigs with weights and a cantilever pulley with a 1:6.30 ratio, meaning that a specimen load of 31 kN required 500 kg of weight. Time to failure was recorded for all specimens, while plate slip was continuously recorded only for one DOL specimen of each type and load level.

3. Short-term tests

After 43 days of outdoor sheltered conditioning, the displacement controlled short-term quasi-static tests were performed in indoor climate with minimal time for the test specimens to acclimatise. The average specimen moisture content at time of testing was 11.7% (+2.6 percentage points since production). 10 specimens of each type were tested at a rate of deformation of 1.2 and 0.6 mm/min for the parallel and perpendicular specimens, respectively, resulting typically in a total test duration of 10 minutes. The results of these short-term referential tests are found in Table 1 and Figure 4, showing that loading parallel to grain is on average 95% stronger than perpendicular loading. Shown in Figure 4 are also typical clear wood shear strengths for Norway spruce for the respective shear strengths in RT and LT directions [17]. The coefficient of variation (COV) is found smaller for the SPDJ than the shear strength of clear wood specimens, and the mean strength of the SPDJ was found greater than that reported in [17] for clear wood.

Primary failures were located in the bond line at all times, often followed by shear plug failure due to contact between dowel and GLT. The possible bond line failure modes considered here are (1) shallow wood shear failure, (2) failure in the adhesive layer including the interlayers, (3) vulcanization failure and (4) rubber failure, see example in Figure 5. All failure modes but rubber failure were found to various degrees at inspection, thus no single failure mode can be identified as a conclusive limiting factor. Inspection of the bond line of the parallel specimens revealed that 60% of the bond line surface was subjected to adhesive failure, while 25% had a shallow wood failure. However, for the perpendicular specimens 85% of the surface was considered wood failure while 12% adhesive failure. Some specimens of both types had weaknesses in the vulcanization, which should be, of course, eliminated by proper manufacturing techniques and quality controls.

The steel plate displacement was measured using linear potentiometers, for which typical results are found in Figure 6. The behaviour resembles that of rubber in shear rather than timber, although the difference in stiffness is caused by

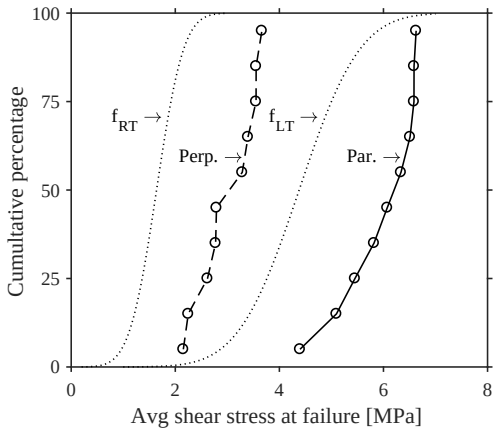

Figure 4: Short-term strength of the SPDJ conditioned in outdoor sheltered conditions for 43 days, loaded both parallel and perpendicular to grain. Dotted lines represent shear strength in RT and LT directions respectively [17].

the timber. The average stiffness of the parallel specimens was 12.6 kN/mm and 7.0 kN/mm for the perpendicular specimens, as determined assuming a linear force–displacement relation between $0.4F_{max}$ and $0.7F_{max}$, and where F_{max} is the ultimate load. The initial stiffness is considerably higher than the presented average, as can be seen in Figure 6.

4. Long-term tests

4.1. Time to failure

The long-term tests were all performed in outdoor sheltered conditions after 48–72 days of on-site conditioning in the facility described in Section 2. The average specimen moisture content at time of test initialization was 15.9%, i.e. +6.8 p.p. since production and +4.2 p.p. compared to short term tests. The specimens were loaded to 80%, 60% or 50% of the average short-term failure load presented in Table 1 in a fast ramp load, usually fully loaded within one minute. Testing of the 80% and 60% test specimens began in late February 2018, while the tests with the 50% specimens started in late March. The results of the long-term tests are found in Table 4, as well as Figure 7 and 8. A high variability in terms of time to failure was found.

Failure status was recorded every minute by a logging system. Complementing daily visual inspections ramped down to weekly inspections during the course of the series were also performed. However, the logging system was inoperable during three time periods of 2–6 days during the entire test. Furthermore, some few specimens failed without activating the logging system and these failures were thus discovered during the visual inspection. For the cases were manual

Table 1: Short-term tests of small scale SPDJ with a total effective plate shear area of 6500 mm^2 each. 10 specimens of each type were tested, thus the minimum failure load is equal to the 5th percentile.

Specimen	Direction	Failure load *5th percentile (avg)*	Shear stress at failure[1] *5th percentile (avg)*	COV
Par−100	Parallel to grain	28.7 (39) kN	4.40 (5.9) MPa	12%
Perp−100	Perpendicular to grain	14.1 (20) kN	2.15 (3.0) MPa	18%

1) Determined by assuming uniformly distributed shear stress.

Table 2: Time to failure for specimens loaded parallel and perpendicular to grain at different load levels in percentage of average short-term failure loads. 10 specimens of each type and load level was tested, and thus minimum time to failure is also the 5th percentile.

Specimen	Load level	Time to failure *min*	Time to failure *max*	Time to failure *median*	COV
Par−80	80%	26 min	406 hrs	26 hrs	120%
Par−60	60%	292 hrs	1111 hrs	839 hrs	45%
Par−50	50%	37 hrs	1210 hrs	772 hrs	40%
Perp−80	80%	1 min	541 hrs	0.3 hrs	290%
Perp−60	60%	9 min	2238 hrs	1712 hrs	50%
Perp−50	50%	571 hrs	2510 hrs	1299 hrs	35%

Figure 5: Illustration of different bond line failure modes of the SPDJ. Failure includes shallow wood shear failure (50%), failure in the adhesive layer including the interlayers (30%) and vulcanization failure (20%). Rubber failure of the tensile type seen here occurred during specimen disassembly, after the tests. The steel plate was intentionally mounted eccentric over the over-sized timber hole in order to facilitate a large enough displacement at failure to register the event in the failure detection system. This specific specimen was in group Par−60, see Table 4.

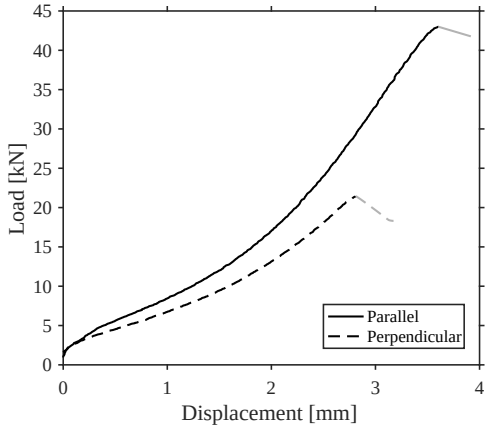

Figure 6: Typical load-displacement curve for short term testing of SPDJ specimens loaded parallel and perpendicular to grain. Grey lines are very fast failure propagation and should thus be considered brittle.

logging was required, the time in between last confirmed status and manual logging was chosen as failure time. This was done for a total of 10 out of 60 DOL specimens.

The failure modes of the DOL specimens are similar to the failure modes of the short-term specimens. Specimens loaded parallel to the grain are more subjected to adhesive failure, whereas specimens loaded perpendicular to the grain show more shallow wood shear failures. One of the specimens loaded perpendicular to the grain in the 60% load level group was removed from the analysis due to setup error.

A smaller than expected difference in terms of time to failure was found between the 60% and 50% load level specimens, regardless of loading direction. The relative humidity during the test period is shown in Figure 8, in which failures times also are included. Outdoor measurements recorded 1.2 km from the facility complement the facility measurements due to system failure.

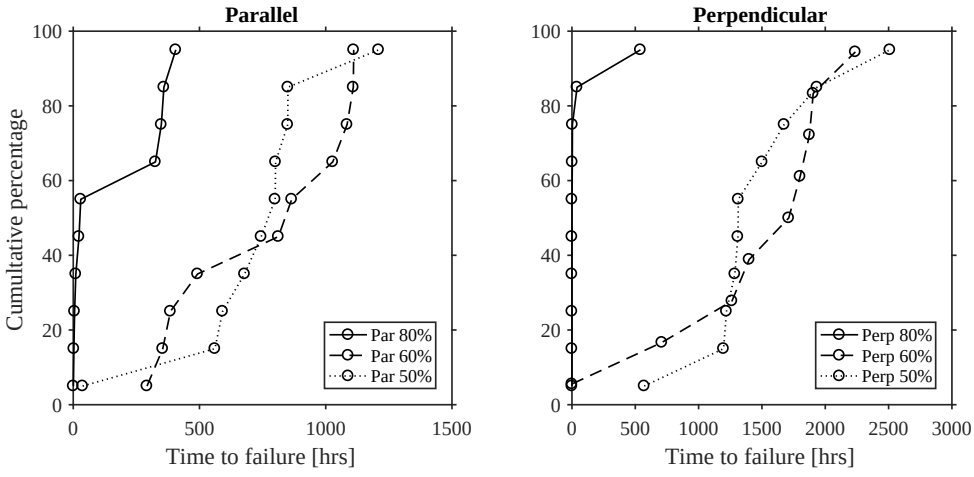

Figure 7: Cumulative distribution of time to failure of the parallel and perpendicular test specimens, all three load levels.

The data does not suggest a higher rate of failure during decreasing relative humidity. The lowest recorded moisture content of a single test specimen was 12.1% in early June, while the highest was 16.3%, recorded at test start in February.

4.2. Matching and fitting

The aim of the study is to find a general strength reduction for a typical SPDJ subjected to load over time. The method of ranked stress level is adopted, based on the assumption that the specimen strength distribution is equal for all load level groups. The results of each group are sorted from low to high, and the load acting on the first failing specimen of each load level group is then divided by the failure load of the weakest short-term specimen to determine its ranked stress level. Such a ranked stress level thus differentiates the load levels based upon the average short-term strength, which is useful in the stress level versus time to failure analysis shown in Figure 9. It has previously been shown that linear-logarithmic functions are suitable to estimate the duration of load behaviour of timber [11]. Such lin-log fits are also chosen for this study, since the statistical significance of the conducted tests is not high enough to suggest otherwise. Reference curves of the shear DOL behaviour of clear wood as determined by Leont'ev [12] and bending DOL behaviour as compiled by Pearson [9] are also shown in the figure, both determined parallel to grain.

The empirical linear logarithmic fit is in general terms expressed as shown in Equation 1, where A and B are fitting parameters, t_0 is a time reference here set to $t_0 = 1h$, $f_{s,Ramp}$ is the fractile s short term ramp loading strength and $\sigma_{s,DOL}$ is the constant load that for strength fractile s of the material is predicted to give a failure at time $t = t_f$.

$$\frac{\sigma_{s,DOL}}{f_{s,Ramp}} = A - B\log_{10}(t_f / t_0) \tag{1}$$

With an R^2 value of 0.78 and 0.73 for parallel and perpendicular tests respectively, the logarithmic fitting parameters found in Table 3.

Even though failure times did not exceed 4 months and thus not a full year cycle, the logarithmic functions can be extrapolated to obtain an estimate in order to be compared for reference period of 50 years. The given logarithmic fits suggest the resulting stress levels at failure to be 13.2% and 34.6% for parallel and perpendicular SPDJ, respectively. The values given in Table 3 for references [12] and [9] correspond to 33% and 52% for shear and bending respectively. By such, the suggested reduction factor k_{mod} for the SPDJ in outdoor sheltered conditions can be estimated to be in the range of 0.10 and 0.30 for SPDJ specimens loaded parallel and perpendicular, respectively. For reference, Eurocode assigns a k_{mod} factor of 0.5 for the corresponding climate class 3, without differentiating for modes of loading (bending/shear), nor for load to grain angle (parallel/perpendicular).

The ranked stress method is based upon the internal rank-

Table 3: Empirical fitting parameters to linear logarithmic fit to DOL testing of the SPDJ.

	A	B
Parallell	101.2	15.60
Perpendicular	81.6	8.34
Ref shear [12]	91.4	10.4
Ref bending [9]	91.5	7

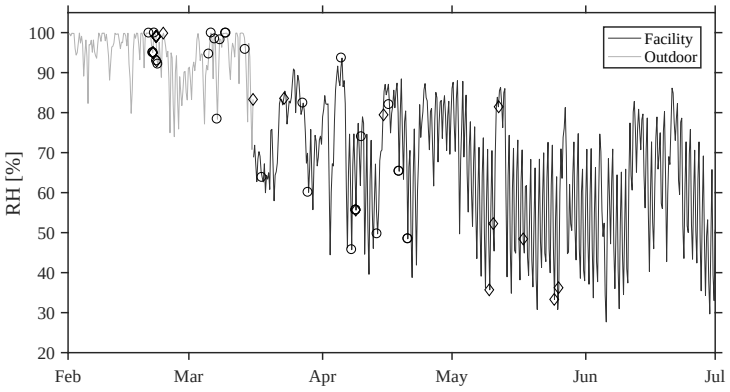

Figure 8: Relative humidity within the test facility or outdoor close to the test facility during the long-term tests. Failures are indicated by circles and diamonds for specimens loaded parallel and perpendicular to grain respectively.

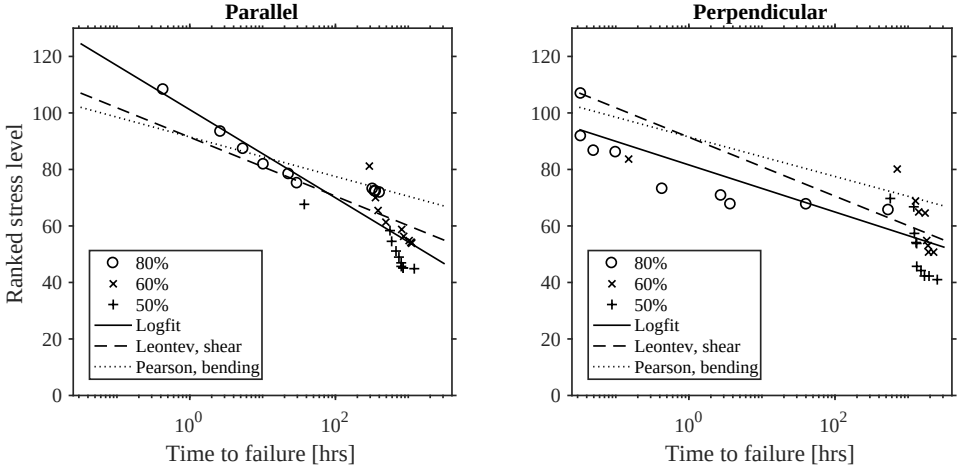

Figure 9: Ranked stress level vs time of specimens loaded parallel to grain (left) and perpendicular to grain (right). Logfit refers to a linear logarithmic fit to test data, while two reference curves also are plotted [9, 12]. The 100% specimens are excluded due to other type of loading.

ing of the grouped test results. The sensitivity of the estimated reduction factors k_{mod} (one for parallel to grain loading and one for perpendicular to grain loading) to this internal ranking were investigated by randomly deleting up to 5 individual test results in each group. For each such new combination of fictitious test results, the corresponding value of k_{mod} was calculated. The obtained distributions of k_{mod} were then statistically evaluated. For the parallel to grain loaded specimens, the statistical analysis suggests an average stress level at failure of 13.9% with a standard deviation of 0.068. Corresponding values for the perpendicular specimens are 35.5% and 0.026. Using the identified k_{mod} distributions, the above mentioned estimates of the reduction factors of 0.10 and 0.30 correspond to the percentiles of 20% and 1.5% for the perpendicular and parallel specimens, respectively.

4.3. Long term deformations

Displacement of the steel shear plate was measured every minute during the test period for one specimen in each group. Plotted in Figure 10 is the average of two linear potentiometers used to measure on each side of a specimen. The raw measurement data contains a few regions in time with unrealistic deformation variations, probably due to an unsteady power supply at the test facility. One region of obviously corrupted data has been removed, but some minor anomalies are still visible in Figure 10. The largest remaining large and fast vari-

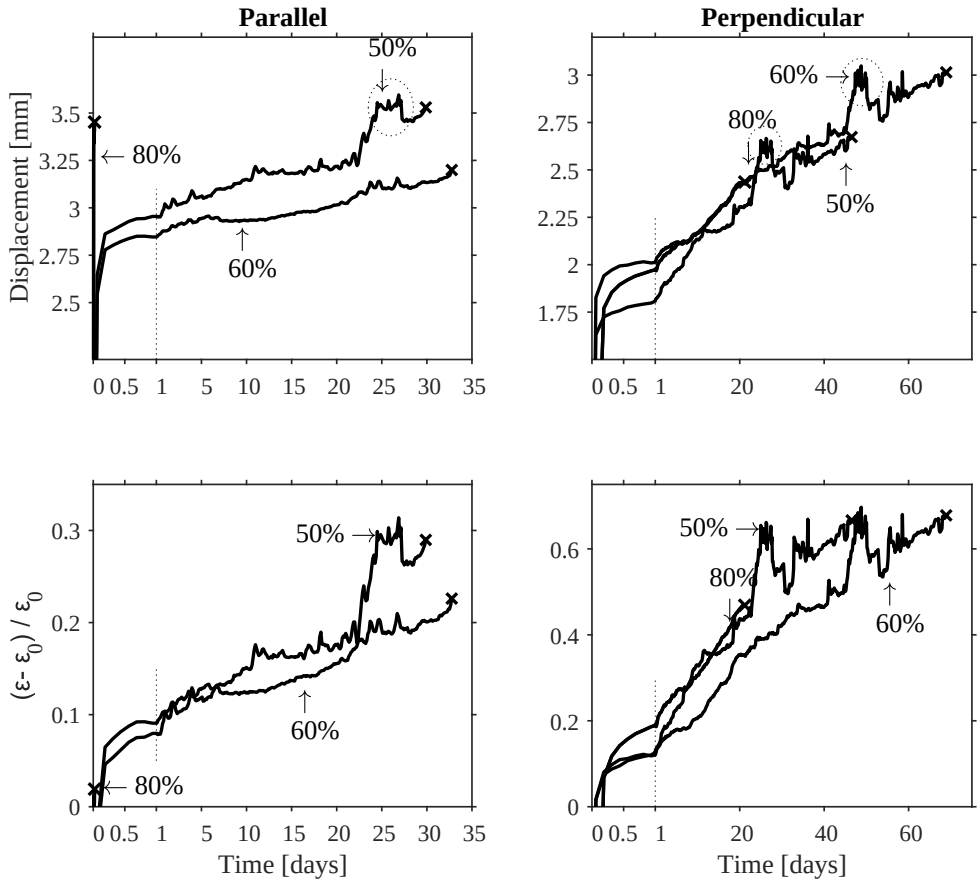

Figure 10: Displacement and normalized creep factor over time for SPDJ specimens loaded parallel and perpendicular to grain at different load levels. Note the different time scales before and after 1 day.

ation of displacement can be seen in all readings as highlighted by circles. All circled data were recorded during the same time period (different start dates), for which the variation is certainly not due to the mechanical loading. The variation might be due to moisture changes, but this is unlikely since no large variations in climate were recorded during the time period in question. Furthermore, a moisture variation would have more significant effect on the specimens loaded perpendicular to grain as the measurement setup here is more influenced by shrinkage and swelling, which is not the case in the readings.

A stiffness discrepancy is shown in Figure 10 for the parallel specimen. The single Par−50 specimen shows a larger deformation than the heavier loaded Par−60 specimen. However, post-failure inspection shows how the Par−50 specimen included an unsound knot on one side of the bond line, and some 5% area of vulcanization failure on the other. These defects decrease the effective bond area and thus increases the deformation. No evident defects were visible in the 60% specimen.

The results are also tabulated in Table 4, where it is evident that the both 50% load level specimens experienced more creep than the 60% specimens. This unexpected result can possibly be attributed to material variation.

The initial deformation is defined as the deformation after 10 minutes of constant loading. The normalized creep factor is defined in Equation 2, which is valid since the thickness of the rubber layer is 1 mm.

$$creepfactor = \frac{\delta - \delta_0}{\delta_0} = \frac{\varepsilon - \varepsilon_0}{\varepsilon_0} \tag{2}$$

5. Effects of long-term outdoor sheltered storage

In addition to the DOL study, the degradation of short-term strength by a year of outdoor sheltered storage was investi-

Table 4: Deformations and creep data for parallel and perpendicular test specimens at different load levels in percentage of average short-term failure loads. All deformations are specified in mm, and the total duration time to failure is shown in parenthesis. The creep factor is defined as deformation at failure divided by initial 10-minute deformation.

Specimen	Load level	Def 10 min	Def 24 h	Def at failure	Creep fact. *20 days*
Par−80	80%	3.38	–	3.45 (0.5 hrs)	–
Par−60	60%	2.61	2.85	3.20 (815 hrs)	0.15
Par−50	50%	2.74	2.96	3.53 (745 hrs)	0.17
Perp−80	80%	1.66	1.97	2.44 (540 hrs)	0.45
Perp−60	60%	1.80	2.02	3.01 (1905 hrs)	0.34
Perp−50	50%	1.60	1.81	2.67 (1290 hrs)	0.43

gated in a comparative manner between the SPDJ and a similar joint but without the rubber layer in the bond line (SPDJ-wr). For this purpose, three specimens of each type were produced and tested.

The average moisture content of the original specimens during testing was 11.3% and 8.6% for the SPDJ and SPDJ-wr specimens respectively. The specimens stored for one year (379 days) had an average moisture content of 16% during testing, for which the results are found in Table 5.

A general strength degradation of the specimens was found after the exposure to the natural moisture fluctuations. However, a larger degradation was expected for the specimens without rubber than for the specimens with rubber, as the rubber layer should accommodate for moisture movements in the timber and minimising cracking. This effect is expected to be more pronounced for larger test specimens than the 65×65 mm^2 used.

Although difficult to unequivocally distinguish the effect of the storage from the effect of different moisture contents during testing, an estimate can be obtained using Equation 3 [18, 19]. The relation suggests that for moisture content between 12 and 20%, the shear strength decreases by 2.5% per 1% increase in moisture content. The equation is based upon clear wood specimens tested in parallel shear, where $f_{v,MC\%}$ is the shear strength at a given moisture content MC (%). $f_{v,green}$ is the shear strength of green wood and M_p the moisture content at the intersection of a horizontal line representing the strength of green wood and an inclined line representing the logarithm of the strength–moisture content relationship for dry wood, i.e. slightly less than the fibre saturation point and typically $M_p \approx 25$.

$$f_{v,MC\%} = f_{v,12\%}\left(\frac{f_{v,12\%}}{f_{v,green}}\right)^{\frac{12-MC}{Mp-12}} \approx f_{v,12\%}\left(1-0.025\left(MC-12\%\right)\right) \quad (3)$$

A 12% strength reduction due to increased moisture content is expected for the SPDJ by means of Equation 3, while 17% for the SPDJ-wr. It can thus be concluded that, for parallel shear, the SPDJ-wr can be considered unaffected of the storage, while a reduction was found for the SPDJ contrary to expectations. However, the tests perpendicular to grain indeed showed a larger reduction for the specimens without rubber.

Table 5: Average short-term strength of the SPDJ after unloaded outdoor sheltered storage for 1 year, with and without a rubber layer in the bond line (SPDJ and SPDJ-wr respectively). Coefficient of variation within parenthesis.

		SPDJ	SPDJ-wr
Parallel	New	39[1] kN (12%)	24 kN (42%)
	1 year	28 kN (17%)	21 kN (22%)
	Decrease	29%	13%
Specimen	New	20[1] kN (18%)	19 kN (16%)
	1 year	19 kN (7%)	12 kN (20%)
	Decrease	4%	40%

1) average of 10 specimens, otherwise average of 3.

6. Evaluation of DOL effects on the SPDJ

The results of this study comprise experimental analyses of the shear plate dowel joint subjected to long term loading. The design of the joint entails a close to uniform shear stress being applied to the GLT body, and thus it is expected that the SPDJ has an upper bound performance level being defined by the shear behaviour of timber. Any other failure mode than shallow wood failure in the bond line should thus decrease the strength of the joint in comparison.

The short-term strength results in Figure 4 show how the SPDJ is stronger in shear than small clear wood specimens [17]. It is reasonable to believe that this difference is in part due to the difference between timber and clear wood. This reasoning is also evident in the fact that the characteristic strength values of longitudinal and rolling shear in Eurocode surpasses the 5th percentile of the presented clear wood strengths in Figure 4. It is found that the 5th percentile of the tested SPDJ specimens exceeds the characteristic strength values in Eurocode in terms of short-term strengths, with an increase of 25% and 80% for parallel and perpendicular direction respectively.

The mixed type of bond line failure mode was similar in the DOL testing as in the short-term tests, suggesting that any specific failure mode was no more prone to time effects than another and that no specific failure mode is considerably weaker than another. It is thus difficult to identify a specific failure initiation mode.

Van de Kuilen [16] conducted comparative duration of load tests on shear connectors in controlled and uncontrolled climate. It was shown how not only timber in bending, but also different types of shear connectors are strongly and negatively influenced by a varying climate during loading. It is reasonable to anticipate that an indoor climate would cause a smaller reduction in strength and thus a higher k_{mod} factor, but it was also shown how a small moisture content variation of only 1% is sufficient to induce mechano-sorptive deformation, a variation which indeed also does occur in indoor climate conditions.

In the deformations recorded of the shear connectors [16], a second process of higher creep rate was triggered by the moisture variations of an uncontrolled climate after approximately 200 days. The creep results of the SPDJ do not indicate such a second process but instead the specimens maintained a high creep rate throughout the relatively short test period. However, the variation in moisture content from test start in combination with a high load level might suggest that such a second phase was initialized early in the test duration, rather than suggesting that the phases do not occur for the current tests.

Based upon the findings of Leont'ev [12], it is reasonable to expect that a perfectly manufactured SPDJ loaded parallel to grain would still be limited to a k_{mod} of approximately 0.3, if the bonded plates are large enough to minimize the influence of peel stresses. However, using the proposed bonding technique and material in outdoor sheltered conditions, a reduction factor k_{mod} of 0.1 was found. These k_{mod} values should be regarded as estimates, as the test duration was too short to establish such reduction factor with satisfying accuracy. The longest recorded test period did not exceed 4 months, and thus did not experience a full year cycle of the varying climate common to the test site.

Although this study might indicate that shear perpendicular to grain is to some degree better than shear parallel to grain as regards DOL behaviour, it must be concluded that the SPDJ without screws is not efficient in terms of long duration loads in outdoor sheltered conditions, and that further studies are needed in order to verify the use in other climate classes.

Such a further duration of load study is currently ongoing at Nanjing Tech University, China, where lap joints with a resilient bond line using rubber are tested under climate control. In addition to the resilient bond line, the specimens also include screws in a total shear area is 12800 mm^2 (approximately double size as compared to this study). The first specimen loaded to 60% has failed after 391 days. Additionally, a single very small-scale resilient lap joint (200 mm^2) was loaded to 25% of short term strength in indoor climate and unloaded after 8 years without failure, succeeding the work of Danielsson and Björnsson [20]. The bonding technique used for these two studies are the same as used in this study, proposing a higher k_{mod} for indoor climate.

7. Conclusion

The presented study concludes the following findings:

- A lack of knowledge and empirical evidence on duration of load effects in timber for shear loading. Conducted research is inconclusive in terms of the duration of load behaviour of shear strength compared to bending strength. More studies in this field is advisable.
- The characteristic short-term strength of the small-scale shear plate dowel joints is higher than the characteristic shear strength of timber according to Eurocode.
- A linear logarithmic fit to ranked stress data over time suggests a significant duration of load reduction factor k_{mod} of 0.10 and 0.30 for parallel and perpendicular SPDJ without screws respectively in outdoor sheltered conditions. This is to be considered a relatively rough estimate based on a 50-year extrapolation of 4-month data.
- The shear plate dowel joint, as produced in this study without any improvements, is not recommended for structural applications in climate classes 2 and 3 as defined in Eurocode.

8. Acknowledgements

The financial support provided by *Stiftelsen Nils och Dorthi Troëdssons forskningsfond* through grant 893-16 is gratefully acknowledged. The authors would like to thank Thomas Johansson at Moelven Töreboda AB for delivering the GLT and Ante Salomonsson at Sika for adhesives and expertise. This study has also been made possible by the Swedish Infrastructure for Ecosystem Science (SITES), in this case by Asa Research Station. Special thanks to the staff at the research station as well as to Michael Lempart and Jessica Dahlström, Structural Mechanics at Lund University, for their work on the DOL measurement system. Associate Professor Huifeng Yang at Nanjing Tech University is kindly acknowledged for sharing unpublished data.

References

1. Crocetti R, Axelson M, Sartori T. Strengthening of large diameter single dowel joints. Tech. Rep. 2010:14; SP Technical Research Institute of Sweden; 2010.
2. Kobel P. Modelling of strengthened connections for large span truss structures. Master's thesis; Division of structural engineering, Lund University; 2011.
3. Yang H, Crocetti R, Larsson G, Gustafsson PJ. Experimental study on innovative connections for large span timber truss structures. *Proceedings of the IASS Working Groups* 2015;12(18).

4. Larsson G, Gustafsson PJ, Crocetti R. Use of a resilient bond line to increase strength of long adhesive lap joints. *European journal of wood and wood products* 2018;76(2):401–11.
5. Gustafsson P. Tests of full size rubber foil adhesive joints. Tech. Rep. TVSM-7149; Div. of Struct. Mech., Lund University; 2007.
6. Larsson G. High capacity timber joints - proposal of the shear plate dowel joint. Licentiate thesis; Division of structural mechanics, Lund University; 2017.
7. Austrell PE. Modeling of elasticity and damping for filled elastomers. Ph.D. thesis; Division of structural mechanics, Lund University; 1997.
8. Wood L. Relation of strength of wood to duration of load. Tech. Rep. 1916; US Department of Agriculture, Forest Service, Forest Products Laboratory; 1951.
9. Pearson R. The effect of duration of load on the bending strength of wood. *Holzforschung-International Journal of the Biology, Chemistry, Physics and Technology of Wood* 1972;26(4):153–8.
10. Madsen B. Duration of load tests for dry lumber in bending. University of Briitish Columbia, Department of Civil Engineering; 1971.
11. Hoffmeyer P. Failure of wood as influenced by moisture and duration of load. Ph.D. thesis; State University of New York. College of Environmental Science and Forestry; 1990.
12. Leont'ev N. Long term resistance of spruce wood to shear along the grain. *Russian Lesn Z Archangel'sk* 1961;4(4):122–4.
13. Spencer RA, Madsen B. Duration of load tests for shear strength. *Canadian Journal of Civil Engineering* 1986;13(2):188–95.
14. Madsen B. Duration of load tests for dry lumber subjected to shear. *Forest Products Journal* 1975;.
15. Gerhards CC. Effect of duration and rate of loading on strength of wood and wood-based materials. Tech. Rep.; FOREST PRODUCTS LAB MADISON WIS; 1977.
16. Van de Kuilen JWG. Duration of load effects in timber joints. Ph.D. thesis; Delft University; 1999.
17. Dahl KB. Mechanical properties of clear wood from norway spruce. Ph.D. thesis; NTNU Trondheim; 2009.
18. USDA Forest Service, Forest Products Laboratory . Wood handbook: wood as an engineering material. Tech. Rep. FPL-GTR-190; 2010.
19. Gehri E. Shear problems in timber engineering–analysis and solutions. In: *Proceedings of 11th World Conference on Timber Engineering, Riva del Garda*. 2010:.
20. Björnsson P, Danielsson H. Strength and creep analysis of glued rubber foil timber joints. Master's thesis; Division of structural mechanics, Lund University; 2005.